THE TEMPORAL GROWTH OF IONIZATION IN HELIUM

by

G.B. Evans, M.Sc.

A thesis submitted to the
University of Keele in candidature
for the degree of Ph.D.

Department of Physics
University of Keele
July 1966

ABSTRACT

Measurements were made of the formative time lag in helium and an analysis due to Davidson was used to obtain the relative contributions of the individual secondary processes to the current growth.

A series of curves was obtained, giving the dependence of the formative time lag on the percentage overvoltage, for overvoltages within 4% of the sparking potential. These curves were obtained at five pressures in the range 14.9 to 62.2 torr and at gap distances from 0.18 to 0.82 cm. The range of E_s/p_o was from 9.8 to 38.7 volt cm^{-1} $torr^{-1}$.

The combination of two processes involving delayed photons gave good agreement with experiment over the intermediate range of E_s/p_o investigated. One of the delayed photon processes was the emission of secondary electrons from the cathode by photons produced by the decay of 2^1S metastable atoms in two-body collisions in the gas. The other was due to photons from the decay of $2^3\Sigma$ metastable molecules which had been produced in three-body collisions involving 2^3S metastable atoms.

Positive ion action at the cathode became important at the highest values of E_s/p_o used. This, in combination with the action of delayed photons from the decay of 2^1S metastable atoms, gave the required agreement with experiment.

Below 11.6 volt cm^{-1} $torr^{-1}$, the observed time lags could not be satisfactorily explained by the processes considered. In this case, it was suggested that examination of the processes involving the action at the cathode of metastable atoms and delayed photons from the decay of metastable molecules might prove fruitful.

ACKNOWLEDGMENTS

I wish to thank Dr. D.E. Davies for suggesting the problem and for his helpful supervision of the work. I also wish to thank Professor D.J.E. Ingram for the use of the laboratory and research facilities at the Department of Physics, University of Keele.

I am greatly indebted to the Director, A.E.R.E. (Harwell), for the provision of a maintenance grant and for the purchase of the greater part of the equipment used during the investigation.

My thanks are due to my former colleagues at the University of Keele for many useful discussions. I am also indebted to Dr. D. Griffiths, formerly of the University College of Swansea, for his valuable suggestions during a discussion of the work. I am also grateful to Mr. D.R. Tilley, of the Mullard Research Laboratories, for helpful advice during the writing of the computer programmes.

I also wish to express my gratitude to the Director of the Mullard Research Laboratories for the use of facilities at the Laboratories during the writing and production of this thesis.

Finally my thanks are due to Miss J. Franks for her care in the drawing of the figures and to Miss R. Merralls for her speed and accuracy in the typing of the manuscript.

CONTENTS

Chapter 1

EXCITATION AND IONIZATION IN HELIUM

The present investigation was begun in an attempt to clarify the complex processes leading to electrical breakdown in helium. In 1959, Davidson[1] published a theory applicable to the temporal growth of ionization in gases, such as helium, where the action of metastable atoms is of importance. This provided a method of establishing, from formative time lag measurements, the relative contributions of the various secondary processes to the current growth. This was the approach adopted in the present study.

Before proceeding to a discussion of the temporal growth of current, it is relevant to consider the ionization and excitation processes occurring in gases with particular reference to helium.

1.1 The atomic structure of helium

The atomic structure of the gas is obviously of great importance in any discussion of the fundamental excitation and ionization processes occurring in a gas discharge. The gas of the present investigation is helium of which the normal atom has only two electrons.

It is possible to calculate the energy levels of the helium atom by wave mechanical methods[2]. The Schrödinger equation for the two-electron system cannot be solved exactly, but it is

possible to obtain approximate solutions. In most problems the only states of importance are those for which at least one electron is in its lowest energy level.

Early spectroscopic investigations showed that the term scheme of helium (figure 1) split into two separate groups, in general there being no transitions between terms of the two groups. These groups of terms are known as parahelium and orthohelium. Once an atom has exhibited the properties of one of the two groups, it rarely subsequently shows the properties of the other. The splitting of the term scheme into two groups can be explained by electron spin considerations[3]. In parahelium the spins of the two electrons are anti-parallel and the parahelium terms are singlets. Since the electron spins are parallel in orthohelium the terms are triplets.

In the unexcited state of the atom, the two electrons complete the K-shell, the ground state configuration being written $1s^2$. This saturated structure of complete shells is characteristic of the noble gases. Together with the high excitation energy of helium, it determines the character of the inter-atomic forces, and these, in their turn, are to a great extent responsible for many of the typical properties of helium.

From the term diagram, it can be seen that there is no 1^3S term - the expected ground state for orthohelium. No lines have been found by spectroscopic methods which would correspond to

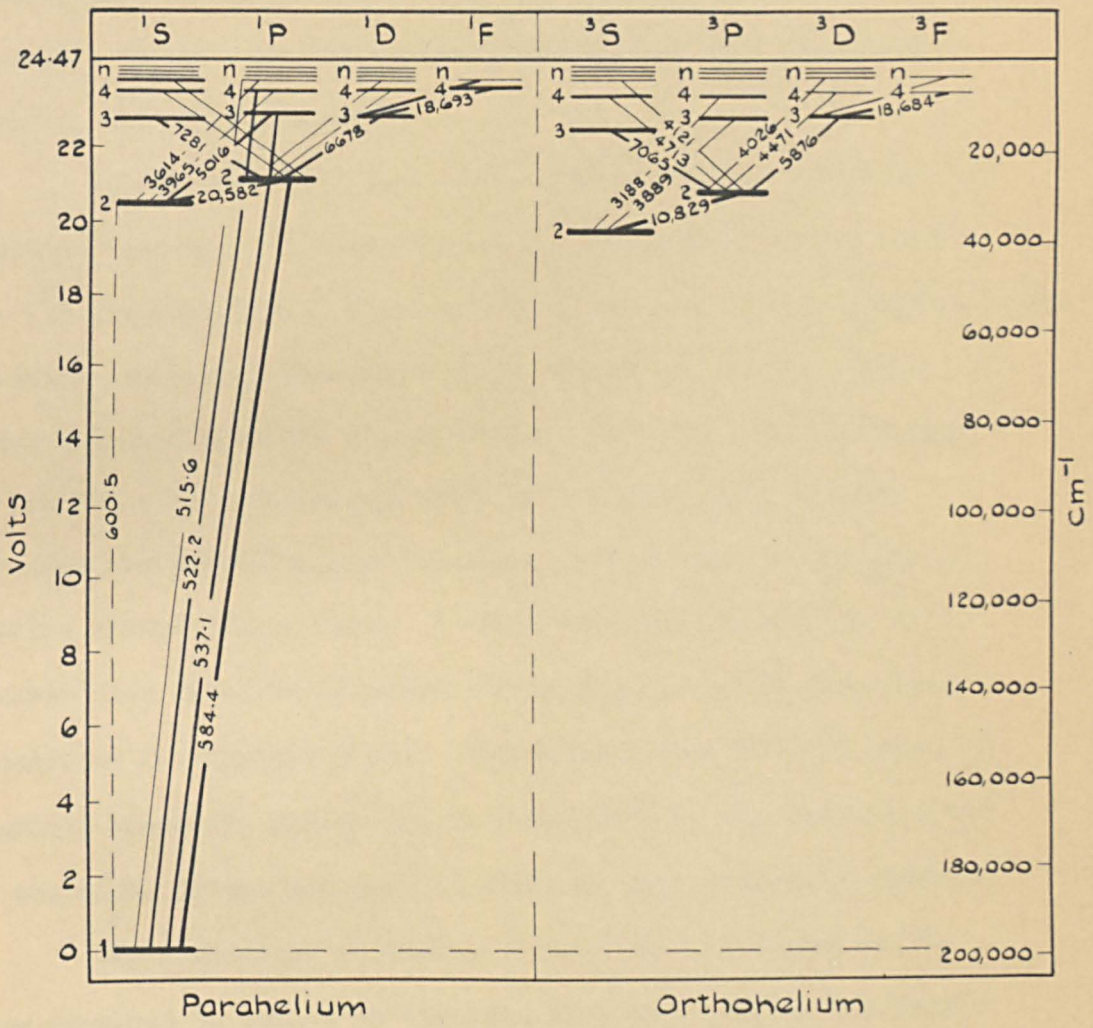

FIG. 1 ENERGY LEVEL DIAGRAM OF HELIUM. THE TRANSITIONS ARE IN ANGSTROM UNITS.

transitions to this term. Further examination shows that, for a 1^3S term, all four quantum numbers would be the same for both electrons. As such an arrangement would violate the exclusion principle, the term is absent.

By the selection rule, $\Delta L = \pm 1$, it can be seen that the transition from the 2^1S state to the 1^1S state and the transition $2^3S - 1^1S$ are forbidden. Those states which cannot pass spontaneously to a lower state with the emission of radiation are metastable. Of the two metastable states of the helium atom, the 2^3S is stronger than the 2^1S. This is because the $2^3S - 1^1S$ transition would contradict the prohibition of an ortho-para transition as well as violating the selection rule. In fact the transition $2^3S - 1^1S$ has never been observed directly, while the $2^1S - 1^1S$ transition can occur in an electric field. Transitions from the 2^3S state to the ground state are mainly due to collisions of the excited atoms with the atoms of the gas and the walls of the containing vessel.

The ionization potential of an atom is defined as the energy required to remove an electron from the atom in its ground state to form the singly charged ion in its ground state. So the ionization potential of the helium atom is the energy of the process: $He \rightarrow He^+ + e$. The value of the ionization potential of helium, as obtained from the limit of the series $1^1S - m^1P$, is 24.46 volts. Quantum mechanics gives the spectroscopic value to within the limits of the accuracy of the calculation[4].

Table 1 gives some of the potentials and spectral lines found from electron excitation of the ground state of the helium atom. It should be noted that the helium spectrum is almost entirely due to transitions of only one electron, the other remaining in its lowest state.

Transition	Wavelength in Å	Potentials in volts	
		Spectroscopically	Electron collision
$1^1S - 2^3S$		19.77	19.75
$1^1S - 2^1S$	600.5	20.55	20.55
$1^1S - 2^1P$	584.4	21.12	21.2
$1^1S - 3^1P$	537.1	22.97	22.9
$1^1S - 4^1P$	522.3	23.62	
$1^1S - 5^1P$	515.7	23.92	
1^1S - ionization	502.0	24.47	24.6

Table 1. Potentials and spectral lines produced by electron excitation of the ground state helium atom[5].

1.2 Electrons, ions and excited atoms in helium

In the absence of an electric field all the particles present, charged and uncharged, move at random through the gas. When thermal equilibrium is attained the velocity distribution of the gas atoms is Maxwellian. The average distance a particle travels between two successive collisions is called the mean free path. The

mean free path λ for gas atoms moving in their parent gas can be obtained from simple collision theory as $\lambda = 1/(\sqrt{2}\ \pi\ N\ d^2)$, where N is the number of gas atoms per cm^3 and d is the diameter of a gas atom. So, at a pressure of 1 torr and 273°K (when $N = 3.56 \times 10^{16}$ atoms cm^{-3}), the mean free path of helium atoms is 0.018 cm.

By treating the electron as a particle of infinitely small radius, classical theory gives its mean free path as $\lambda_e = 4\sqrt{2}\ \lambda$. However, experiment has shown that λ_e varies with the electron energy. The number of collisions made by an electron in travelling 1 cm through a gas at 1 torr and 273°K is known as the collision probability P_c and $P_c = 1/\lambda_e = NQ$, where Q is the effective cross-section for a collision between a gas atom and an electron. Thus, at 1 torr and 273°K, when N has the value given above, $Q = 0.281 \times 10^{-16}\ P_c\ cm^2$.

It follows that the effective collisional cross-section also depends on the electron energy. This is known as the Ramsauer effect, and can be explained by considering the diffraction of the electron wave by the potential field of the atom. By this application of wave mechanical methods to the problem, Allis and Morse[6] obtained good agreement between theory and experiment. The probabilities of electron-atom collision in helium and in hydrogen, at varying electron energies, are compared in figure 2. Helium has one of the smallest effective cross-sections of any atom. This is to be

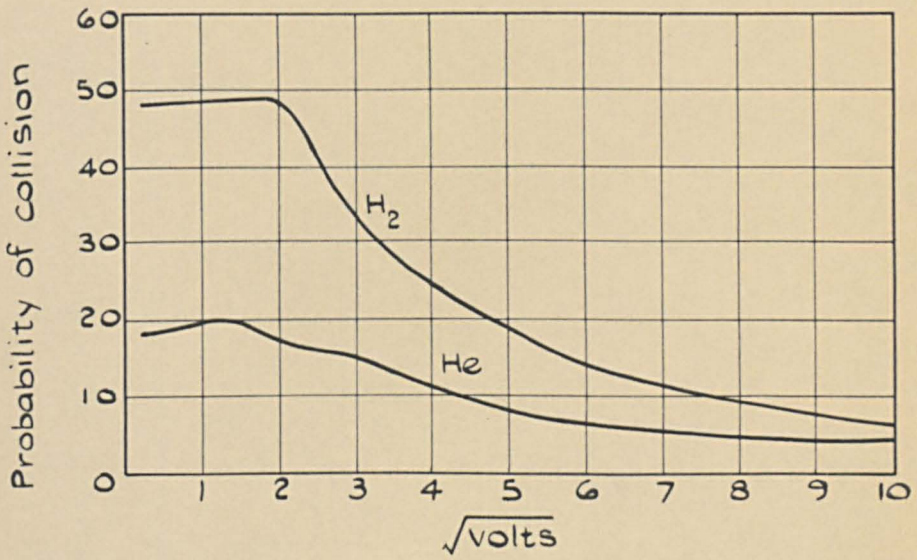

FIG. 2 THE PROBABILITY OF ELECTRON-ATOM COLLISION IN HYDROGEN AND HELIUM AS A FUNCTION OF ELECTRON VELOCITY. AFTER BRODE[7], PHELPS, FUNDINGSLAND AND BROWN[9], VARNERIN[10] AND GOULD AND BROWN[8].

expected, since P_c is inversely proportional to the ionization potential and helium has the highest known ionization potential.

It is often convenient to keep the mean energies of the charged particles constant while other parameters, such as the gas pressure, change. The energy gained by an electron from the electric field E depends on the potential drop per mean free path in the direction of the field which is given by $E\lambda_e$. Now $\lambda_e = \lambda_1/p_o$, where λ_1 is the mean free path of an electron at 1 torr and 273°K and p_o (= 273 p/T, where T is the temperature in °K) is the reduced gas pressure. Thus $\lambda_e E = \lambda_1 E/p_o$, λ_1 being a constant for a given gas. So the ratio E/p_o must be kept constant if the mean energies of the electrons (and other charged particles) are to remain constant. In general, since E/p is proportional to E/p_o at a given temperature, E/p is kept constant and the reduction to p_o can be made later if required.

At each collision the energies of the colliding particles will change. Elementary considerations give the following expression for the mean fractional loss of energy at collision, allowing for collisions at all possible angles: $\Delta = 2\,mM/(m + M)^2$, where m and M are the masses of the colliding particles. It should be noted that this is only strictly true for elastic collisions, that is, those collisions in which there are no internal changes of energy in the colliding particles. For ions in collision with atoms of their parent gas, m = M and $\Delta = \frac{1}{2}$. For electrons, $m \ll M$ so $\Delta \approx 2m/M$ and,

for helium, $\Delta \approx 2.7 \times 10^{-4}$, which is considerably lower than the value for ions. Because of this, electrons can attain much higher mean energies in an electric field than can ions. So electrons will play the more important role in the excitation and ionization of gas atoms.

Even though an electron has sufficient energy to excite a gas atom to a given level, it is not certain that this will occur. The ratio of the effective cross-section for the particular excitation (or ionization) to the total effective cross-section gives the probability of the excitation (or ionization) taking place at collision. The probabilities for the excitation of the 4^1P and 3^3P states of helium are given in figure 3(a). The shapes of the curves show the characteristic difference between singlet and triplet levels, the difference being most marked for the P states. It can be seen that, for electrons of low energy, excitation of the triplet state is more probable than excitation of the singlet state and vice versa for high energy electrons. This difference in excitation probabilities for singlet and triplet states can be explained by use of wave mechanics[11].

The dependence of the probability of ionization on electron energy is shown in figure 3(b) which compares values for helium and neon. For helium, the probability increases to a maximum at electron energies of about 110 volts. Here, by common usage, the electron-volt energy unit has become shortened to the volt.

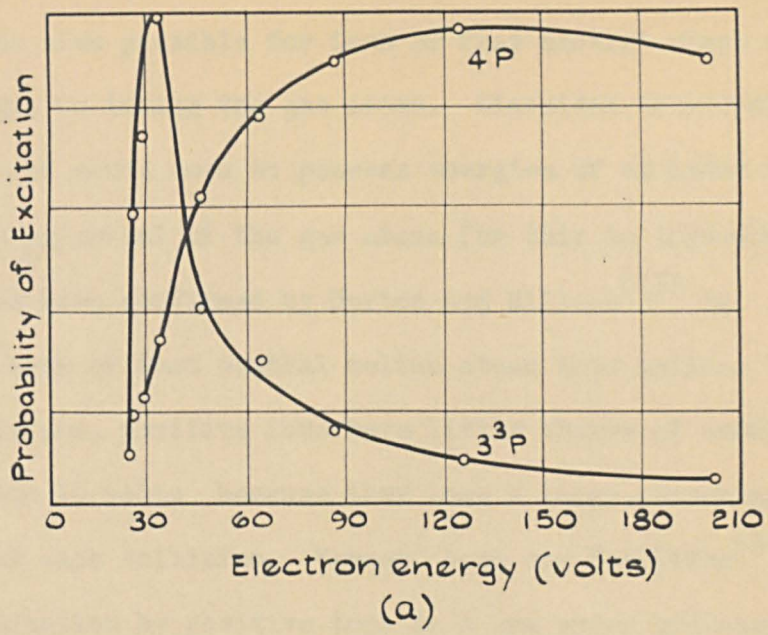

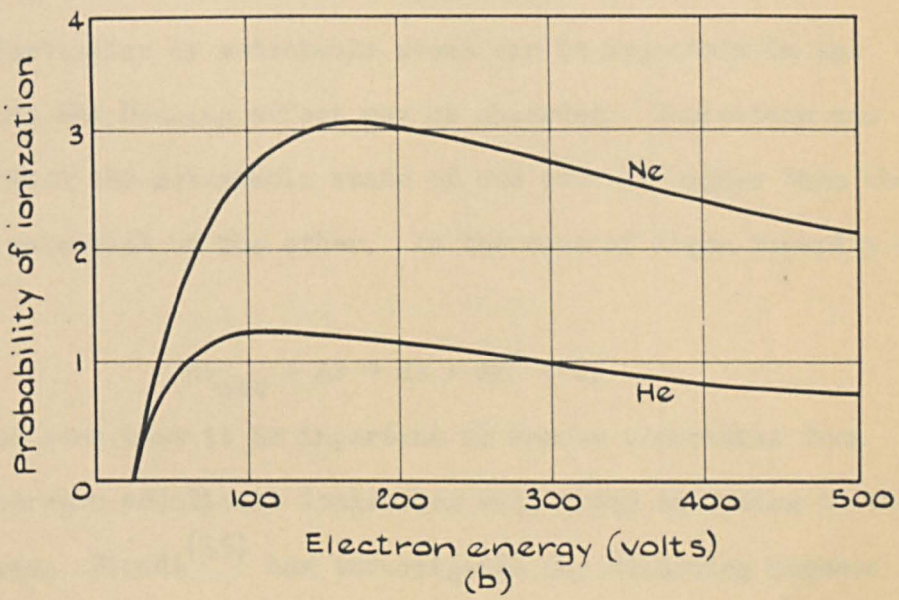

FIG. 3 EXCITATION AND IONIZATION PROBABILITIES AS A FUNCTION OF ELECTRON ENERGY. (a) EXCITATION FUNCTIONS FOR THE 4^1P AND 3^3P LEVELS OF HELIUM (b) PROBABILITY OF EXCITATION IN HELIUM AND NEON (12).

It is also possible for ions or fast neutral atoms moving in their own gas to ionize the gas atoms. Classical treatment shows that the ions and atoms need to possess energies of at least twice the ionization potential of the gas atoms for this to take place. This result has been confirmed by Horton and Millest[13] by introducing a beam of fast neutral helium atoms into helium. Under ordinary conditions, positive ions have little chance of achieving energies of even 10 volts because they lose a large percentage of their energy at each collision. Varney, Loeb and Haseltine[14] state that ionization by positive ions in a gas under ordinary sparking conditions, and even at low pressure and high E/p, is virtually ruled out.

Ionization by metastable atoms can be important in gas mixtures when the Penning effect may be observed. Ionization can take place when the metastable state of one atom is higher than the ionization potential of the other. In the case of argon impurity in helium,

$$He_{met} + Ar \rightarrow He + Ar^{+} + e.$$

So it can be seen that it is important to remove impurities from helium, otherwise additional ionization will occur according to the above process. Biondi[15] has investigated the following process which could possibly occur in pure helium:

$$He_{met} + He_{met} \rightarrow He + He^{+} + e.$$

However, he states that it is only likely to occur in the positive column of a d.c. discharge where it must be taken into account.

Since electrons are the main cause of excitation and ionization of the atoms of a gas, the form of their energy distribution is of great importance. Heylen and Lewis[16] calculated the energy distribution of electrons in helium and obtained good agreement with other published distributions. The curves they obtained at various values of E/p are given in figure 4. It can be seen that, as E/p decreases, so the distribution becomes narrower. Reder and Brown[17] have also given a method for obtaining the electron energy distribution in helium. From their distribution theory, they made an indirect determination of the average energy of electrons in helium as a function of E/p (figure 5). These results were in good agreement with values obtained at low E/p (< 10 volts cm^{-1} $torr^{-1}$) by Townsend and Bailey[18] and by Smit[19].

Although a swarm of charged particles may have velocities distributed in all directions about an average velocity, an electric field will move the swarm bodily. The average speed with which the centre of the swarm moves in the direction of the field is called the drift velocity. The electron drift velocity has been measured in helium as a function of E/p by, among others, Phelps, Pack and Frost[20]. They used a double-shutter tube method at low values of E/p (< 1 volt cm^{-1} $torr^{-1}$). At higher E/p, they obtained their values from microwave methods which had been used to measure

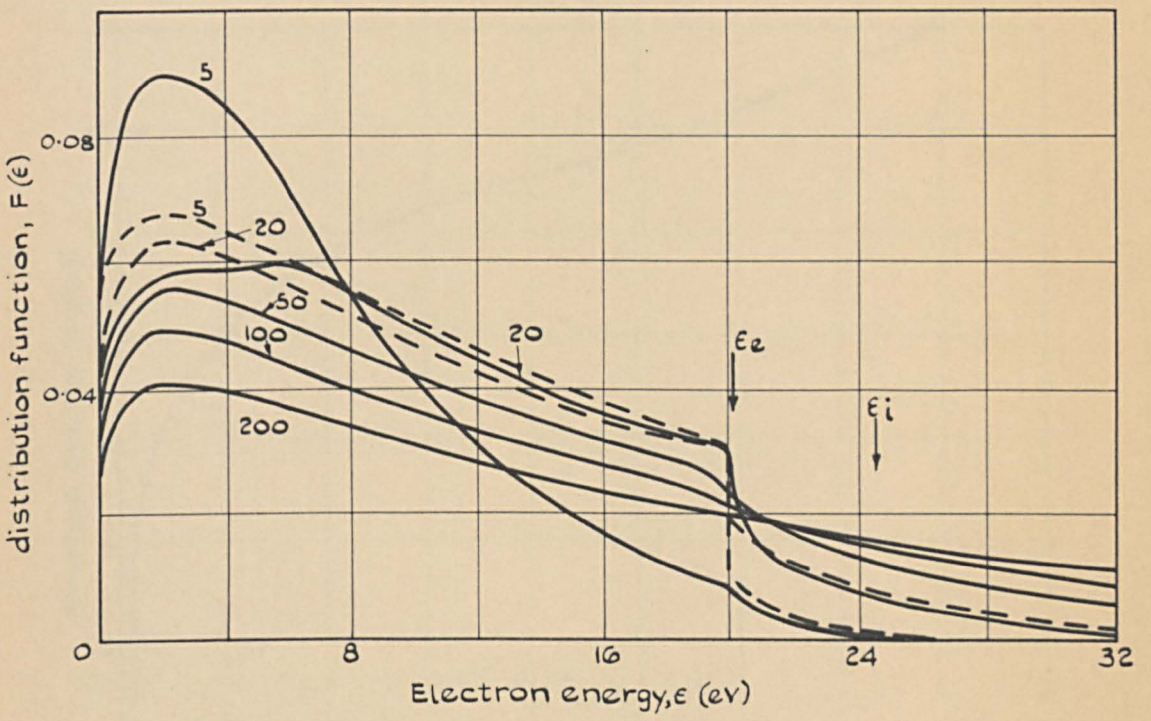

FIG. 4 ELECTRON ENERGY DISTRIBUTION FOR HELIUM AT VARIOUS VALUES OF E/P. THE DISTRIBUTIONS SHOWN BY DASHED LINES WERE OBTAINED BY NEGLECTING ELASTIC LOSS.

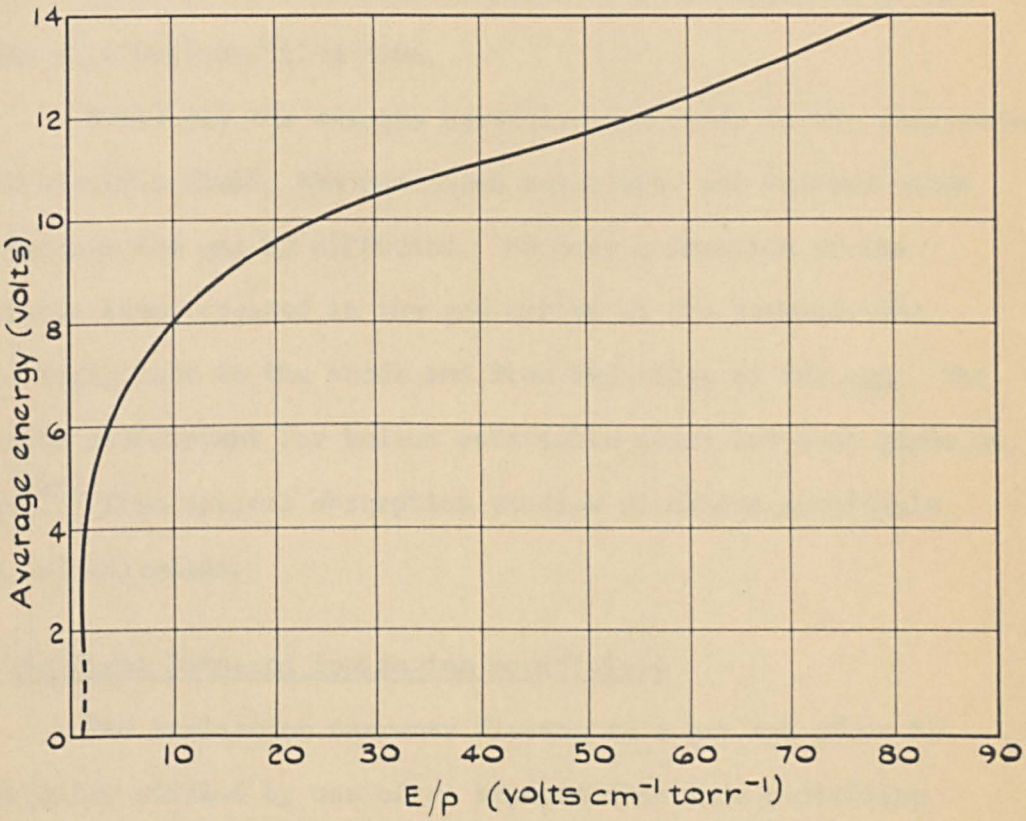

FIG. 5 AVERAGE ENERGY OF ELECTRONS IN HELIUM AS A FUNCTION OF E/p.

the electron density in the positive column of a low pressure discharge. The drift velocities of molecular and atomic ions in helium have been measured by Hornbeck[21]. His method relied upon the measurement of transient currents resulting from the release of a very short (0.1 μsec) pulse of photoelectrons at the cathode of a helium-filled tube.

While all the charged particles are drawn to the electrodes by the electric field, the uncharged metastable and excited atoms move through the gas by diffusion. So only a fraction of the metastable atoms created in the gas arrive at the cathode, the others being lost to the anode and from the sides of the gap. The diffusion coefficient for helium metastable atoms has been given by Phelps[22] from optical absorption studies on helium metastable atoms and molecules.

1.3 The first Townsend ionization coefficient

The ionization currents flowing in a gas can often be conveniently studied by use of an experimental tube containing parallel electrodes where the inter-electrode distance can be varied. A steady source of electrons is usually provided in the gap, commonly by ultra-violet illumination of the cathode. The anode current i may then be measured at various values of gap distance d, E/p being kept constant. On plotting a graph of log i against d, a straight line results up to a limiting value of d. This linear relationship

can be readily explained by considering ionization of gas atoms by electrons which have gained sufficient energy from the electric field. If the number of ion-pairs produced by an electron in moving 1 cm in the direction of the field is defined as α, the following relation can be obtained at constant E/p:

$$i = i_o \exp \alpha d, \qquad (1)$$

where i_o is the externally maintained current at the cathode and α is known as the first Townsend, or the primary, ionization coefficient. $1/\alpha$ thus represents the average distance travelled in the field direction by an electron in creating a new ion-pair. The number of electrons produced by one electron in moving a distance x in the direction of the field is $e^{\alpha x}$ and these electrons constitute an electron avalanche. If conditions are such that the distance d_o the electrons have to travel from the cathode before attaining their equilibrium energy distribution is significant, the expression is modified to

$$i = i_o \exp \alpha (d - d_o) \qquad (2)$$

at constant E/p and constant d_o.

A coefficient which is often found useful is η, which is the number of ion-pairs created by an electron in falling through a potential difference of 1 volt. This leads to the following expression for the anode current, again at constant E/p:

$$i = i_o \exp \eta (V - V_o), \qquad (3)$$

and the constant V_o is similar to the d_o of equation 2. α and η are related by $\eta = \alpha/E$, and η is itself a function of E/p.

Although α is not a unique function of E/p, α/p is and it can be related to E/p from elementary considerations[23]. The energy gained by an electron from the electric field E in a free path l is E e l, where e is the electronic charge. The probability of an electron ionizing a gas atom of ionization potential V_i is taken to be unity when $E\ e\ l \geq e\ V_i$ (figure 3(b) shows that this is, in fact, inaccurate) and zero when $E\ e\ l < e\ V_i$. Then the chance that an electron will cause ionization depends on the probability of the occurrence of free paths greater than the ionizing free path. The following expression may then be obtained:

$$\alpha/p = A \exp\left[-B/(E/p)\right], \qquad (4)$$

where A and B are constants. von Engel[24] gives the values of A and B for a number of gases, indicating the range of E/p over which the equation holds. For helium, when A = 3 ion-pairs cm^{-1} $torr^{-1}$ and B = 34 volts cm^{-1} $torr^{-1}$, the equation is valid for E/p from 20 to 150 volts cm^{-1} $torr^{-1}$. Again, for helium, with A = 3 ion pairs cm^{-1} $torr^{-1}$, but with B = 25 volts cm^{-1} $torr^{-1}$, the equation is valid over $3 \leq E/p \leq 10$ volts cm^{-1} $torr^{-1}$.

If greater accuracy is required, theoretical calculations of α/p must take into account the energy distribution of the electrons, the excitation and ionization probabilities and the energy losses

which occur when electrons collide with gas atoms. In a rigorous treatment of the problem, Heylen and Lewis[16] compared their calculated values of α/p in helium with the experimental results of Townsend and McCallum[25] and with the theoretical values of Dunlop[26] who extended Smit's[19] work. It can be seen from figure 6(a) that good agreement was obtained with Dunlop at low E/p. At higher values of E/p, the calculated values were about 20% less than the experimental ones.

Recent experimental measurements of the primary ionization coefficient in helium have been made by Davies, Llewellyn Jones and Morgan[27] and by Fletcher[28]. Spectroscopically pure helium (supplied by B.O.C. in both cases) was used in these determinations. Fletcher studied the effect of gas purity on α/p. He used the helium with no further purification, purified by activated charcoal at liquid nitrogen temperature and, finally, purified with the aid of cataphoresis techniques. Although Davies, Llewellyn Jones and Morgan used metal taps to prevent grease contamination of the gas, Fletcher used greased stop-cocks throughout. Measurements of α/p were also carried out by Chanin and Rork[29] who used nickel electrodes in a stainless steel system. They also used cataphoresis techniques to help purify the gas. The results of the three investigations are compared in figure 6(b), which shows that there is still some uncertainty as to the true value of α/p, especially at higher values of E/p (greater than, say, 15 volts $cm^{-1}torr^{-1}$).

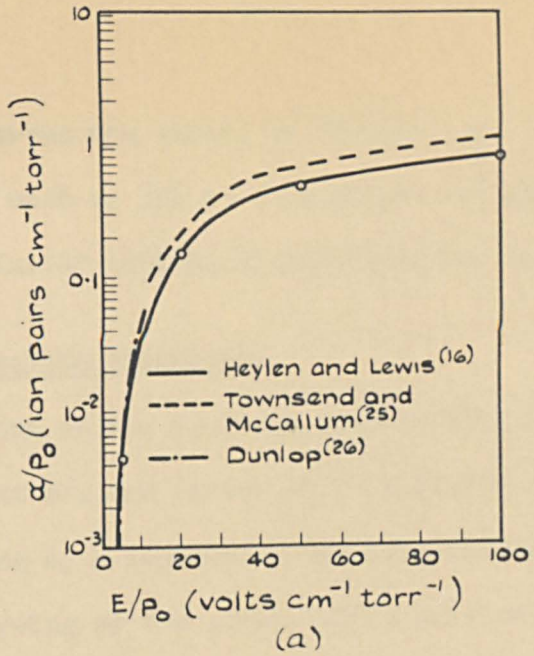

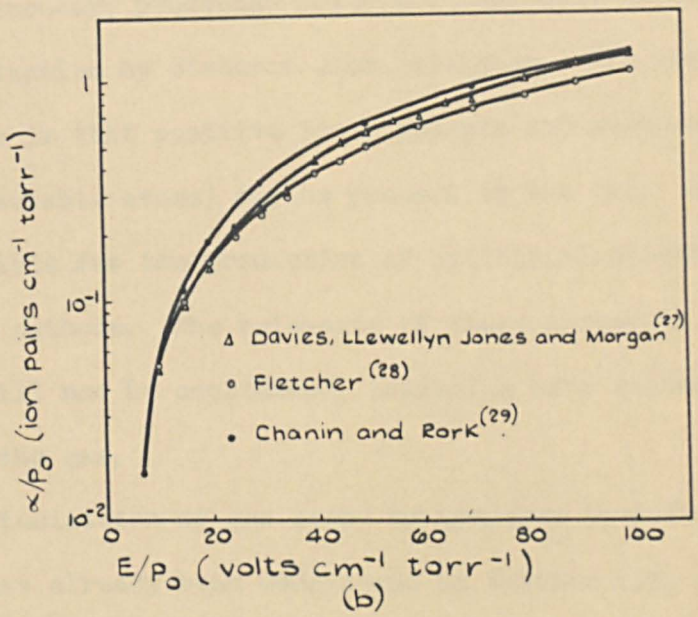

FIG. 6 THE TOWNSEND FIRST IONIZATION COEFFICIENT FOR HELIUM. (a) THEORY (16, 26) COMPARED WITH EXPERIMENT (25); (b) RECENT EXPERIMENTAL DETERMINATIONS.

The disagreement between the values of Fletcher and those of Chanin and Rork (as much as 30% at some values of E/p) is especially surprising, since similar methods of purification were used.

1.4 Secondary ionization processes

It was shown in the previous section that plots of log i against d at constant E/p are linear up to limiting values of d. On further increasing d, a departure from linearity is observed in the form of an upcurving of the graph. At a critical value d_s of the gap distance, the current becomes very large and breakdown of the gap occurs. The upcurving is due to the production of additional charged particles by secondary processes which are dependent on the primary process of ionization by electron-atom collision. One result of the primary process is that positive ions, photons and excited atoms (including metastable atoms) may be present in the gas. Any of these may be responsible for the production of additional electrons in the gas and at the cathode. The relevance of these processes to the present work will now be considered, beginning with secondary ionization in the gas.

The ionization of gas atoms by positive ions and by metastable atoms has already been considered in section 1.2, and it is unlikely that these processes occur in pure gases under discharge conditions similar to those encountered in the present work.

Photo-ionization may take place in the gas if a gas atom absorbs a sufficiently energetic quantum. The energy with which an electron is emitted from the atom is given by $\frac{1}{2} mv^2 = h\nu - eV_i$, where h is Planck's constant and ν is the frequency of the radiation. The maximum probability of ionization or excitation taking place occurs at energies about 0.1 to 1 volt above the minimum energy for the particular process[30]. It is obvious that, for pure gases, the photons emitted in the decay of excited atoms to the ground state have not sufficient energy to ionize the ground-state gas atoms. However, if such a photon is absorbed by a gas atom which has already been excited, ionization may take place. The helium atom has a metastable level at 19.8 volts and its ionization potential is 24.5 volts. So ionization of this metastable atom can be caused by photons with energies exceeding 4.7 volts. Nevertheless, it is generally considered[31] that photo-ionization in the gas is not an important secondary mechanism at low pressures (< 760 torr).

Having seen that secondary processes in the gas are of negligible importance in the present work, secondary processes at the cathode must now be considered. Electron emission from the cathode depends on the surface work function ϕ, which is defined as the minimum work necessary to remove an electron from the solid. The cathode can be considered to be a potential well in which the energy of an electron in the ground state is lower than that of an

electron outside by an amount χ. According to the Fermi-Dirac statistics, the electrons have energies distributed up to a maximum ζ, and $\phi = \chi - \zeta$.

It is possible for positive ions incident on a metal surface to cause the emission of electrons provided $KE_{ion} + eV_i \geq 2\ e\ \phi$, where KE_{ion} is the kinetic energy of the ion. Here the energy would be in ergs if V_i and ϕ were in eV (strictly, a factor of 300 needs to be included for the conversion to e.s.u.). The factor 2 appears in the relationship because, for each electron emitted from the surface, another escapes to neutralize the ion. The process is characterized by the coefficient γ, which is the number of electrons emitted from the cathode by positive ion action per ionizing collision in the gas. The coefficient γ_i is also used and is the number of electrons emitted from the cathode per incident positive ion, and $\gamma_i = \gamma$.

The usual method by which a positive ion causes the emission of an electron is by the Auger process. An electron from the conduction band of the metal neutralizes an ion near the surface and the energy released by the electron is then absorbed by a second electron in the metal, where the wave functions of the electrons overlap. Providing that the energy transferred to the second electron is sufficient, and its momentum is in the right direction, it can escape from the metal. Hagstrum[32] studied the interaction of helium and other ions with atomically clean tungsten (figure 7(a)). He concluded that the small dependence of γ_i on the ion kinetic energy showed that the ejection

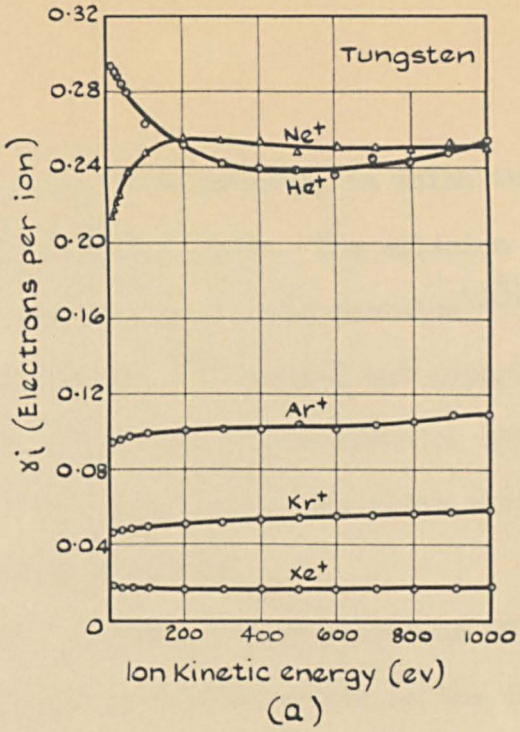

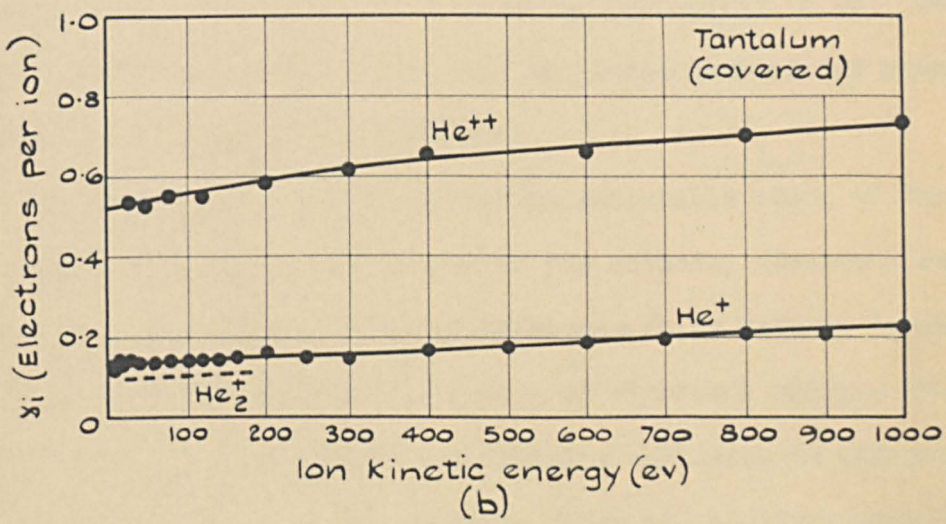

FIG. 7 TOTAL ELECTRON YIELD AS A FUNCTION OF ION KINETIC ENERGY. (a) SINGLY CHARGED IONS OF THE NOBLE GASES ON ATOMICALLY CLEAN TUNGSTEN; (b) HELIUM IONS ON GAS-COVERED TANTALUM.

process was the single-stage Auger process, in which the ion kinetic energy plays only a very secondary role. The emission due to He^+, He^{++} and He_2^+ incident on gas-covered tantalum[33] is shown in figure 7(b). Propst and Lüscher[34] carried out experiments for He^+ incident on tungsten, which was either clean or covered with hydrogen or nitrogen. Their results for the clean surface agreed well with those obtained by Hagstrum.

Because of the exponential multiplication of electrons across the gap, the majority of the particles active in the discharge are created near the anode. As ordinary excited atoms have a short ($\sim 10^{-8}$ seconds) lifetime, it is unlikely that they reach the cathode in sufficient numbers to be of importance. On the other hand, metastable atoms have a relatively long lifetime (extending to 10^{-1} sec and above, depending on the conditions) and large numbers can reach the cathode under favourable conditions.

Providing that the energy of the metastable state of the atom is higher than the work function of the cathode, electrons may be emitted from the surface. The coefficient ε/α is used to describe this process and is defined as the number of electrons emitted from the cathode by metastable action per ionizing collision in the gas. Metastable atoms diffuse to the cathode, while the positive ions drift to the cathode under the influence of the applied electric field. So the metastable process is the slower acting of the two. Diffusive loss of the metastable atoms can be large and many of them can be

destroyed in the gas. If metastable action is of importance, it should be indicated by a decrease in the generalized secondary coefficient (section 1.5) as the gap distance increases at constant E/p. The number of electrons emitted from the cathode per incident metastable atom is defined as γ_m. Not surprisingly, the condition of the cathode surface can have a large effect on γ_m. If the excess potential energy $V_{met} - \phi$ (where V_{met} is the energy of the metastable state) is large, as is the case with helium metastable states in combination with most surfaces, then γ_m is large. Dorrestein[35] has given experimental values of γ_m for helium metastable atoms incident on a platinum surface covered with a gas film. He found that, for the 2^3S metastable atom, $\gamma_m = 0.24$ and, for the 2^1S atom, $\gamma_m = 0.40$.

As with the other active particles, the majority of the photons in a discharge are produced near the anode. About half of these photons will be lost to the anode. Some of the photons directed towards the cathode will be lost from the sides of the gap and others will be absorbed by the gas atoms.

It is possible for quanta emitted by the gas atoms to be delayed in their passage through the gas by being absorbed and, after a short time, re-emitted by other atoms. Once a photon reaches the cathode an electron may be emitted if $h\nu \geq e\phi$. The coefficient describing this process is δ/α, which is defined as the number of electrons emitted from the cathode by photons from the discharge per ionizing collision in the gas. In fact, only a fraction of the expected

number of electrons is emitted depending on the nature of the surface and on the wavelength and polarization of the radiation. The photoelectric yield γ_p is the number of electrons emitted per incident quantum. Values for the photoelectric yield of a well-degassed nickel surface have been given by Kenty[36]. The surface was illuminated by the short wavelength radiation given out by the positive columns of helium, neon and argon. Kenty's results for nickel and other surfaces are given in figure 8.

1.5 The second Townsend ionization coefficient and breakdown

By considering the secondary processes to act simultaneously, the following expression for the anode current can be obtained:

$$i = \frac{i_o \exp \alpha d}{1-(\omega/\alpha)(\exp \alpha d-1)} \qquad (5)$$

at constant E/p. If d_o (section 1.3) is significant, then d may be replaced by $(d - d_o)$. ω/α is a generalized secondary coefficient and is the linear sum of the coefficients already considered, hence

$$\omega/\alpha = \gamma + \delta/\alpha + \varepsilon/\alpha + ... \qquad (6)$$

When processes other than those described by these three coefficients are of importance, the relevant coefficients must be included in ω/α. The coefficient ω/α is the second Townsend ionization coefficient or the secondary ionization coefficient. When ω/α reduces to zero, equation 5 becomes that given when the primary process acts alone.

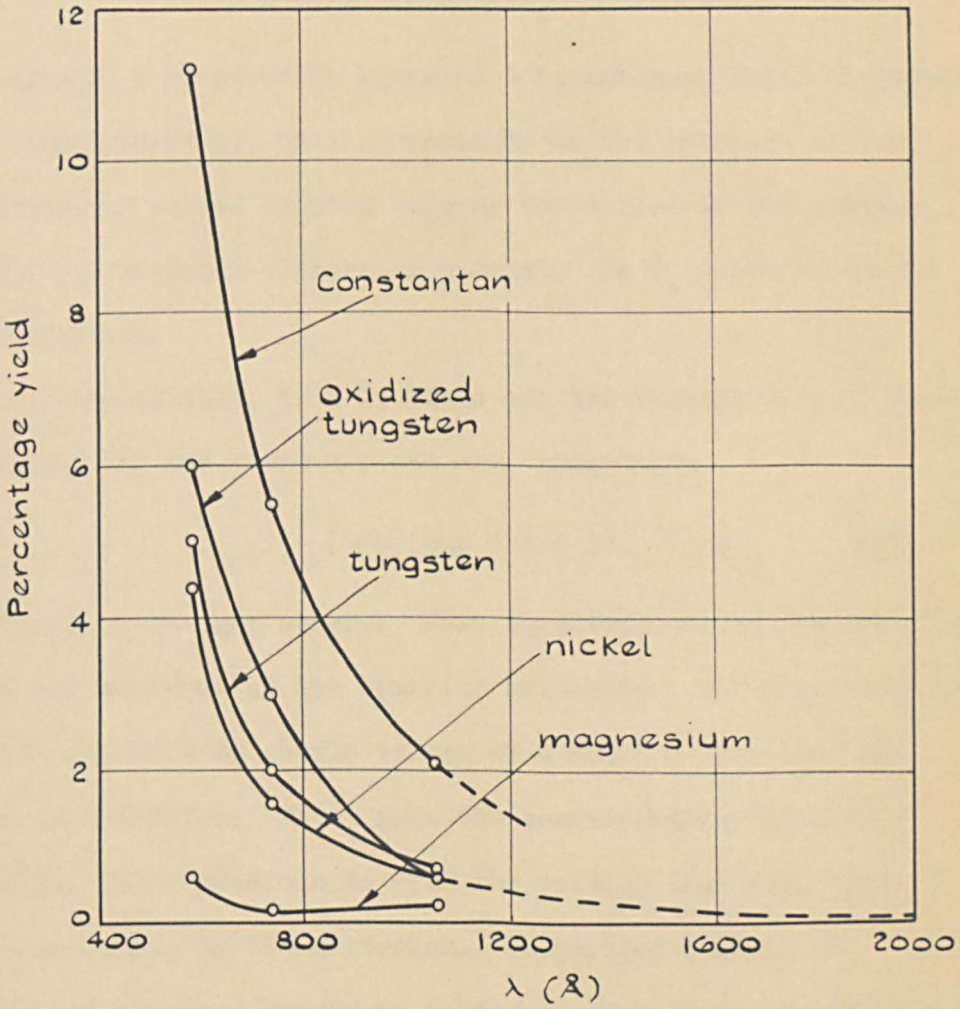

FIG. 8 PHOTOELECTRIC YIELDS AS A FUNCTION OF WAVELENGTH.

If the gap distance is increased keeping E/p constant, hence keeping α/p and ω/α constant, a value d_s is reached such that

$$1 - (\omega/\alpha)(\exp \alpha d_s - 1) = 0$$

and the current i as given by equation 5 is mathematically indeterminate. Experimentally, this corresponds to the increase of the anode current to values limited only by the nature of the voltage supply and the external electrical circuit. So d_s is known as the sparking distance.

Alternatively, if d is fixed and the voltage is increased, so increasing E/p and hence α/p and ω/α, eventually

$$1 - (\omega/\alpha)(\exp \alpha d - 1) = 0 \qquad (7)$$

and breakdown of the gap occurs. This equation defines the onset of breakdown and is known as the sparking criterion. For a given value of d, it is possible to obtain values of α and ω/α such that the criterion is satisfied. Then, from the corresponding value of E/p (= V/pd), it is possible to find the voltage that will give breakdown according to the criterion. Comparison between the calculated and observed breakdown voltages gives close agreement for short gaps at reduced pressures, so establishing the validity of the criterion.

At $(\omega/\alpha)(\exp \alpha d - 1) < 1$, that is, below breakdown, the current is not self-maintained and i ceases if i_o is cut off.

However, at breakdown and above, the discharge is self-maintained.

Physically, $(\omega/\alpha)(\exp \alpha d - 1) = 1$ is a replacement condition. This can easily be seen if, for simplicity, the γ-process alone is considered. The criterion (equation 7) then becomes $\gamma(\exp \alpha d - 1) = 1$. One electron leaving the cathode will cause the production of $(\exp \alpha d - 1)$ positive ions as it crosses the gap. The number of secondary electrons produced by these positive ions is $\gamma(\exp \alpha d - 1)$. If this is equal to unity the original electron is replaced. Thus the process is regenerative and the discharge is self-maintained.

If $(\omega/\alpha)(\exp \alpha d - 1) > 1$, the current increases in time and is only limited by the nature of the external electrical circuit. The greater the amount by which $(\omega/\alpha)(\exp \alpha d - 1)$ exceeds unity, the more rapid is the current growth.

Since α/p and ω/α are functions of E/p, we may write $\omega/\alpha = F_1 (V/(pd))$ and $\alpha/p = F_2 (V/(pd))$. The breakdown criterion then becomes:

$$1 - \left\{ F_1(V/(pd)) \right\} \left\{ \exp\left[F_2 (V/(pd))\ pd \right] - 1 \right\} = 0,$$

and it is clear that, for a given value of pd, there is a particular value of the breakdown potential V_s. Thus, $V_s = F(pd)$ and the breakdown potential is a function of the product pd alone. This relationship is known as Paschen's law.

Experimental determinations of the breakdown potential obey this relation. A typical Paschen curve, obtained by Townsend and

McCallum for helium[25], is given in figure 9. The minimum in the curve is to be expected from elementary considerations. The number of atoms in the gap is proportional to pd. At low pressures the electron mean free path is large and few electron-atom collisions take place. To produce sufficient ionization for breakdown to occur, the voltage has then to be increased as p decreases, d remaining constant. At large p, the electron mean free path is small and few electrons gain enough energy over λ_e to cause ionization. The ionization probability has to be increased to give breakdown and this is effected by increasing the voltage. So a minimum is predicted in the Paschen curve.

McCallum and Klatzow[37] observed deviations from Paschen's law in neon and in argon. As d increased (p being adjusted to keep pd constant) the sparking potentials in neon and argon increased. However, no such variation was observed on carrying out similar experiments in helium. They explained the difference in the behaviour of the gases on the basis of the rate of electron diffusion perpendicular to the field direction. In neon and in argon this rate is much greater than in helium. Thus, in these gases, as d increases, electrons are lost in increasing numbers from the sides of the gap. For helium, it was unlikely that this effect was appreciable, so the sparking potential remained constant as d increased.

From the sparking criterion, it can be seen that V_s depends on ω/α, so V_s should be dependent on the nature of the cathode.

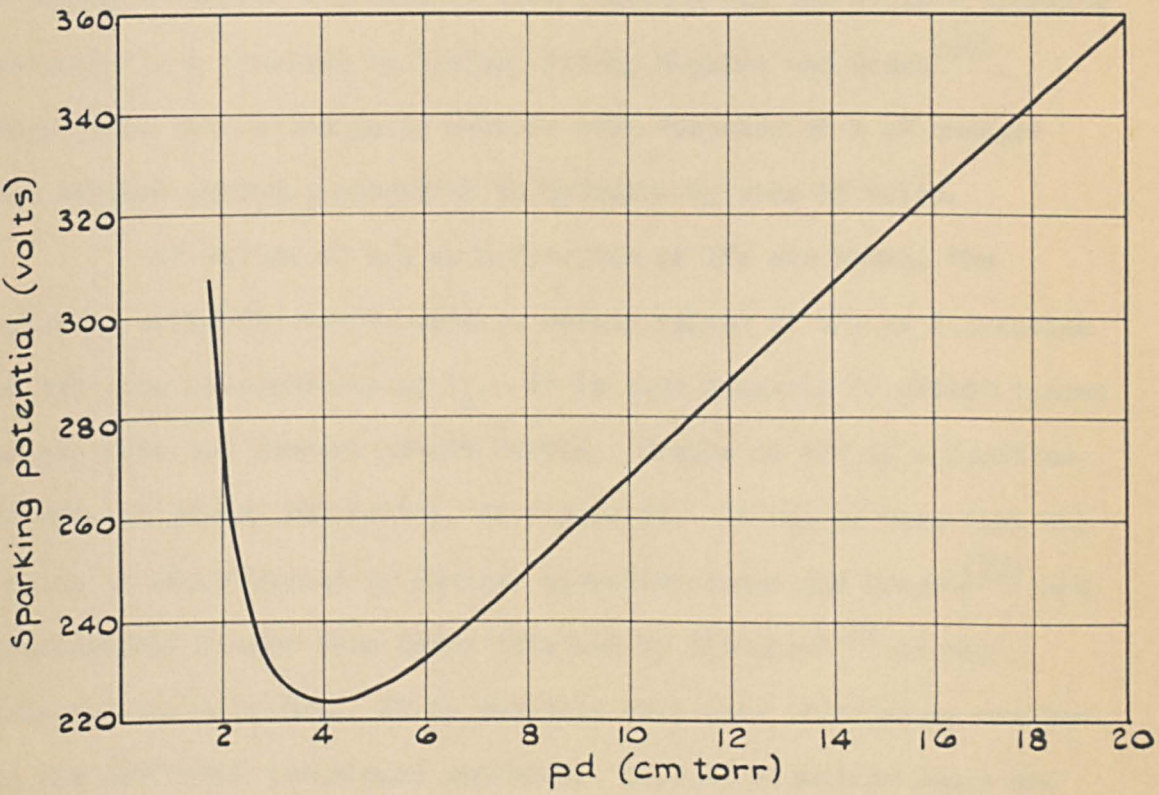

FIG. 9 PASCHEN CURVE IN HELIUM OBTAINED BY TOWNSEND AND McCALLUM.[25]

This was confirmed by Llewellyn Jones[38] in his experiments on six different cathode materials in hydrogen. Furthermore Llewellyn Jones and Davies[39] observed large changes in the minimum sparking potential as a result of the deposition of films of alien metal on the cathode. A relation between the cathode work function and the minimum sparking potential was obtained by Davies, Fitch, Hopkins and Gozna[40]. They found that a change in cathode work function of 1 eV changed the minimum sparking potential in hydrogen by some 55 volts.

If values of α/p as a function of E/p are known, the sparking criterion may be used to obtain values of ω/α as a function of E/p from measurements of V_s. It is also possible to obtain values of ω/α from the current growth curves. Graphs of ω/α as a function of E/p are given, for helium, in figure 10. It can be seen that the values of ω/α obtained by Davies, Llewellyn Jones and Morgan[27] are considerably higher than those obtained by Fletcher[28] at any selected value of E/p. It is possible that this discrepancy was due to the different techniques employed. Davies, Llewellyn Jones and Morgan used silver electrodes, whereas Fletcher used gold films deposited on glass substrates.

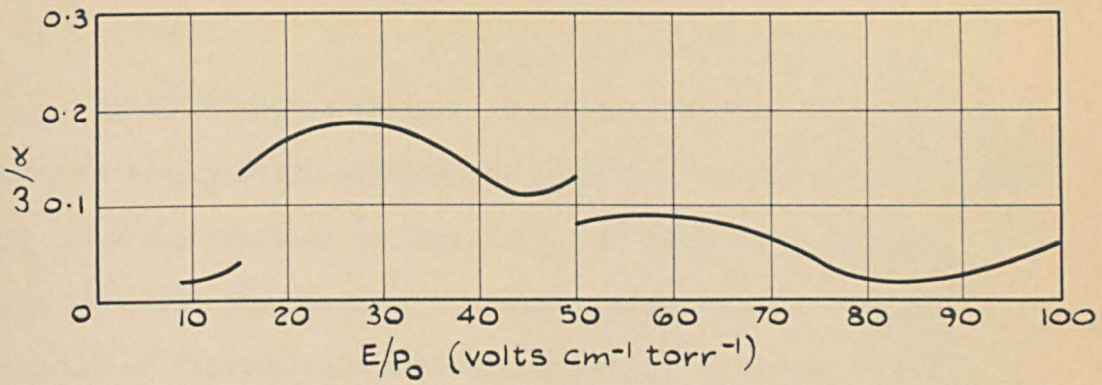

(a)

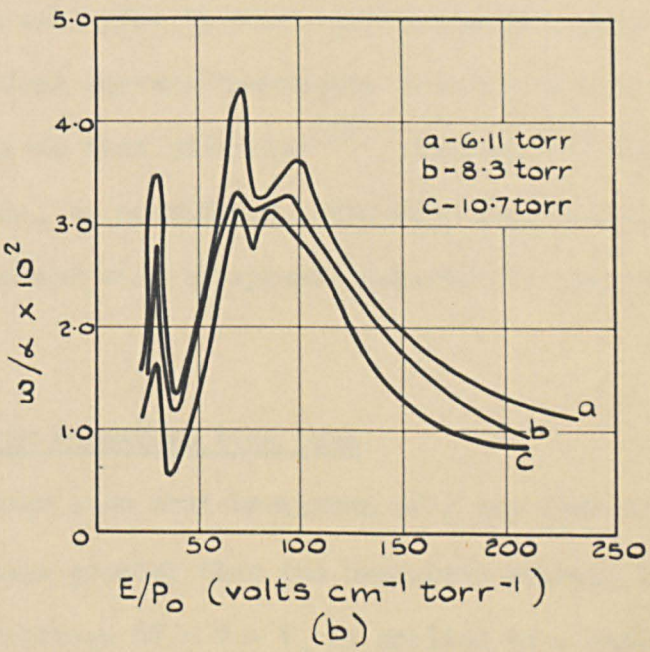

(b)

FIG. 10 EXPERIMENTAL VALUES OF ω/α AS A FUNCTION OF E/P_0. (a) DAVIES, LLEWELLYN JONES AND MORGAN[27]; (b) FLETCHER[28] AT DIFFERENT VALUES OF PRESSURE.

Chapter 2

THE TEMPORAL GROWTH OF IONIZATION

In the previous chapter, the discussion was largely confined to steady state conditions. However, the ionization currents flowing in a gas can vary in time. If, for example, a constant voltage less than the sparking potential is applied to a gap and a short pulse of initiating electrons introduced by an interrupted beam of ultra-violet light, transient currents will flow in the gap. Alternatively, when the photocurrent is kept constant and a voltage greater than the sparking potential is applied to the gap, the ionization current will grow in time until breakdown occurs.

As transient current techniques were not used in the present study, work similar to that of Molnar[41], Hornbeck[42] and Varney[43] will not, in general, be considered. However, some transient current theory may be discussed when it appears relevant to the present problem.

2.1 Statistical and formative time lags

It has been seen that breakdown of a gap does not take place immediately a voltage greater than the breakdown voltage is applied to it. If an overvoltage $\Delta V = V - V_s$ is applied to a gap, the ionization processes can only begin when an electron appears in the gap to initiate them. The delay between the application of the overvoltage and the appearance of the initiatory electron is the statistical

time lag t_s. The current flowing in the gap then increases until breakdown occurs, which is usually indicated by the start of the collapse of the gap voltage. The time taken for the ionization processes to generate sufficient current to cause breakdown is the formative time lag t_f. This is the time that elapses between the appearance of the initiatory electron and breakdown. The total time lag t is given by the sum $t_s + t_f$.

The statistical time lag can be obtained by measuring the total time lag t, since, in practice, t_f is often very much smaller than t_s. If t_f is required, t_s must be reduced to zero. This is usually effected by adequate ultra-violet illumination of the cathode.

The formative time lag obviously depends on the ionization processes which, in turn, depend on E/p. So it is usual to specify the value of E/p in connection with measurements of t_f. An indication of the manner in which t_f depends on the percentage overvoltage, $\Delta V\% = 100\ (V - V_s)/V_s$, can easily be obtained. If, for given values of p and d, $\Delta V\%$ is increased, E/p must also increase. This means that α and ω/α increase, and faster time lags ensue as $\Delta V\%$ increases.

2.2 Early theories of the current growth

Perhaps the earliest treatment of temporal growth was carried out by Steenbeck[44], who derived the equations for the growth of a discharge using the first and second ionization coefficients. He assumed that the current grew exponentially with time about a certain

average build-up time τ, which was set as the characteristic time constant of the process. The current i flowing at time t after the voltage application was given by $i = i_o \exp(t/\tau)$, τ being associated with the formative time lag. He assumed that the γ-process was the only source of secondary electrons and obtained the following relation from which τ could be calculated:

$$\frac{\gamma\alpha}{\alpha - 1/(\tau W)} \exp\left\{\left[\alpha - 1/(\tau W)\right] d - 1\right\} = 1, \quad (8)$$

where $1/W = 1/W_+ + 1/W_- \simeq 1/W_+$ and W_+ and W_- are the positive ion and electron drift velocities.

It can be seen that equation 8 reduces to the sparking criterion (equation 7) when τ is large and $1/(\tau W)$ approaches zero. In this treatment of the problem, space charge distortion of the field was neglected.

Schade[45] approached the problem by first obtaining four expressions for the electron and positive ion currents at the cathode and at the anode. He then considered that, for a small overvoltage, α changed to $\alpha + \delta\alpha$ while γ remained constant. Using equation 4 for α/p, he gave the following approximate expression for the formative time lag at a given pressure:

$$t_f = \left[a/(V - V_s)\right] \exp(-b/V). \quad (9)$$

The constants a and b could be obtained by matching a curve drawn from equation 9 to two experimental points. Schade's measurements

in neon supported his view that the formative time was given by an expression of the form of equation 9.

A simple treatment was given by Druyvesteyn and Penning[46], who considered positive ion action at the cathode to be the only secondary process taking place. One ionization cycle was considered to be completed in a time approximately equal to the transit time t_i of a positive ion moving from anode to cathode. Each of the electrons leaving the cathode produces $\exp(\alpha d) - 1$ ion-pairs in travelling to the anode. The mean number of electrons liberated at the cathode by the ions created by one primary electron is $\gamma(e^{\alpha d} - 1) = M$ where M is the multiplication factor. Then the photocurrent at the cathode i_o (corresponding to n_o electrons per second) is assumed to become $i_o(1 + M)$ at time t_i and $i_o(1 + M + M^2)$ at $2t_i$. At $t_f = nt_i$ the electron current at the cathode is $i = i_o(M^{n+1} - 1)/(M - 1)$, from which the following expression for t_f may be obtained

$$t_f = t_i \frac{\log\left[(M - 1)\, i/i_o\right]}{\log M}. \qquad (10)$$

So far the only secondary process considered has been the γ-process. The secondary process of electron emission from the cathode by photons produced in the gas was included in Bartholomeyczyk's solution of the problem[47]. Here the cathode was considered to be exposed to constant ultra-violet illumination and, at time zero, the

potential difference of the electrodes was suddenly increased and then maintained constant. Ionization of the gas atoms was assumed to be the result of the α-process alone. Then, by considering an elemental volume and balancing the increase in electrons and ions due to the α-process and the decrease due to the net movement of charge, the important continuity equations were obtained

$$\frac{1}{W_-}\frac{\partial i_-}{\partial t} = -\frac{\partial i_-}{\partial x} + \alpha i_- \qquad (11)$$

$$\frac{1}{W_+}\frac{\partial i_+}{\partial t} = \frac{\partial i_+}{\partial x} + \alpha i_- , \qquad (12)$$

where i_- and i_+ are the electron and positive ion currents. The boundary conditions to which equations 11 and 12 were subject were taken to be

$$i_-(0, t) = \gamma i_+(0, t) + \delta \int_0^d i_-(x, t)\, e^{-\mu x}\, dx, \qquad (13)$$

$$i_+(d, t) = 0. \qquad (14)$$

From these equations, Bartholomeyczyk obtained the following approximate expression for the current amplification:

$$i_-(x, t) \exp(-\alpha x) = C \exp\left[\lambda (t - x/W_-)\right]. \qquad (15)$$

Here C is a constant and λ is the real root satisfying F(d) = 0, where

$$F(x) = 1 - \frac{\alpha\gamma}{\phi}(e^{\phi x} - 1) - \frac{\delta}{\psi}(e^{\psi x} - 1),$$

$$\phi = \alpha - \lambda/W,$$

$$\psi = \alpha - \mu - \lambda/W_{-},$$

and $$1/W = 1/W_{-} + 1/W_{+} .$$

This solution was later criticized and modified by Davidson[48] (see section 2.3).

The effect of metastable atoms on the current growth was taken into account by Engstrom and Huxford[49]. Although their theory was evolved for application to experiments on transient currents, the main features are of interest. They defined γ_m to be the number of secondary electrons per positive ion created in the gas which are released by metastable action at the cathode. If α_m is the number of metastable atoms produced per cm per electron, α_m/α is the ratio of the number of metastables to positive ions produced in the discharge. Only a fraction f of the metastables produced diffuse to the cathode where each metastable atom releases an average of ε electrons. Then, $\gamma_m = \varepsilon f \alpha_m/\alpha$ and the steady state Townsend equation becomes:

$$i = \frac{i_o \exp \alpha d}{1 - (\gamma + \varepsilon f \alpha_m/\alpha)(\exp \alpha d - 1)} .$$

For metastable atoms reaching the cathode by diffusion, the probability of arrival at time t per unit time is closely approximated by

$$P(t) = \frac{1}{\tau_o} \exp\left(-\frac{t}{\tau_o}\right) \qquad \text{for } t \geq 0 \qquad (16)$$

and $P(t) = 0$ for $t < 0$.

Here τ_o is the average interval between the creation in the gas (at $t = 0$) and arrival at the cathode for those metastables which reach the cathode. The differential equation describing the diffusion of metastables is

$$\frac{\partial m(x, t)}{\partial t} = D \frac{\partial^2 m(x, t)}{\partial x^2},$$

where $m(x, t)$ is the linear density of metastable atoms at distance x from the cathode at time t and D is their coefficient of diffusion. The spatial distribution of metastable atoms, when created, is assumed to be $m(x, 0) = 0$ for $x < x_m$ and $m(x, 0) \propto \exp \alpha(x - x_m)$ for $x_m \leq x \leq d$, where x_m is the distance which an electron must travel in the direction of the field to obtain the energy of excitation of the metastable state. Engstrom and Huxford then gave the following solution of the diffusion equation:

$$\tau_o = \frac{d^2}{12D}\left[1 + \frac{2}{15}\alpha d + \frac{1}{180}\alpha^2 d^2 + \ldots. + \frac{x_m}{d}\left(2 - \frac{2}{5}\alpha d - \frac{1}{45}\alpha^2 d^2 + \ldots.\right) + \frac{x_m^2}{d}\left(-1 + \frac{2}{5}\alpha d + \frac{1}{36}\alpha^2 d^2 + \ldots.\right) + \ldots\ldots\ldots\ldots\ldots\ldots\right]. \quad (17)$$

Thus the probable delay time of the arrival of the metastable atoms is known in form from equation 16 and in magnitude from equation 17.

The following expression was then obtained for the form of the lagging current response to a constant photoelectric current initiated at time t = 0:

$$i_{rise}(t) = 1 - (1 - i_a) \exp\left[- (i_a/\tau_o)\, t \right], \quad (18)$$

where the maximum equilibrium current was referred to as unity. If the photoelectric source was cut off at $t = T$ ($t^1 = 0$) when the rising current lacked saturation by an amount i_c, the falling characteristic could be represented by:

$$i_{fall}(t^1) = (1 - i_b - i_c) \exp\left[- (i_b/\tau_o)\, t \right]. \quad (19)$$

Here i_a and i_b represented the fraction of non-lagging current for the rise and for the fall characteristic respectively and it could be shown that $i_a = i_b$. Equations 18 and 19 could be used in the analysis of the time lag data.

2.3 Theoretical approaches to the problem made since 1950

Kachickas and Fisher[50] obtained an expression for the formative time lag by considering that the only secondary process of significance was the δ/α-process. They assumed that all the photons produced in the gas are created very near the anode and that the time for a photon to cross the gap is negligible. The number of photoelectrons produced at the cathode per ion-pair created in the gas was defined by them as γ_p. A single electron starting from the cathode at time zero gives rise to $\gamma_p^n (\exp \alpha d - 1)^n$ photoelectrons

from the cathode at time nt_e, t_e being the electron transit time and n the number of electron crossings. It was assumed that a spark occurs when the number of electrons liberated from the cathode reaches N, this number being the result of a single electron emitted at an earlier time. Then

$$\gamma_p^n \ (\exp \alpha d - 1)^n = N \qquad (20)$$

is the condition for a spark to occur after n electron transits. Here electrons liberated from the cathode by an external source at times later than zero were not taken into account. This was considered to be justified since the experimental results showed that the time lags were independent of i_o.

The breakdown criterion (equation 7) in this case is

$$\gamma_p \ (\exp \alpha_s d - 1) = 1 , \qquad (21)$$

where α_s is the value of α at the threshold. Now $\exp \alpha_s d \gg 1$ and so equations 20 and 21 give:

$$\exp (nd \ \Delta\alpha) = N \qquad (22)$$

where $\Delta\alpha = \alpha - \alpha_s$. Since $nd = t_f W_-$, equation (22) becomes:

$$t_f = \frac{\log N}{W_- \Delta\alpha} . \qquad (23)$$

If positive ion action at the cathode is considered instead of photon action, equation 23 shows that the time lags would be longer by the ratio of the velocities of electrons and positive ions. The theory leading to equation 23 was used by Kachickas and Fisher to

explain the formative times they obtained in nitrogen at pressures from 150 to 700 torr.

In contrast to the above approach, Davidson[48] returned to Bartholomeyczyk's continuity equations (equations 11 and 12). The boundary conditions used by Bartholomeyczyk were inadequate, since the photocurrent i_o was not included in the boundary condition for $i_-(0, t)$ (equation 13). Moreover, Davidson pointed out that Bartholomeyczyk's solutions are not accurate, since they do not reduce at $t = 0$ to the charge distributions actually present at that time. However, Davidson showed that, if λ is given Bartholomeyczyk's value, and if

$$P = 1 - \gamma\,(e^{\alpha d} - 1) - \frac{\delta}{\alpha - \mu}\left[e^{(\alpha-\mu)d} - 1\right],$$

a short calculation confirms that

$$i_-(x, t)\exp(-\alpha x) = i_o/P + C\exp\left[\lambda\,(t - x/W_-)\right], \qquad (24)$$

together with an accompanying expression for $i_+(x, t)$, satisfies the continuity equations and the corrected boundary conditions. The constant C may be given a value which gives approximate agreement with the initial conditions. Thus, if the initial value of $i_-(0, t)$ is c, the solution can be made to have that initial value of $i_-(0, t)$ by taking C as $c - i_o/P$.

Davidson's approximate solution (equation 24) still does not satisfy the initial conditions completely, giving any prescribed initial distribution of positive and negative charge in the whole

range x = 0 to d. F(d) = 0 (see Bartholomeyczyk's solution) has, in addition to the real root, an infinite number of complex roots. So the last term of equation 24 must be replaced by a summation containing these various λ's and with C's determined by the initial conditions. The accurate solution is then obtained in the form of series expressions for $i_-(x, t)$ in two parts: the value which it would have if the initial charge distribution were absent and the value it would have if the constant generation i_o were absent. From these series expressions, it is possible to calculate the electron or ion density at any point x in the gap at any time t after the production of the initial electrons.

In a later paper, Davidson[51] gave an alternative form of his exact solution which is more convenient for discussing the earliest stages of the growth. He also subsequently explained his proof of the exact solution more fully and gave new forms of the solution[52].

The continuity equations (equations 11 and 12) provided Auer[53] with a convenient starting point for his discussions of current growth. In the most recent of the three papers referred to, he considered only positive ion and photon action at the cathode and neglected any space charge distortion of the field. If, initially, no charge is present in the gap, the solutions of equations 11 and 12 are subject to the boundary conditions: $i_-(0, t) = f(t)$, $i_+(d, t) = 0$ and $f(t)$ is zero for $t < t_o$. Here t_o is the starting time, which is later

set equal to zero. The function f(t) is specified through the secondary mechanisms and is the cathode electron current density.

For photon and positive ion secondary mechanisms only, the Townsend model gives:

$$f(t) = i_o(t) + \gamma\, i_+ (0, t) + \delta \int_o^d i_- (x, t)\, dx \quad (25)$$

and $i_o(t) = f(t) = 0$ for $t < 0$.

By considering general solutions of the continuity equations in conjunction with equation 25, the cathode current density is given by:

$$f(t) = i_o(t) + \alpha\gamma W \int_{t-\bar{t}}^{t} e^{\alpha W(t-s)} f(s)\, ds$$

$$+ \delta W_- \int_{t-t_e}^{t} e^{\alpha W_-(t-s)} f(s)\, ds, \quad (26)$$

where $t_e = d/W_-$ = electron transit time, $t_+ = d/W_+$ = positive ion transit time and $\bar{t} = d/W = t_e + t_+$.

Once a solution of equation 26 is obtained, the current characteristics of the gap are fully specified. For mathematical convenience, Auer considered only one secondary mechanism to be operative. Two solutions could then be obtained, corresponding to two different sets of experimental conditions. Either the avalanche process

starts at t = 0 with a unit pulse of charge, no other charge entering the system from external sources at later times, or the cathode is subject to constant illumination, resulting in a steady i_o.

Bandel[54] also began his discussion with the continuity equations (equations 11 and 12) and considered that the α, γ and δ/α processes were the only relevant mechanisms. An expression for $i_-(0, t)$ was obtained which, for $t > d/W$, reduced to Davidson's solution[48]. To explain the disagreement between theory and experiment in air at high pressures ($\sim$ 700 torr), Bandel considered the possibility of the photon action being delayed, for example, by the entrapment of resonance radiation. However, he suggested that a metastable process having a lifetime of the right order could account for the observed discrepancy. Such a process is the three-body collision, in which a metastable atom collides with two normal gas atoms to give an excited molecule and a normal atom. The excited molecule then falls to the ground state with the emission of a photon. However, no definite conclusions were given. In an attempt to explain the hyper-exponential increase in current observed just before breakdown, Bandel concluded with considerations of the field distortion due to positive ions.

Miyoshi[55] also approached the problem by considering the continuity equations. As before, the only secondary processes considered were those of positive ion and photon action at the cathode. A solution was given in three forms corresponding to times shorter than the

electron transit time t_-, times longer than t_- but shorter than the resultant transit time $\bar{t}$ $(= t_- + t_+)$ and times longer than the resultant transit time. The calculations were carried out for a constant i_o and an instantaneous release of photoelectrons at the initial time. Davidson later showed[52] that one of his solutions was an accurate form of an approximate solution proposed by Miyoshi. Miyoshi[56] used his analysis to calculate the development of space charge in the transient Townsend discharge. He suggested that the formative time is a preliminary stage for developing the anode region of the glow discharge in the photon predominant case and for developing the cathode region of the glow discharge in the positive ion predominant case.

Menes[57] essentially used Bartholomeyczyk's simple exponential build-up theory to analyse his results for argon. He considered only the case where the secondary mechanism is due to positive ions or to a simple delayed-photon process. For positive ion action at the cathode, the boundary conditions to which equations 11 and 12 are subject are: $i_+ (d, t) = 0$ and $i_- (0, t) = \gamma_i\, i_+ (0, t)$. A definition of γ_i is given in section 1.4. For delayed photon action, it was assumed that photons are emitted from an excited state having a mean lifetime τ and that they proceed unhindered, a fraction g arriving at the cathode. The number of excited states created in the discharge is given by $\bar{\delta}$ which is the number of excitations per electron per cm drift. Then the second boundary condition is replaced

by:

$$i_{-}(0, t) = \gamma_p \overline{\delta} g \int_0^d \int_{-\infty}^{t} e^{-(t-t^1)/\tau} i_{-}(x, t^1)\, dt^1\, dx$$

where γ_p is as defined in section 1.4.

Menes then assumed solutions which are exponential in time and of the form: $i(x, t) = j(x) \exp \lambda t$, where λ is the growth constant of the discharge. Expressions can then be obtained for the rate of build-up λ in terms of the parameters of the discharge. For positive ion action:

$$\frac{\gamma_i \alpha}{\alpha - \lambda/W} \left[e^{(\alpha - \lambda/W)d} - 1 \right] = 1$$

and for delayed photon action:

$$\frac{\gamma_p g \delta}{(1+\lambda\tau)(\alpha - \lambda/W_{-})} \left[e^{(\alpha - \lambda/W_{-})d} - 1 \right] = 1.$$

Setting $\tau = 0$ in the second equation gives the case of undelayed photon action.

Having measured λ, it is possible to obtain values of τ from these expressions. Menes compared values of τ for argon with both calculated imprisonment times for resonance radiation and delay times for molecular radiation (see discussion of Bandel's work) as observed by Colli[58]. He observed that the imprisonment times were of the right magnitude to explain the build-up rates obtained. The

Colli-process delay times were in fair agreement with data at higher pressures (~ 500 torr), but at lower pressures (~ 50 torr) were too short to explain the observed build-up rates.

Recently Davies, Evans and Llewellyn Jones[59] gave a numerical method which enabled the growth of the discharge to be traced from its initiation to the transition to the glow discharge involving fields distorted by space-charge. Again only the α, γ and δ/α processes were considered. The theoretically predicted curves of voltage collapse agreed with those observed experimentally in hydrogen when the field distortion was taken into consideration.

2.4 Metastable atoms and the temporal growth

The first accurate mathematical treatment to include metastable action at the cathode was given by Davidson[60]. He also dealt with the secondary cathode process due to fluorescent light, in which electrons are released from the cathode by photons which have been repeatedly absorbed and re-emitted by the gas atoms. These photons can be considered to move through the gas by a diffusion process. Finally, Davidson considered the general case where, in addition to these diffusion processes, there is secondary action at the cathode due to positive ions and unscattered photons.

At first, Davidson assumed that the secondary processes only occur at the cathode and that they depend on the diffusion of (a) metastable atoms and (b) repeatedly scattered photons. The formulae used

to represent the two cases resemble each other and conciseness is gained by taking advantage of this resemblance. The diffusion equation satisfied by the active particles (metastables and photons) is written:

$$\frac{\partial n(x,t)}{\partial t} = D \frac{\partial^2 n(x,t)}{\partial x^2} + \alpha_1 e^{\alpha x} i_- (t - \frac{x}{W_-}) - \frac{n(x,t)}{\tau_1} . \tag{27}$$

Here $n(x,t)$ is the spatial density of the particles, α_1 is the number of active particles an electron creates in travelling unit distance in the x-direction and $1/\tau_1$ is the fraction of active particles in any region which are destroyed per unit time by collisions with unexcited atoms. In case (a), the diffusion coefficient D is given by $D = 1/3\ \ell\ \bar{v}$, where ℓ is the mean free path for metastable atoms and $\bar{v}$ is their mean kinetic velocity. In case (b), D is given by:

$$D = \frac{\ell^2}{3\ (\tau + \ell/c)(1-F^1)} .$$

This is obtained by considering the fraction of the free photons which become bound per unit time to be c/ℓ, where c is the velocity of light and ℓ is the collision mean free path for photons. On re-emission, they retain a fraction F^1 of their original resultant momentum.

With the correct boundary conditions, equation 27 can be solved to obtain an expression for the cathode current as a function of time. Davidson obtained his solution in two forms. One form is

valid at all times, the other is valid when t/T is a fairly small fraction, say 1/4, and is of limited interest (T is the average time an active particle takes to diffuse to the cathode). Here we shall only consider the solution which is valid at all times.

The equation for the electron current density at the cathode i_- may be written:

$$\frac{i_-}{i_o} = \frac{1}{1-(\gamma/\alpha)(\exp \alpha d - 1)} + \frac{2(\lambda^2-\alpha^2)(1-\exp[-2\lambda d])\exp D\lambda^2 t}{\lambda \left(\frac{\partial \theta}{\partial z}\right)_\lambda} . \tag{28}$$

λ is the real value satisfying $\theta(z) = 0$, i.e. satisfying:

$$(\alpha-z)\left[(\alpha+z)F + \delta_1\right]e^{-2zd} + 2\delta_1 z\, e^{(\alpha-z)d} - (\alpha+z)\left[(\alpha-z)F + \delta_1\right] = 0, \tag{29}$$

where δ_1 is given by:

$$\frac{\delta^1}{\alpha} \left(\text{or } \frac{\varepsilon}{\alpha}\right) = \frac{\delta_1}{\alpha^2 d} \frac{(\exp \alpha d - \alpha d - 1)}{\exp \alpha d - 1}, \tag{30}$$

depending on which of the two processes (δ^1/α process due to trapped radiation or ε/α process due to metastable atoms) is considered. F is given by:

$$F = 1 - (\gamma + \delta/\alpha)(\exp \alpha d - 1).$$

The other symbols have their usual meanings.

The procedure for the calculation of the formative time lag as a function of percentage overvoltage $\Delta V\%$ can now be outlined. At given values of p and d, the sparking potential is measured and ω/α is calculated from the sparking criterion. A value of $\Delta V\%$ is chosen and the corresponding value of α is obtained from previous measurements. By choosing arbitrary values of the secondary coefficients, γ, δ/α, ..., λ may be obtained from equation 29. Once λ is known,

$$\left(\frac{\partial \theta}{\partial z}\right)_{\lambda} = 2\lambda F - \delta_1 - 2\delta_1(\lambda d-1)\, e^{(\alpha-\lambda)d} - e^{-2\lambda d}\left\{ 2Fd\,(\alpha^2-\lambda^2) + 2d\,\delta_1\,(\alpha-\lambda) + 2\lambda F + \delta_1 \right\} \qquad (32)$$

may be obtained.

Experimental values of i_- and i_o, together with the values obtained for ω/α, α, d, λ and $\left(\frac{\partial \theta}{\partial z}\right)_{\lambda}$, can be substituted in equation 28. If i_- is chosen to be the value of the cathode current when breakdown occurs, t becomes the formative time lag t_f. The equation may then be solved to give Dt_f and knowledge of D gives t_f for the given conditions. Repetition of this procedure for different values of $\Delta V\%$ gives the required calculated curve.

In the above it was assumed that the trapped radiation could be treated as a diffusion process characterized by a diffusion coefficient. Also d/W_- and d/W_+ were regarded as being very much

less than t. All contributions to the current arising from the imaginary roots of equation 29 were neglected. Finally, it was assumed that there was negligible destruction of the diffusing particles in the gas.

Davidson[61] extended his treatment of the problem to include consideration of processes such as the conversion of atomic ions into molecular ions, metastable atoms into metastable molecules and the transition of atoms from metastable and resonant states with the production of undelayed photons. He also considered the transfer of resonant photons through the gas, in accordance with Holstein's theory[67], and included delayed radiation from excited states which have a long lifetime τ_1. He first obtained the following expression for the cathode current at time t for secondary action due to positive ions and delayed radiation:

$$\frac{i_-(0,\ t)}{i_o} = \frac{1}{F(0)} + \sum \frac{\exp(\lambda t)}{\lambda\, F^1(\lambda)} ,$$

where $$F(p) = 1 - \frac{\delta\,(e^{\psi d} - 1)}{\psi(1 + p\,\tau_1)} - \frac{\alpha\,\gamma\,(e^{\phi d} - 1)}{\phi} ,$$

$$\psi = \alpha - p/W_-, \quad \phi = \alpha - p/W, \quad F^1(p) = \frac{\partial F(p)}{\partial p}$$

and $$\frac{1}{F(0)} = \frac{1}{1 - (\delta/\alpha + \gamma)(\exp \alpha d - 1)} .$$

The summation extends over all values λ of p which satisfy $F(\lambda) = 0$. At large values of t the complex λ's become relatively negligible and the expression for $i_-(0, t)$ reduces to the form

$$\frac{i_-(0, t)}{i_o} = \frac{1}{F(0)} + \frac{\exp \lambda t}{\lambda F(\lambda)} ,$$

which may be written

$$i_-(0, t)/i_o = A - B \exp \lambda t.$$

If $V > V_s$, the term A may be omitted at sufficiently large t and

$$i_-(0, t)/i_o = - B \exp \lambda t.$$

Davidson then proceeded to find the general solution for the case where the trapped photons obey the law of Holstein radiation. Previously it had been wrongly assumed that the diffusion law for trapped radiation was analogous to that for metastable atoms. Davidson's first step was to set up, for all types of active particle, expressions of the form $i_k (x, t) = i_k (x, 0) \exp \lambda t$. By treating the problem in this general manner, he obtained the expression for $i_-(0, t)$ at large t:

$$i_-(0, t)/i_o = A - Be^{\lambda t} \qquad (33)$$

where: $A = 1/F(0)$ and $B = - 1/\lambda F^1(\lambda)$.

λ is the real value satisfying $F(\lambda) = 0$, the complex λ's being neglected.

$F(\lambda)$ is given by

$$F(\lambda) = 1 - \sum \gamma_k f_k(\lambda),$$

where $f_k(\lambda) = i_k(0, t)/i_-(0, t)$, $i_k(x, t)$ being the current of each type of active particle, and, in the simple exponential solution, $i_k(x, t) = i_k(x, 0) \exp \lambda t$.

Of all the differential equations and boundary conditions which have to be satisfied, there is only one equation in which the coefficients γ_k of secondary ionization occur. These coefficients appear in the equation describing the condition that the cathode electron current at time t is the sum of i_o and the electron currents generated at the cathode by the secondary action of the various types of active particle.

Phelps[66], in considering processes acting in helium, calculated the value of λ from an expression he obtained for $F(\lambda)$. This function $F(\lambda) = 1 - \sum \gamma_k f_k(\lambda)$ was a complicated expression. However, equation 33 remains valid when the F specified by Phelps is inserted.

If V is only slightly greater or less than V_s, the λ of the simple exponential solution is of small magnitude, and so we can write $F(0) = F(\lambda) - \lambda F^1(\lambda)$ by neglecting terms in higher powers of λ. Since $F(\lambda)$ is zero, equation 33 becomes $i_-(0, t)/i_o = (1-\exp \lambda t)/F(0)$.

McClure[62] began his treatment of the problem by considering an electron leaving the cathode at time t = 0, when the applied

voltage is V. On the average, this electron causes, say, L (V, t) dt secondary electrons to leave the cathode during the interval (t, t + dt). Thus:

$$i_-(t) = i_o + \int_{-\infty}^{t} L\,(V,\ t - T)\ i_-(T)\ dT \qquad (34)$$

If i_o and V are time independent, the solution of equation 34, with $i_-(0) = i_o$, is:

$$i_-(t) = i_o \left[\frac{1 - K\,(V)\ \exp\,(t/\theta)}{1 - K\,(V)} \right] , \qquad (35)$$

where $K\,(V) = \int_o^\infty L\,(V,\ t)\ dt$. K (V) is the total number of secondary electrons a typical electron from the cathode subsequently causes to leave the cathode. At small overvoltages, the time constant θ is given by:

$$\theta \Delta V = \int_o^\infty \frac{t\ R\,(V_b,\ t)\ dt}{\left(\frac{dK}{dV}\right)_b} \qquad (36)$$

where the subscript b implies that the quantity is evaluated for the conditions existing at breakdown. The usual definition of V_b is given by $K\,(V_b) = 1$, which is the requirement for a self-sustaining discharge. In equation 36, $R\,(V,\ t) = L\,(V,\ t)/K\,(V)$. Equation 36 shows that the delayed secondary emission occurring during (t, t + dt) contributes to θ in proportion to the length of the delay t and in proportion to the rate of release of secondaries $R\,(V_b,\ t)$. The rate of build-up is $1/\theta$.

McClure discussed these equations for the particular case of a Townsend discharge in neon at low pressures and over-voltages of less than one volt. He assumed that the discharge was entirely sustained by the return of positive ions and metastable atoms to the cathode. He evaluated $\gamma\Delta V$ in terms of independently observed parameters and compared these calculated values with direct observations of the build-up of the discharge. The general features of the experimental results agreed with the calculated values, but the experimental values of $\gamma\Delta V$ as a function of $p_o d$ lay below the calculated values by about some 15%, indicating that the discharge built up faster than predicted. McClure had previously concluded that the predominant contribution to $\gamma\Delta V$ was due to metastable atoms, the ions being expected to contribute only a few per cent, even though about ten times as many ions as metastables reach the cathode. So he suggested that the discrepancy between the values for $\gamma\Delta V$ was due to the effect of metastable action not being as large as he had predicted.

Chapter 3

PREVIOUS MEASUREMENTS OF FORMATIVE TIME LAGS IN HELIUM

The previous chapters have been concerned with general ionization growth theory and the ionization and excitation processes occurring in helium, so the particular case of the temporal growth of ionization in helium may now be considered. It would seem that the only previous measurements of the temporal growth of current in helium were those of von Gugelberg[63] and Davies, Llewellyn Jones and Morgan[64]. These will now be reviewed in turn.

3.1 von Gugelberg's measurements

von Gugelberg carried out his experiments on seven gases. Besides helium, these included argon, krypton, xenon, hydrogen, nitrogen and a neon-argon mixture. He used five sealed-off tubes containing plane parallel electrodes, the cathode being illuminated through holes pierced in the anode. Two of the tubes contained movable electrodes enabling d to be varied while the others had gap distances fixed at 1.3, 3.0 and 7.5 mm. The electrodes used were either clean nickel or nickel which had been coated with barium and its nitride.

von Gugelberg followed a theoretical approach which was similar to that of Steenbeck and Bartholomeyczyk. A difference was that he took into account the externally maintained current i_o, by replacing the boundary condition (equation 13) by the expression:

$$i_-(0, t) = i_o + \gamma\, i_+(0, t) + g\gamma_p \int_o^d i_-(x, t)\, f(x)\, e^{-\mu x} dx, \qquad (37)$$

where g is a geometrical factor for photon arrival at the cathode, f(x) is the ratio of photons to electrons produced at a distance x from the cathode and μ is the photon absorption coefficient.

It was assumed that the current grows exponentially with time about an average build-up time τ, which is characteristic of the particular breakdown conditions. Then $j_-(x, t) = e^{t/\tau}\, j_-(x)$, and the quantity τ is associated with the formative time lag. von Gugelberg obtained the breakdown relation:

$$1 = i_o/i_-(0, t) + \gamma \int_o^d \alpha\, e^{\int_o^x (\alpha - \lambda/W)dx}\, dx + g\gamma_p \int_o^d f(x)\, e^{\int_o^x (\alpha - \lambda/W_-)dx - \mu x}\, dx\,. \qquad (38)$$

He then obtained the relation given by Steenbeck (equation 8) for positive ion action, together with a corresponding relation for combined positive ion and photon action. Finally, he obtained the following expressions for the growth constant λ:

$$\lambda_{ion} = W_+ \left\{ \alpha - \frac{1}{d} \ell n \frac{1}{\gamma} \left(1 - \frac{gf\gamma_p}{\alpha - \mu}\, e^{(\alpha-\mu)d}\right)\right\} \qquad (39)$$

$$\lambda_{photon} = W_- \left\{ \alpha - \mu - \frac{1}{d}\, \ell n\, \left(\frac{\alpha - \mu}{gf\gamma_p}\right)\right\} \qquad (40)$$

according to whether positive ion or photon action was predominant.

It was then possible to plot a calculated curve for the reciprocal of the time against values of d or V, for given values of E and p. If, as in von Gugelberg's case, the time t was taken to be that for the current to grow from 10^{-11} to 10^{-4} amp, $j_-(x, t)/j_-(x) = 10^7 = \exp(\lambda t)$ and $1/t \approx \lambda/16$.

In figure 11 the calculated curves are given for positive ions and photons each acting alone. The third curve was obtained by assuming a photoelectric contribution of 0.3% to the combined action of ions and photons.

Similar curves were plotted for each gas for varying ratios of γ and γ_p. The curve which gave the closest fit to the experimental results for the given conditions gave the relative contributions of the two actions. Thus, for helium at a pressure of 7.5 torr and $E_s/p \approx 140$ volts cm^{-1} $torr^{-1}$, it was shown that photons contributed less than 0.1% to the total ionization, the rest being due to positive ion and, possibly, metastable atom action.

The effect of metastable action was noticeable in the measurements, even though it was not included in the theoretical treatment. Near and below the threshold for positive ion action, long build-up times were observed. Where these occurred, the curves of 1/t against V showed a steep rise at onset. The long, nearly horizontal portion of the curves went through a point of inflexion and reached the value of 1/t which was characteristic of ions. The metastable effect was largest in helium and decreased for the

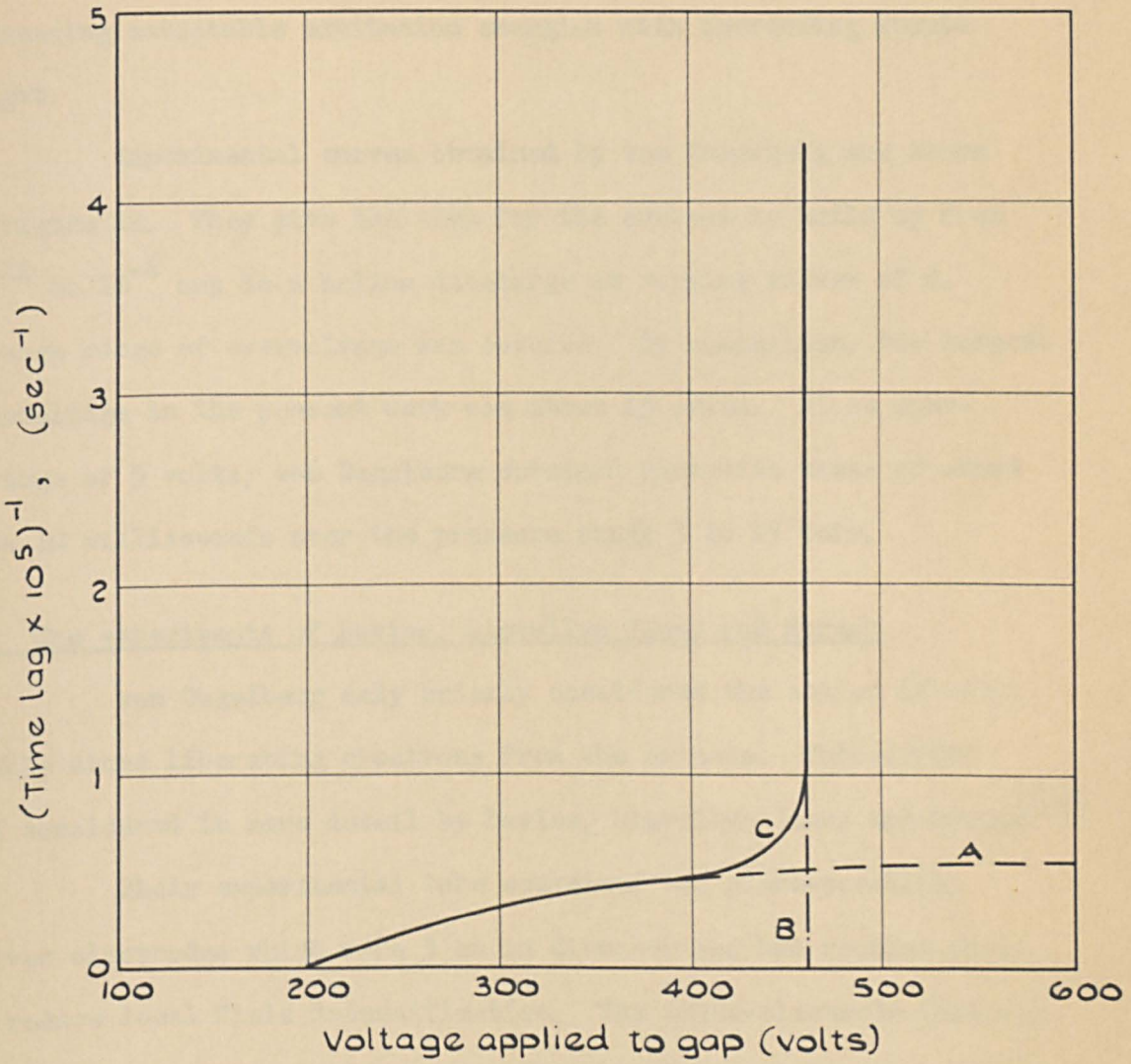

FIG. 11 CALCULATED CURVES[63] OF THE RECIPROCAL OF THE TIME LAG IN HELIUM AS A FUNCTION OF VOLTAGE. A, POSITIVE IONS ALONE; B, PHOTONS ALONE; C, PHOTON CONTRIBUTION OF 0·3% TO THE COMBINED ACTION OF PHOTONS AND POSITIVE IONS.

heavier inert gases. This variation was probably related to the decreasing metastable excitation energies with increasing atomic weight.

Experimental curves obtained by von Gugelberg are shown in figure 12. They give the time for the current to build up from 10^{-11} to 10^{-4} amp in a helium discharge at varying values of d. A large range of overvoltage was covered. By comparison, the largest overvoltage in the present work was about 15 volts. At an overvoltage of 5 volts, von Gugelberg obtained formative times of about 1 to 10 milliseconds over the pressure range 3 to 19 torr.

3.2 The experiments of Davies, Llewellyn Jones and Morgan

von Gugelberg only briefly considered the action of metastable atoms liberating electrons from the cathode. This effect was considered in more detail by Davies, Llewellyn Jones and Morgan[64].

Their experimental tube contained two plane-parallel, silver electrodes which were 3 cm in diameter and had rounded edges to reduce local field intensification. The inter-electrode distance was fixed at 0.817 cm and the borosilicate glass envelope was fitted with a quartz window so that the cathode could be illuminated with ultra-violet light through fine holes in the anode. The 8 cm diameter envelope was fitted with an earthed metal screen in contact with the inside wall of the tube to prevent build up of charge.

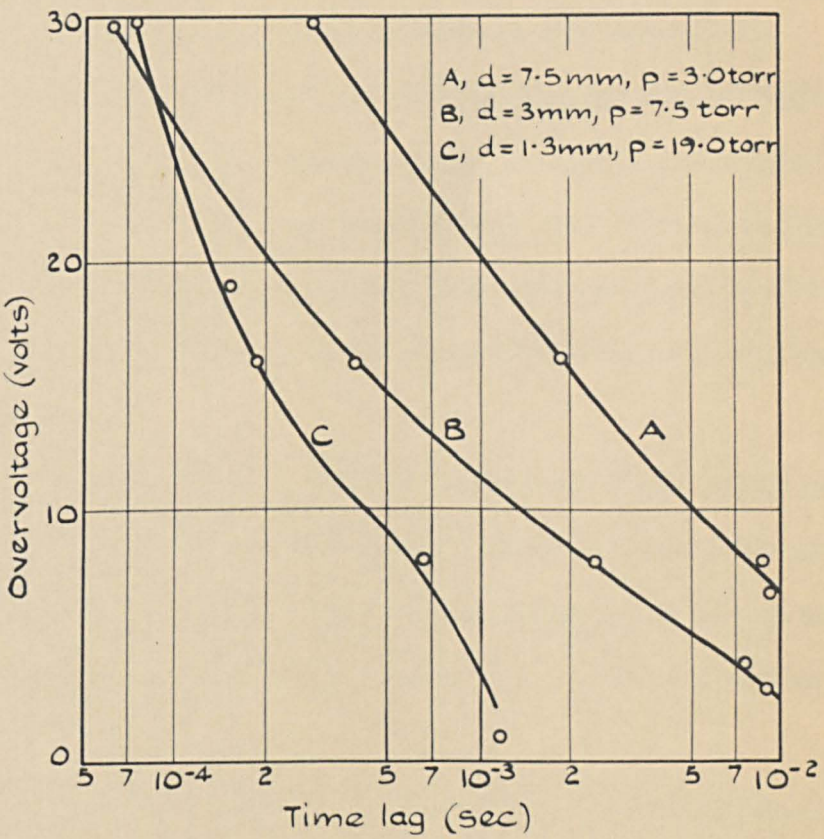

FIG. 12 TIME LAG AS A FUNCTION OF OVERVOLTAGE IN HELIUM. AFTER VON GUGELBERG (63).

By means of standard techniques, in which an Alpert-type ion pump was used, pressures of the order of 10^{-8} torr were achieved before introduction of gas to the experimental tube. To reduce possible sources of gas contamination, metal taps were used and the gas pressure was measured by a bellows micro-manometer, used as a null detector, in conjunction with an oil manometer. The helium was supplied by the British Oxygen Company and contained 2 parts per million of carbon dioxide, 4 ppm of oxygen and 2 ppm of other carbonaceous gases. Further purification was carried out by passing the helium through a trap containing activated charcoal at liquid oxygen temperature and a vessel containing titanium hydride at room temperature.

The curves obtained by Davies, Llewellyn Jones and Morgan are shown in figure 13, which gives the variation of the formative time lag with percentage overvoltage. By varying the helium pressure from 5 to 40 torr, seven curves were obtained at different values of E_s/p.

In an attempt to explain these results, Davies, Llewellyn Jones and Morgan assumed that the only secondary processes acting were those due to the incidence of positive ions, photons and metastable atoms at the cathode. Using Davidson's analysis[60] (section 2.4), families of curves of formative time against percentage overvoltage were calculated corresponding to various assumed combinations and proportions of the secondary coefficients γ, δ/α and ε/α. These

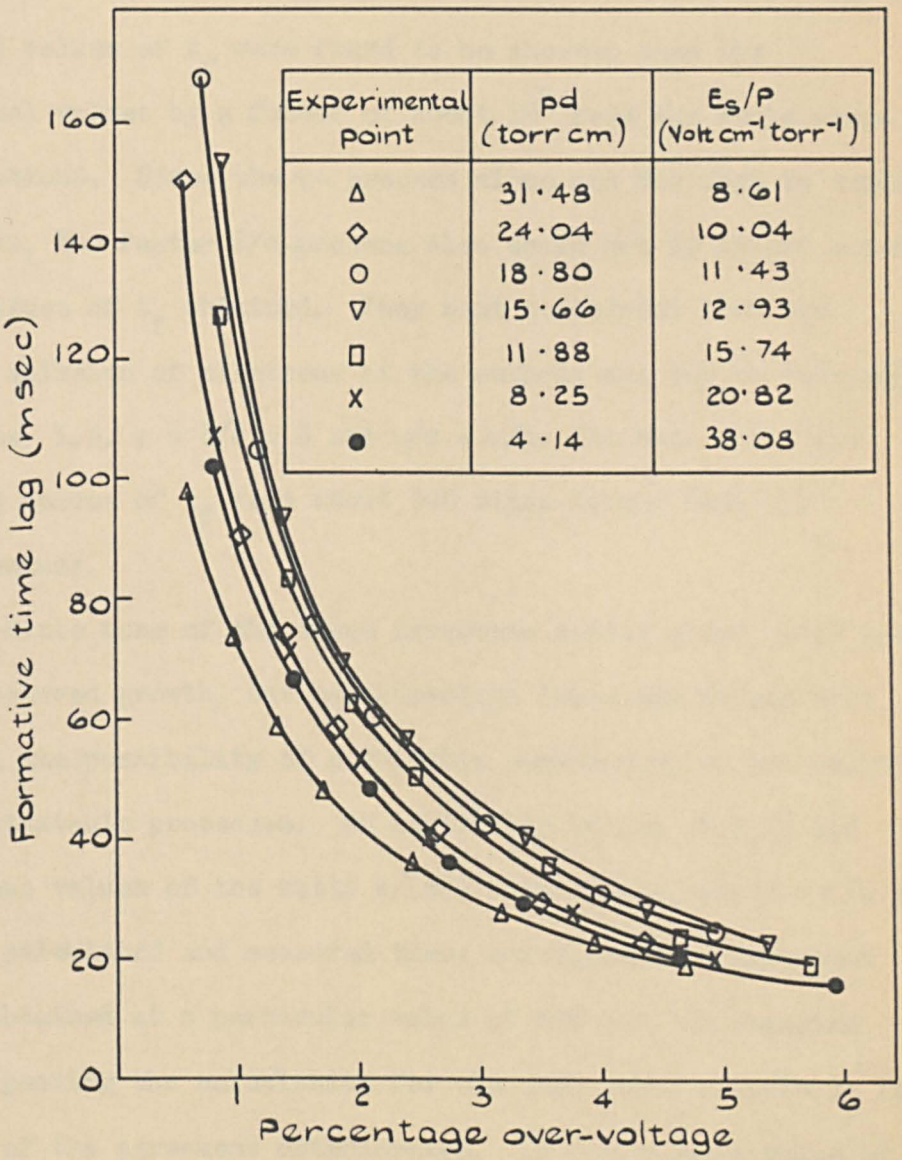

FIG·13 VARIATION OF FORMATIVE TIME LAG WITH PERCENTAGE OVER-VOLTAGE, DAVIES, LLEWELLYN JONES AND MORGAN[64].

curves were then compared with the experimental data.

The secondary emission was first assumed to be entirely due to positive ions, i.e. $\delta/\alpha = \varepsilon/\alpha = 0$ and $\omega/\alpha = \gamma$. Here the calculated values of t_f were found to be shorter than the experimental values by a factor of about 10^2 over the whole range of observations. Since the γ- process alone was too fast to explain the results, the faster δ/α-process also could not by itself account for the values of t_f obtained. They next considered that the secondary emission of electrons at the cathode was due to metastable atoms alone, i.e. $\gamma = \delta/\alpha = 0$ and $\omega/\alpha = \varepsilon/\alpha$. In this case, the calculated values of t_f were about 100 times longer than the measured values.

Since none of the three processes acting alone could account for the observed growth, Davies, Llewellyn Jones and Morgan next considered the possibility of a suitable combination of the positive ion and metastable processes. At particular values of E_s/p and $\Delta V\%$, various values of the ratio $\varepsilon/(\alpha\gamma)$ were chosen, for $\gamma + \varepsilon/\alpha = \omega/\alpha$, until the calculated and measured times corresponded. Agreement could be obtained at a particular value of $\Delta V\%$ but, on changing $\Delta V\%$ and repeating the calculation for the same value of $\varepsilon/(\alpha\gamma)$, the closeness of the agreement deteriorated. At the highest value of E_s/p (31.48 volts cm^{-1} $torr^{-1}$), when $\varepsilon/\alpha = 19.5\%$ and $\gamma = 80.5\%$ of ω/α there was fair agreement between the observed and calculated values for $0.86 \leq \Delta V\% \leq 5.93$. But at low values of E_s/p, the growth

was not satisfactorily explained by this combination of ε/α and γ. At E_s/p = 8.61 volts cm^{-1} $torr^{-1}$, the combination giving the closest agreement was ε/α = 4.2% and γ = 95.8%. Even so, the agreement was very poor.

These combinations of γ and ε/α represented the optimum results based on a wide range of combinations of the secondary processes considered, so the authors suggested that these three processes were inadequate to explain the observed growth times. They ended by proposing that other processes should be investigated, such as the action of delayed photons at the cathode. This they did in a subsequent paper which is the subject of the next section.

3.3 Additional discussion of their 1963 results by Davies, Llewellyn Jones and Morgan

Davies, Llewellyn Jones and Morgan soon presented a further discussion[65] of the secondary ionization processes in helium based on the formative time lag measurements given in their previous paper[64].

The discussion opened with a review of the delay times of the various secondary processes acting in helium. The delay time τ_1 is the time between the appearance of an electron at the cathode and the subsequent release of a further electron from the cathode by the process considered.

The majority of the particles active in the discharge are created near the anode. Thus the positive ion delay time is the sum of the electron and positive ion transit times and is $d/W_- + d/W_+$. Since $W_- \gg W_+$, the ion delay time may be written d/W_+. For d = 1 cm and for the range of E_s/p considered (when $W_+ \approx 10^5$ cm/sec), the delay time associated with the γ-process is $\sim 10^{-5}$ sec. Under similar conditions, the delay time for unscattered photons (δ/α-process) is $\sim 10^{-7}$ sec. The delay time for the arrival of metastable atoms at the cathode (ε/α-process) is given by $d/W_- + d^2/D_{met}$, where D_{met} is the appropriate diffusion coefficient. As in the positive ion case d/W_- can be neglected. Thus, for a 1 cm gap, the delay time for the ε/α process is $\sim 10^{-3}$ sec. The values of W_-, W_+ and D_{met} are those given in the papers referred to in section 1.2.

Previously, Davies, Llewellyn Jones and Morgan had concluded that a process faster than the ε/α-process, but slower than the γ-process, was required to explain the observed formative time lags. From the above consideration of delay times, such a process would be expected to have a delay time of about 10^{-4} sec. Possible processes, which were not considered in the previous paper, were those of photoelectric emission from the cathode by imprisoned resonance radiation and by collision-induced non-resonance radiation.

The main source of non-resonance photons in helium was shown by Phelps[66] to be the destruction of 2^1S metastable atoms

in 2-body collisions with neutral gas atoms. The collision frequency for this 2-body process is proportional to p and the effective cross-section for this volume destruction of 2^1S metastables at 300^oK is 3×10^{-20} cm^2 (66). The time elapsing between the production of a 2^1S metastable and the emission of a non-resonance photon can be calculated to be $1/(192\ p)$. Over the range of pressures used by Davies, Llewellyn Jones and Morgan (5 to 40 torr), this time is $\sim 10^{-4}$ sec. By comparison, the transit times of electrons and photons can be neglected, giving a delay time for the action of non-resonance photons at the cathode $\sim 10^{-4}$ sec.

The motion of resonance photons through the gas can be hindered by the repeated absorption and re-emission of the radiation by ground state gas atoms. The delay time for electron emission at the cathode by resonance radiation is partly determined by the number g^{-1} of absorptions and re-emissions made in traversing the electrode distance. It is also determined by the lifetime τ_o of the particular resonant state of the gas atom. The time spent by the photon in travelling between successive emissions and absorptions can be neglected. So the time taken for the radiation to cross the gap is $g^{-1}\ \tau_o$. An expression for g was given by Holstein(67) in terms of the impact broadening of spectral lines and an expression for τ_o was given by Mitchell and Zemansky(68). Combining the two expressions gives:

$$g^{-1}\tau_o = \frac{m c \lambda_o^2}{8\pi^2 e^2 f} \frac{g_2}{g_1} \left(\frac{3\pi^2 d}{\lambda_o} \right)^{\frac{1}{2}} \frac{1}{1.15} \cdot \qquad (41)$$

According to Phelps[66], only one type of resonance photon reaches the cathode in appreciable numbers in pure helium at pressures above 3 torr. These are the photons arising from the spontaneous $2^1P - 1^1S$ transition, for which $\lambda_o = 584$ Å. The ratio of the statistical weights g_2/g_1 for this transition is 3, the oscillator strength f is 0.275[69] and the other symbols of equation 41 have their usual meanings. For the conditions existing in the experiments of Davies, Llewellyn Jones and Morgan, equation 41 gives $g^{-1}\tau_o \sim 10^{-6}$ sec. Thus, neglecting the electron transit time, which is an order of magnitude faster, the delay time for the resonance photon process is $\sim 10^{-6}$ sec.

From this consideration of delay times, it would seem that the non-resonance photons, and not the resonance photons, are likely to be responsible for the observed time lags. Davies, Llewellyn Jones and Morgan then proceeded to make a detailed quantitative analysis of the measured time lags using Davidson's[61] treatment of the problem.

For both non-resonance and imprisoned resonance photons, the cathode current is given by*:

---

* The expressions given by Davies, Llewellyn Jones and Morgan differ slightly from the ones given here. For example, i_o does not appear in their formulation of equation 42. It would seem likely that these errors were typographical.

$$\frac{i_-(0, t)}{i_o} = A - B\, e^{\lambda t} \tag{42}$$

where:

$$A = \frac{1}{F(0)} \tag{43}$$

$$B = - \frac{1}{\lambda \left[\frac{\partial F(p)}{\partial p} \right]_{p=\lambda}} \tag{44}$$

$$F(p) = 1 - \frac{\delta_1}{\psi} \frac{e^{\psi d} - 1}{1 + p\tau_1} \tag{45}$$

$$\psi = \alpha - \frac{p}{W_-} \tag{46}$$

and λ is the real root of

$$F(p) = 0 . \tag{47}$$

The type of radiation considered affects the coefficient δ_1 of equation 45. It will be recalled that δ_1 is the number of photoelectrons produced at the cathode by delayed radiation as a result of one electron travelling 1 cm in the field direction. For collision-induced non-resonance radiation $\delta_1 = \frac{1}{2} \alpha_1 \gamma_1$, where α_1 is the number of metastable atoms produced by an electron in travelling 1 cm in the field direction and γ_1 is the number of cathode electrons released by each photon emitted by a metastable atom in 2-body collision. For imprisoned resonance radiation

$$\delta_1 = \tfrac{1}{2} \alpha_1 \gamma_1 / \left[1 + 0.175\, (\psi d)^{2/3} \right] .$$

The factor $1/\left[1 + 0.175\ (\psi d)^{2/3}\right]$ is introduced[66] to account for the reduction in the current of resonance photons reaching the cathode as the result of preferential scattering of photons to the anode. This factor varies from 1 for $\alpha d = 0$ to about 0.6 for $\alpha d = 8$. α_1 is now the number of excited atoms in the 2^1P state produced by an electron in travelling 1 cm in the field direction, and γ_1 is the number of electrons produced by a resonance photon on striking the cathode.

For simplicity, only one of the two possible delayed photoelectric mechanisms was at first assumed to occur. The delay time τ_1 was taken as 10^{-4} sec, which was the value indicated in the previous paper[64], and this value was substituted in the expression for F(p) (equation 45) together with known values of δ_1 $(= \omega)$, α and W_-. The growth constant λ was calculated from $F(p) = 0$ and this value of λ used in the calculation of t_f which was then compared with the measured value. The procedure was repeated for various values of τ_1, until agreement was obtained between the calculated and observed growth times and the value of τ_1 which gave the required agreement was used to calculate a complete curve of t_f against $\Delta V\%$. If agreement was obtained between the calculated and experimental curves, it was assumed that the delayed photon process characterized by the particular value of τ_1 was responsible for the growth.

Davies, Llewellyn Jones and Morgan obtained seven values of τ_1 which gave agreement between the calculated and observed times

over the range of E_s/p_o from 8.61 to 38.08 volts cm^{-1} $torr^{-1}$. These values are given in the third column of table 2.

p_o torr	E_s/p_o volt cm^{-1} $torr^{-1}$	$\tau_1 \times 10^4$ sec	$\tau_1 (= \frac{1}{192} p_o) \times 10^4$ sec
38.51	8.61	1.2	1.3
29.43	10.04	2.4	1.8
23.01	11.43	2.1	2.2
19.17	12.93	2.3	2.7
14.54	15.74	1.5	3.6
10.10	20.82	1.7	5.1
5.07	38.08	1.5	10.0

Table 2. Radiation delay times.

The average of these values of τ_1 is approximately 1.8×10^{-4} sec which is about 10^2 times longer than the value predicted for resonance radiation. So they concluded that secondary emission due to trapped radiation was not significant in their work.

They then compared the calculated values of τ_1 with the values for the volume destruction rate of 2^1S metastables, given by $\tau_1 = 1/(192\ p_o)$ which are shown in the fourth column of table 2. For $p_o > 19$ torr, there was reasonably good agreement between the two sets of values but at lower values of p_o, the agreement

deteriorated until at p_o = 5.07 torr the delay times given by $1/(192\ p_o)$ were about six times longer than required. This led them to suggest that, at the lower pressures, the secondary action might be explained by positive ions and delayed non-resonance photons acting together at the cathode.

In this case, equation 45 becomes:

$$F(p) = 1 - \frac{\delta_1}{\psi}\,\frac{(e^{\psi d} - 1)}{(1+p\tau_1)} - \frac{\alpha\gamma}{\phi}\,(e^{\phi d} - 1) \qquad (48)$$

and τ_1 is now $1/(192\ p_o)$, $\omega/\alpha = \gamma + \delta_1/\alpha$ and $\phi = \alpha - p/W$. In the expression $F(p) = 0$ all the quantities are known except for γ and δ_1/α. Since ω/α $(= \gamma + \delta_1/\alpha)$ is known, any given choice of the ratio $\gamma:\delta_1/\alpha$ allows γ and δ_1/α to be determined, and λ can be calculated. The formative time lag can then be obtained from the expression for the cathode current (equation 42). Thus, at a given value of E_s/p_o, the ratio $\gamma:\delta_1/\alpha$ can be varied until agreement is obtained between the calculated and measured curves of t_f against $\Delta V\%$. The percentage contributions of δ_1/α and γ to ω/α, as obtained by Davies, Llewellyn Jones and Morgan, are given in table 3.

E_s/p_o volts cm^{-1} $torr^{-1}$	δ_1/α %	γ%
8.61	100	0
10.04	100	0
11.43	88	12
12.93	76	24
15.74	43	57
20.82	37	63
38.08	24	76

Table 3. Relative importance of the γ and δ_1/α processes.

These values can be explained by considering the dependence on E/p of the ratio of the number of exciting to ionizing collisions (α_1/α)[70]. At low values of E/p ($\lesssim$ 10 volts cm^{-1} $torr^{-1}$), the number of excitations to metastable states greatly exceeds the number of ionizing collisions by a factor $\gtrsim$ 10. So photoelectric emission by non-resonance photons is the dominant secondary process. At high values of E/p_o, the ratio is much reduced to $\alpha_1/\alpha \approx 2$*. Also, over the range of pressure considered, the rate of destruction of metastables is reduced by a factor of almost 8. For these reasons, the non-resonance photon contribution to ω/α is reduced as E/p increases.

Davies, Llewellyn Jones and Morgan concluded by suggesting that, at pressures lower than those considered by them, ω/α is likely to be due to the combination of positive ion and metastable action at the cathode since, because of the low collision frequency at the lower pressures, the diffusing metastables are not likely to be destroyed in the gas.

---

* This value may have been obtained by extrapolation, since Corrigan and von Engel's curves only extend to 10 volts $cm^{-1}torr^{-1}$.

Chapter 4

APPARATUS AND EXPERIMENTAL PROCEDURE

The experimental work was carried out in two phases. The first vacuum system used was, with some modifications, that which had been used for measurements in connection with a hydrogen discharge[71]. Two experimental tubes were used in conjunction with this system and these were designed so that work function determinations could be carried out in addition to formative time lag measurements.

As a result of the experience gained from this arrangement, the vacuum system and experimental tubes were later re-designed and completely re-built. The second vacuum system had the advantage that the helium was nowhere in contact with greased stopcocks or manometer oil, as it had been in the previous system. In the third and fourth experimental tubes the spacing of the electrodes was made variable, so it would have been inconvenient to have included a vibrating reference electrode and the work function measurements were discontinued. Tube 3 contained glass substrates on to which gold could be evaporated to form the electrodes; tube 4 contained nickel electrodes.

Before discussing the apparatus in detail, it is pertinent to begin this chapter by considering the purity of the helium used.

4.1 Helium purification

The helium atom has the highest known ionization potential, so electrons which have not sufficient energy to ionize the helium atoms may ionize any impurity atoms which may be present. It is obvious that this would affect α and the other discharge parameters, so it is important that the helium should be obtained in a high state of purity. Therefore as much residual gas as possible should be removed from the system before the introduction of helium and this entails special regard to the vacuum techniques to be employed.

The helium was supplied in 1-litre Pyrex flasks by the British Oxygen Company and was specified as being spectroscopically pure, containing not more than 2 parts per million of carbon dioxide, 4 ppm oxygen and 2 ppm other carbonaceous gases. Two methods of purifying the helium were considered which involved the use of activated charcoal and the phenomenon known as cataphoresis.

(a) Activated charcoal

Activated charcoal has the property of sorbing gases and, as a result, has often been used as a form of vacuum pump. At a temperature of -190°C and a pressure of 120 torr, 0.377 ccs (reduced to STP) of helium are sorbed per gramme of activated charcoal[72]. For nitrogen, at -190°C and 33 torr, 80.7 ccs (at STP) are sorbed per gramme[72]. Even though the pressure of nitrogen is lower than the pressure of helium, some 200 times more nitrogen than helium

is sorbed by volume by the charcoal and oxygen is sorbed even more readily[72]. The sorption of gases is related to their critical temperature and, in general, the sorption increases with an increase in critical temperature. As helium has the lowest critical temperature of any gas ($\approx 5^{\circ}K$), it is least readily sorbed by charcoal.

This selective sorption of different gases by charcoal can be used for the purification of suitable gases. When it is necessary, as in the present case, to obtain pure helium, charcoal in liquid air may be used to remove gases such as nitrogen, oxygen and hydrogen[73]. Liquid air is often used as a coolant since the physical adsorption of gases increases with a decrease in temperature.

(b) Cataphoresis

When a d.c. glow discharge runs in a mixture of gases, the mixture often becomes enriched in one of the gases at the cathode and another of the gases at the anode. When this effect is due specifically to a drift of one gas towards the cathode, the process is termed cataphoresis. Cataphoresis was discovered as early as 1893[74] and has been studied experimentally by Skaupy[75] and theoretically by Druyvesteyn[76].

Other experiments have been carried out by Riesz and Dieke[77] who used a long, cylindrical discharge tube filled to a pressure of at least 10 torr with helium containing a trace of neon. A d.c. discharge was maintained in the gas at currents of 10 to 30 mA and the intensity of any spectral line could be recorded at any point

along the axis of the tube. When the discharge was first turned on in spectroscopically pure helium, the neon lines showed up very weakly and they were uniformly distributed in intensity throughout the tube. Gradually, the intensity of the neon lines built up in the vicinity of the cathode and the process reached equilibrium in about two hours. The gradual decline in neon intensity observed for longer times was probably due to the clean-up of neon into the cathode.

The time taken for neon and any other impurity gases to be pumped to their equilibrium distributions in the discharge tube depended on the amount of impurity present and the total volume of the gas. With a volume of 2 litres at 20 torr, and such impurities as were present in the helium used, the time taken was about 2 hours for a 20 mA discharge.

The effectiveness of the cataphoretic action is controlled by the current, pressure and the proportions of the gas mixture. The effect of pressure and current on cataphoretic clean-up in helium with neon impurity is shown in figure 14. This shows that the slope of the neon distribution curve increases as the pressure or current is raised, indicating that the process of gas purification is increased by increasing the gas pressure or discharge current.

Riesz and Dieke were limited by experimental difficulties to pressures less than 30 torr and currents less than 30 mA. They believed that increases in pressure and current above these values would further enhance the effect. They concluded that the minor

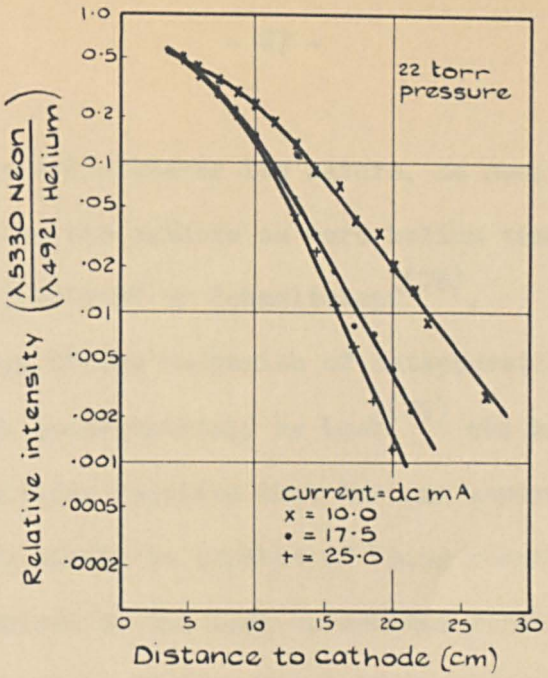

(a)

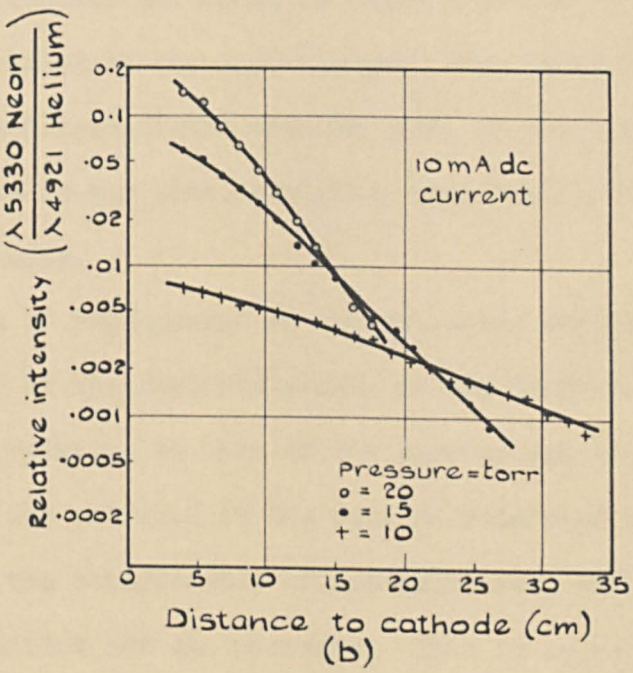

(b)

FIG. 14 DEPENDENCE OF CATAPHORESIS IN COMMERCIAL HELIUM ON (a) CURRENT (b) PRESSURE; RIESZE AND DIEKE[77].

constituent was removed whatever its nature, so neon traces in helium were pumped to the cathode as were helium traces in neon. This was later contradicted by Schmeltekopf[78].

The theory of the mechanism of cataphoretic segregation has been dealt with quantitatively by Loeb[79] who maintained that the cataphoretic process requires that the gas separated by movement towards the cathode should be capable of being readily and more or less completely ionized by the ions or excited states of the carrier gas. The minority gas would then have a much greater fraction (if not all) of its population ionized in the discharge, while the carrier gas would have only perhaps 1 in 10^3 or 10^4 of its atoms ionized. So the minority gas would be rapidly driven to the cathode by the current relative to the majority gas. The impurity ions would then be neutralized at the cathode, and, as the impurity atoms began to accumulate in the cathode region, they would start to diffuse backwards to the anode.

The rate of segregation of the two gases depends on the rate of ionization of the impurity atoms, on the drift velocity of the impurity ions relative to that of the carrier gas ions and on the ion transport current relative to the rate of return of impurity atoms by diffusion. So the cataphoretic effect increases, within limits, with increasing current and gas pressure. This is so because an increase in pressure increases the rate of formation of impurity ions through various types of impact with states of the carrier gas atoms

if these have ionization potentials greater than those of the impurity atoms. Increased gas pressure also retards the return diffusion of the impurity atoms.

Once the impurity ions are neutralized at the cathode, the atoms cannot diffuse far towards the anode before they are re-ionized and again attracted to the cathode. Rapid and effective segregation is likely if the ionization potential of the carrier gas atoms lies above that of the impurity atoms. The presence of large numbers of gas ions ensures almost complete ionization of impurity atoms by charge-exchange processes.

Experiments on cataphoresis in helium-neon mixtures were also carried out by Schmeltekopf[78] who ran a discharge in the gas mixture until equilibrium was established and then carried out a mass spectrometric analysis of the gas at the cathode, at the centre of the tube and at the anode. The results showed that the neon concentration was always greatest at the cathode even when the mixture was 99% neon. This contradicted the observations of Riesz and Dieke, who found thatthe minority gas always moved towards the cathode.

Schmeltekopf suggested that this disagreement might have been due to the different methods of measurement used. Riesz and Dieke observed the ratio of light intensity of a neon line to a helium line as a function of position in the discharge tube and this method is only valid if the excitation conditions remain constant along the

tube. Very large fields exist at the cathode in a glow discharge and all the gases are excited, but in the positive column the gases with the lowest ionization potential are excited to a higher degree. Schmeltekopf observed that, for 99% neon in helium, strong radiation from the 5875 Å helium line appeared at the cathode indicating that the helium concentration was high contrary to the result obtained by mass spectrometric measurements.

The purity of the gas at the anode improved as the cathode-anode distance was increased. Schmeltekopf introduced a quantity d, the quality of the cataphoresis, which was the distance between the anode and the point at which the neon light became visible. He obtained the curves given in figure 15 for 1% neon in helium and it can be seen that d improved rapidly at first with increasing current, but the rate of increase diminished at a current only a few tens of milliamperes higher than the onset current. In general, the quality of the cataphoresis decreased with decreasing pressure.

Schmeltekopf found that the best cataphoresis tube was 50 to 70 cm long and 4 mm inside diameter in the positive column and anode region. The anode was a very small disc or wire and the cathode was 5-8 cm in diameter enclosed in a slightly larger diameter bulb. The long, narrow tube was kept as cool as possible and operated at a high pressure. A current regulator and a large ballast resistor were needed to make the discharge stable so the cataphoresis could work efficiently.

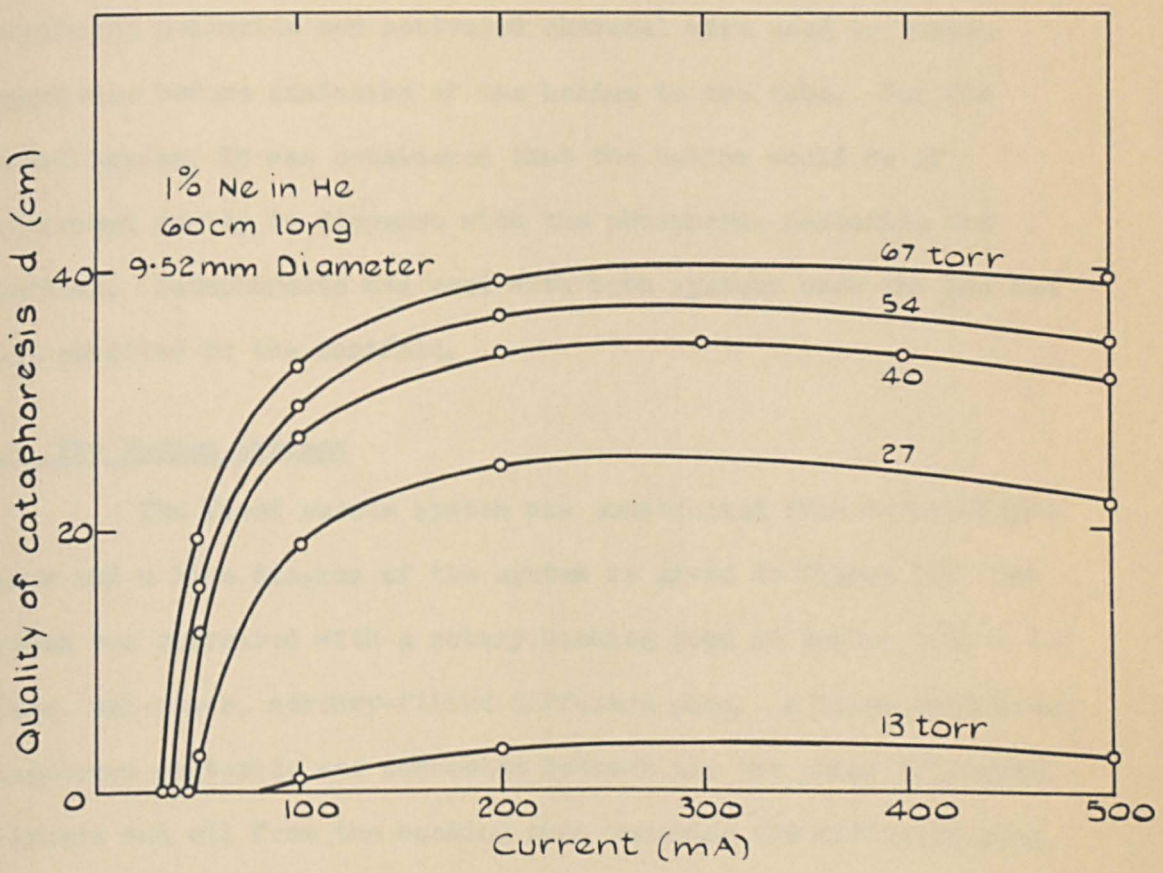

FIG. 15 THE QUALITY OF CATAPHORESIS AS A FUNCTION OF CURRENT AT SEVERAL PRESSURES. 1% NEON IN HELIUM, SCHMELTEKOPF [78].

In the present investigation, the first system used was such that the helium would be in contact with a number of sources of contamination before it was admitted to the experimental tube. So phosphorus pentoxide and activated charcoal were used to remove impurities before admission of the helium to the tube. For the second system, it was considered that the helium would be of sufficient purity to dispense with the phosphorus pentoxide and charcoal. Cataphoresis was used with both systems once the gas had been admitted to the manifold.

4.2 The vacuum systems

The first vacuum system was constructed from borosilicate glass and a line diagram of the system is given in figure 16. The system was evacuated with a rotary backing pump in series with a two-stage, all-glass, mercury-filled diffusion pump. A flask containing phosphorus pentoxide was connected between the two pumps to prevent moisture and oil from the backing pump reaching the diffusion pump. Two freezing traps were placed between the manifold and the pump to prevent mercury vapour reaching the manifold. A Penning gauge was connected just below the asbestos table on which the manifold was built and only two greased stopcocks were provided in this part of the system.

The gas-handling system was evacuated by the same backing pump, but here the diffusion pump was oil filled and this system could be isolated from the manifold by the greased stopcock T_3. The

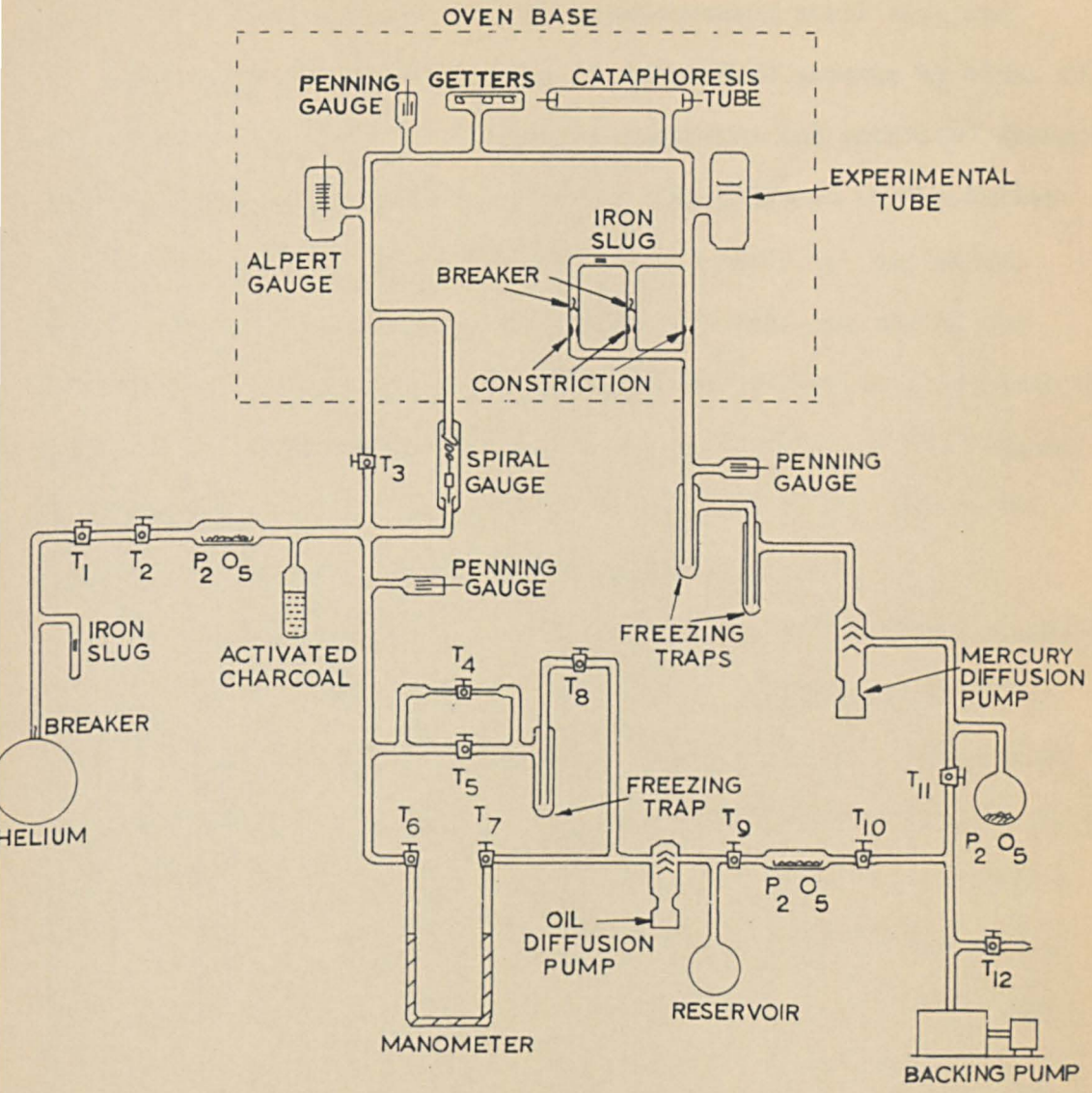

FIG. 16 THE FIRST VACUUM SYSTEM. T, GREASED STOPCOCK

helium flask was closed with a thin glass seal which could be broken by a magnetically-operated glass-encased steel slug and the helium passed into the system in controlled amounts by means of the stopcocks T_1 and T_2. Phosphorus pentoxide and activated charcoal were included as shown in the figure. The pressure of the helium in the system was measured by means of a 3 metre oil manometer, which contained silicone oil (D.C.703). In use, one arm of the manometer was open to the diffusion pump and so was at a pressure of about 10^{-6} torr while the other was at the pressure of the helium. A Penning gauge was also included in this part of the system to monitor the pressure before admittance of the helium.

The all-glass manifold was built above the asbestos table and was constructed so that an oven could be placed around it to bake it at 450°C. On to the manifold were sealed an Alpert gauge, Penning gauge, getter tube, cataphoresis tube and experimental tube. Between the manifold and the pumps was a series of constrictions and breakers, so that the manifold could be closed to the pumps by sealing a constriction, and re-opened by breaking one of the thin glass seals (breakers) with a glass-encased steel slug. The manifold could also be opened and closed to the gas handling system by use of the greased stopcock T_3. A spiral gauge was connected between the manifold and the gas handling system.

The second system (figure 17) was also constructed from borosilicate glass and was similar in some respects to the first.

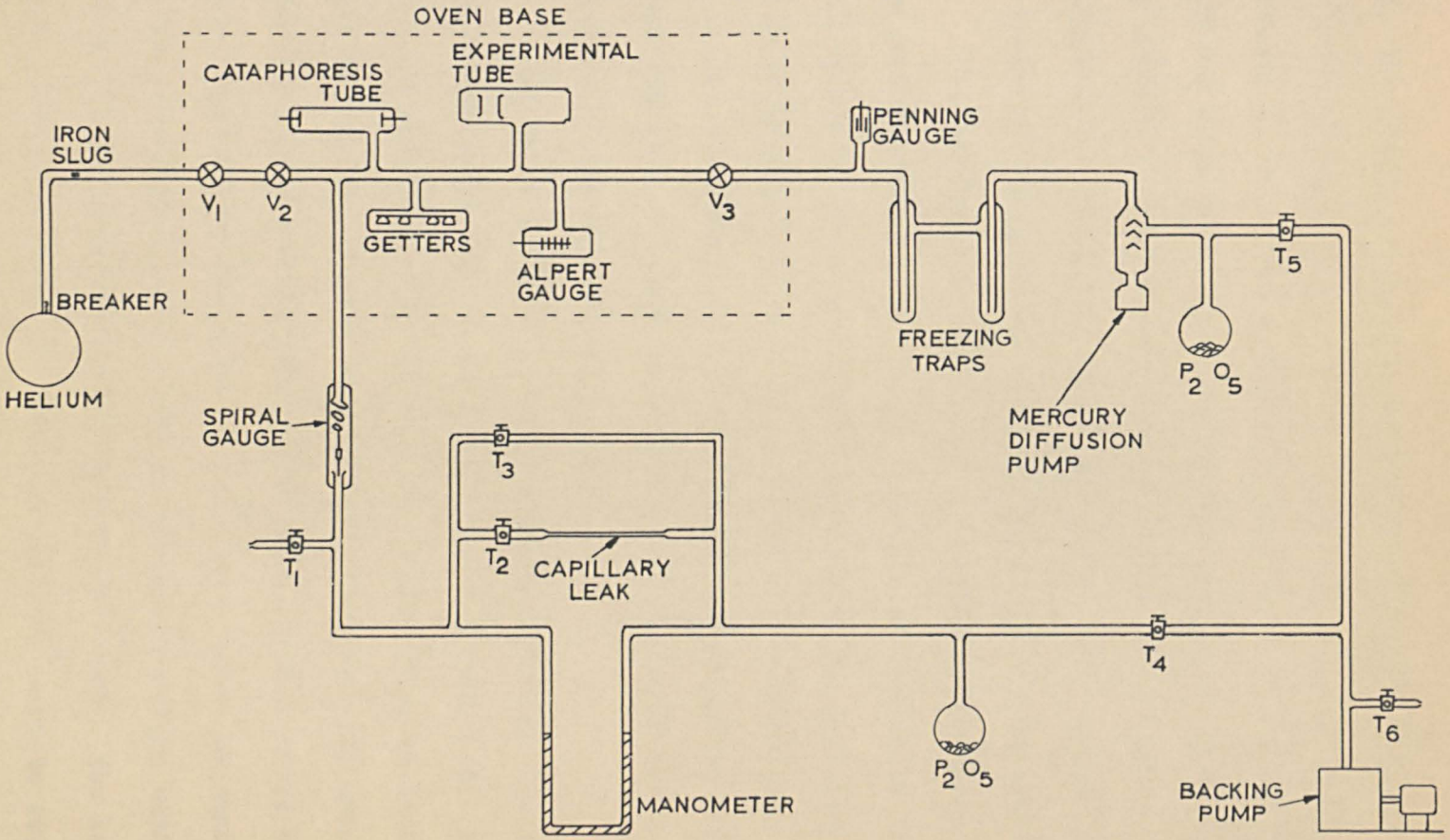

FIG. 17 THE SECOND VACUUM SYSTEM. T, GREASED STOPCOCK; V, METAL CLOSURE VALVE.

However, the manifold could be isolated from the pumps by a bakeable metal closure valve (Edwards MCV 1) V_3, which replaced the constrictions and breakers of the first system. A torque of 35 ft lb was needed to close the three metal taps used in this system, so they were rigidly mounted on the asbestos table by means of a length of 1 in. angle-iron. As before, the experimental tube, getter tube, Alpert gauge and cataphoresis tube were connected to the manifold.

The gas handling system was considerably different from the one just described. The helium flask was connected to the manifold by way of two metal closure valves and the gas supply system could be pumped to the same pressure as the manifold. At first, a tube containing activated charcoal was included, but this was later removed. Controlled amounts of helium could be let into the manifold by the two valves V_1 and V_2.

The third section of the system was concerned solely with pressure measurement and was evacuated by the backing pump used to evacuate the manifold. This part of the system could be isolated from the pump by the greased stopcock T_4. A 1-metre oil manometer was used for pressure measurement, both arms of which could be pumped to pressures of the order of 10^{-3} torr. When the manometer was in use, the taps T_3 and T_2 were closed and the right hand arm (figure 17) of the manometer maintained at 10^{-3} torr. The left hand arm could be maintained at any pressure from 10^{-3} torr to atmospheric, this variation being achieved by either letting in air through the

atmospheric leak by opening T_1 or by extracting air through the capillary leak by opening T_2. A spiral gauge was connected between one arm of the manometer and the manifold.

4.3 The experimental tubes

Tubes 1 and 2 were identical except for a difference in the electrode spacings, so it is sufficient to describe the design and construction of only one of the tubes.

A schematic diagram of the tubes is given in figure 18. A C9 pinch with 7 tungsten leads was the base on which the tube was constructed. A frame was formed from 5 mm diameter glass rod and was mounted on the stem of the pinch. Substrates were made in the form of glass discs of diameter 2.5 cm and 3 to 4 mm thick by pressing molten glass rod between two carbon plates. While the substrates were still hot, tungsten rods (1 mm diameter, 2 cm long) were pressed into them to provide an electrical contact. Glass rods were added as supports for the substrates which were then carefully annealed. When cold, each substrate was ground flat using successively finer grades of carborundum powder, finishing with jeweller's rouge. A spot of Aquadag (colloidal graphite) was placed on the exposed end of each tungsten rod to prevent oxidation and to ensure good contact with the metal surface when deposited.

The glass discs were then mounted in position on the frame. The disc which was to form the anode was rigidly mounted and a second

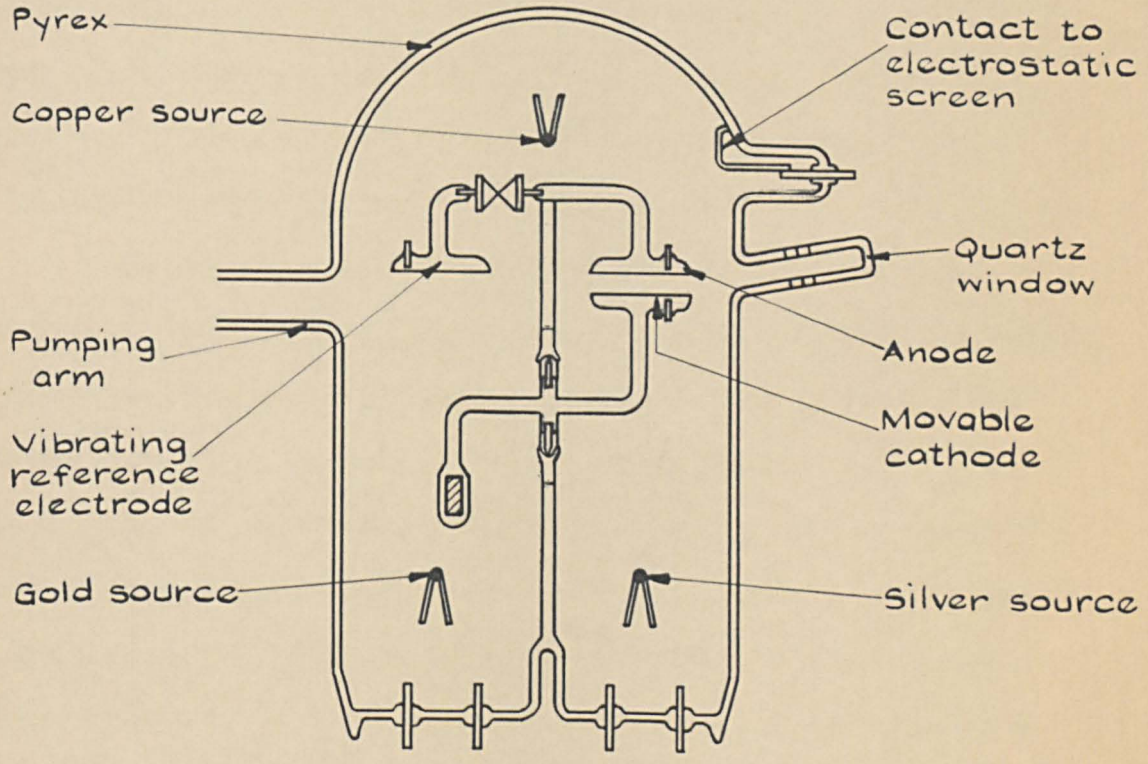

FIG. 18 SCHEMATIC DIAGRAM OF TUBES 1 AND 2

disc was joined to a spring made of two tungsten strips so that it could be made to vibrate, mainly in the vertical plane, at 20 to 30 c/s. The third disc was mounted on a glass hinge arranged so that it had two stable positions: under the anode and under the vibrating electrode. While this disc was being mounted, a machined plastic spacer was used to obtain parallelism between it and the anode. A glass-encased steel slug was added so that the electrode could be moved by the action of a magnet and the slug also served to balance the weight of the electrode.

A film of pure metal was deposited in vacuum on to each substrate by evaporation from a heated bead of the appropriate metal. These beads were made from high purity gold, silver and copper wire provided by Johnson Matthey Co. Ltd. A length of the appropriate wire (10 cms, 0.3 mm diameter) was wound on to a V-shaped heater of 0.5 mm diameter tungsten wire, which was spot-welded to two lengths of 24 s.w.g. nickel wire. The high purity metal wire was heated to melting point in a stream of hydrogen, so forming a molten bead in the V of the heater. This heating also served to reduce any oxides present and helped to remove impurities. On completion of the heating process, a cylindrical nickel shield was spot-welded in position around the bead to ensure that the metal surface would be deposited on the substrate alone, so preventing possible shorting of the electrical leads. The three assemblies were placed in position so that each bead could see the appropriate substrate. Gold was to be

deposited on the vibrating electrode, silver on the fixed anode and copper on the movable cathode.

The electrical connections were made to the pins of the pinch with nickel wire. In the case of the vibrating and movable electrodes, the connections were made with nickel tape in such a way that the free movement of the electrodes was unimpaired.

The envelope used was a commercial C9 hard-glass envelope enlarged by glass-blowing to give increased clearance between the electrodes and the walls of the tube. Three side-arms were joined to the envelope, one of which provided the connection to the vacuum system and another a lead-out for a connection to the electrostatic screen. The third side-arm was connected to a quartz window via a graded seal and was carefully positioned so that ultra-violet light could be shone through it on to the cathode. The envelope was washed in nitric acid and distilled water and dried in an oven. Then the lead making the connection to the electrostatic screen was positioned in the side-arm by means of a tungsten seal. The inside of the envelope was coated with Aquadag, leaving a window in the coating so that the anode-cathode spacing could be checked after the drop-seal had been completed.

Before the electrode assembly was sealed into the envelope, the movable electrode (cathode) was positioned under the fixed electrode (anode) and the gap distance d was measured with a cathetometer. The electrode assembly was carefully positioned inside the envelope and

the envelope was drop-sealed to the pinch. The tube was then complete and was ready to be sealed to the vacuum system.

Tube 3 (figure 19) differed in many ways from tubes 1 and 2 but the constructional methods were often similar. As before, the basis of the tube was a glass frame mounted on a seven-pin pinch. Two glass substrates were made as described above, but their diameter was now approximately 3 cm. The substrate forming the cathode was fixed to the glass frame. A sliding mechanism was made from 5 mm glass rod and a sleeve of glass tubing of slightly greater diameter; and the mechanism was mounted on the frame. A substrate was joined to the glass rod, which was then inserted into the sleeve and a glass-encased steel slug added to the rod as shown in the figure. This slug both balanced the system and enabled the substrate to be moved by the action of a magnet. At this stage, the electrodes were adjusted so that they were parallel by holding them together and softening the sleeve support until it rested on the rod. The assembly was positioned as it would be when in use and tested for parallelism by use of the cathetometer. The electrical connection between the movable electrode and one of the pins of the pinch was made by nickel tape so that the anode retained its freedom of movement. The cathode connection of fine nickel wire was spot-welded to the tungsten pin and the free end welded to a tungsten seal.

Five side-arms were joined to the glass envelope, a sixth side-arm being joined to a quartz window by means of a graded seal and

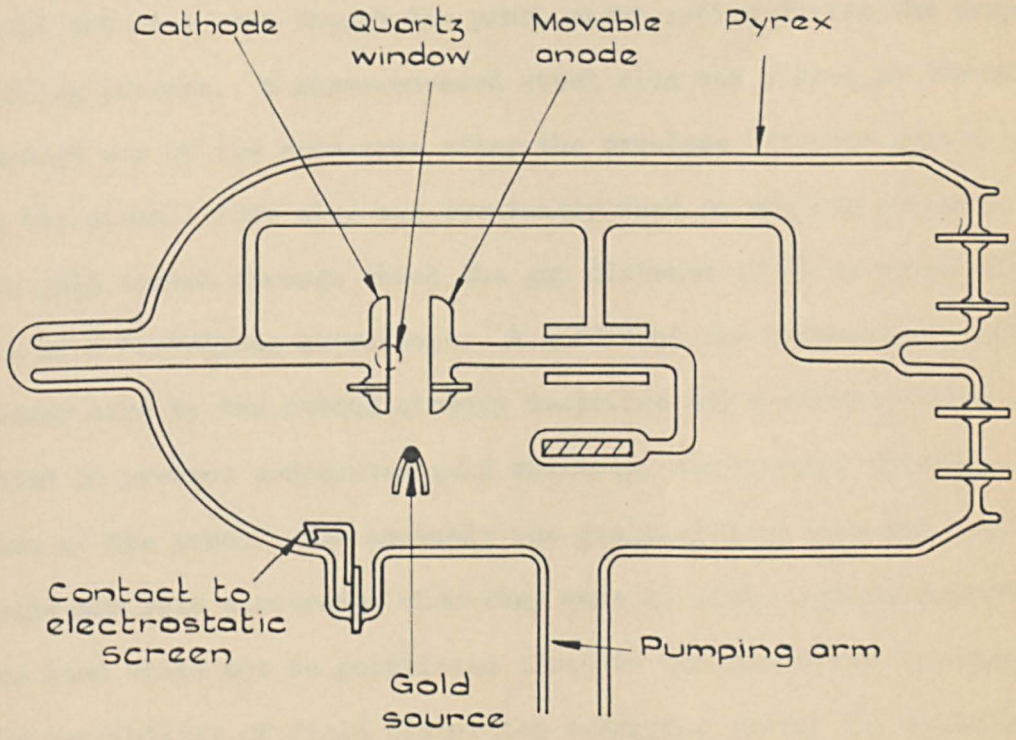

FIG. 19. SCHEMATIC DIAGRAM OF TUBE 3.

placed so that ultra-violet light could be shone on to the cathode. The electrostatic screen was provided by subsequent evaporation of gold on to the walls of the tube.

The electrode assembly was carefully positioned inside the envelope and the glass rod support was sealed into its side-arm. By this means, the electrode system was firmly held in position and would not move even though the pinch might soften during the drop-sealing process. A glass-encased steel slug was placed in the tube through one of the side-arms after the envelope had been drop-sealed to the pinch. This slug was eventually used to provide a window in the gold screen through which the gap distance could be measured by use of a travelling microscope. A gold bead was prepared on tungsten heater wire by the method already described and a nickel screen added to prevent evaporated gold reaching, and perhaps shorting, the pins of the pinch. The assembly was positioned so that the bead could see both electrodes when they were at their maximum separation. The bead could not be positioned close to the electrodes because of the possibility of field distortion occurring during the experiments. The bead assembly was positioned in a 20 mm diameter side-arm by means of two tungsten seals. The connection to the cathode was sealed into the appropriate side-arm and the tube was ready to be joined to the manifold.

Tube 4 (figure 20) was similar to tube 3. The only differences arose from the fact that nickel electrodes were used. These electrodes were

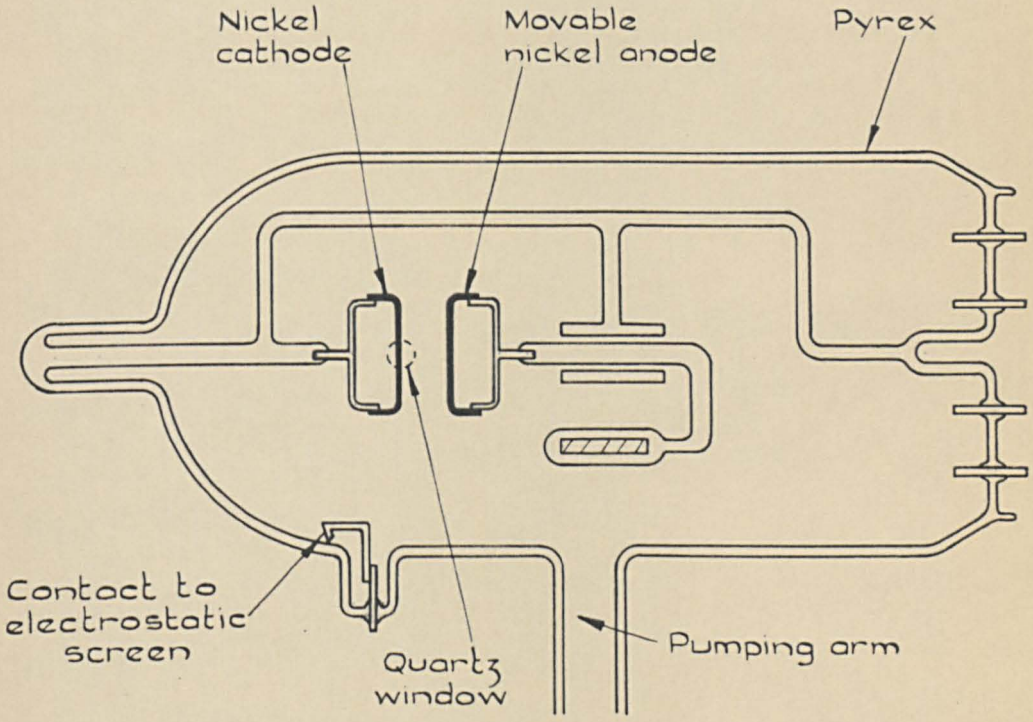

FIG. 20. SCHEMATIC DIAGRAM OF TUBE 4

formed from nickel sheet in a hydraulic press using specially made steel dies, such that the finished electrodes were 3 cm in diameter and had rounded edges. The electrodes were spot-welded to nickel wire on to which tungsten seals had been welded so that each electrode could be joined to a length of glass rod. There was now no need for the evaporation of metal, so the bead assembly, one of the side-arms and the second slug were eliminated. The electrostatic screen was now provided by a coating of Aquadag on the envelope walls, leaving an opening in the coating so that the gap distance could be measured.

4.4 Pressure measurement

Initially, when the system was being evacuated with the backing and diffusion pumps, it was useful to monitor the pressure over the range 10^{-4} to 10^{-6} torr and for this purpose a Penning gauge was constructed in the laboratory[71].

An Alpert gauge was used for the lowest pressure measurements (10^{-9} to 10^{-10} torr). The gauge used with the first system was assembled in the laboratory[71] and the pressure was then given by $p \approx \frac{1}{10} i_c/i_g$, where i_c is the collector ion current and i_g the electron current to the grid. Later, commercial gauges (Mullard IOG-12) were used for which $p \approx \frac{1}{12} i_c/i_g$. When pressure measurements were being made with the gauges, they were operated at low grid currents ($\sim$1 mA) for as short a time as possible to reduce the effect of the pumping action. The collector current at pressures greater than

10^{-7} torr was measured with a Cambridge multi-range galvanometer and, at pressures lower than this, a Vibron 33B electrometer was used.

It was also necessary to know the pressure of the gas in the manifold, which usually ranged from 7 to 70 torr. To give greater accuracy than that available from a mercury manometer, manometers filled with silicone oil (D.C. 703) were used and a conversion factor[71] was applied to the oil manometer reading to give the pressure in torr.

To prevent the gas in the manifold from coming into contact with the manometer oil, a spiral gauge was connected between the systems as shown in figures 16 and 17. A difference in pressure across the gauge caused rotation of the spiral and the mirror attached to it, the rotation being observed by a lamp and scale arrangement. The system was pre-set so that, when no pressure difference existed across the gauge, the light spot on the scale was at zero. To measure the pressure in the manifold, the pressure in the gas system was adjusted to give zero deflection of the gauge and the appropriate manometer reading gave the required pressure.

4.5 Electrical measurements

(a) Work function measurements

The contact potential difference between two metals placed in contact is given by: c.p.d. = $|\phi_1 - \phi_2|$, where ϕ_1 and ϕ_2 are the work functions of the two metals[80]. This relationship is used in

the Kelvin method of measuring work functions, in which the surface of unknown work function and a vibrating reference surface form the plates of a capacitor. When the reference surface is made to vibrate, an oscillating potential appears across a high resistance connecting the surfaces. A variable reverse potential is applied to the plates and, when this is equal in magnitude to the contact potential, the oscillating potential vanishes. This provides a method of measuring the contact potential and, if the work function of the reference surface is known, the unknown work function can be determined.

In the present work, the reference surface was a gold film evaporated on to a glass substrate and the work function of such a film has been given by Riviere[81] as 4.7 eV. However, it was not important that this should be known accurately, since the main interest was in changes of work function. The changing potential across the high resistance (10^8 Ω) was amplified by a conventional low frequency amplifier[71], the output signal of which was displayed on an oscilloscope. The backing-off potential was adjusted until the amplitude of the sinusoidal trace on the oscilloscope reached a minimum and this value of the voltage gave the required contact potential. Since ϕ_1 was known, ϕ_2 was immediately available. In these measurements, it was important that the electrical components were carefully screened, otherwise the signal was masked by electrical interference.

(b) Formative time lag measurements

The voltage supply to the experimental tubes was provided by a bank of 120 volt H.T. batteries connected in series. Coarse adjustment of the voltage was supplied by adding to or subtracting from the number of batteries and fine adjustment was provided by a voltage divider across one of the batteries. The batteries were connected across a calibrated resistance chain which had several tapping points (figure 21a), and the voltage across part of the chain was measured by means of a potentiometer. In this way, the voltage supplied to the tube could be measured to better than $\pm$ 0.1%.

The formative time lags were expected to be of the order of milliseconds, so a mercury switch (measured rise time $\sim$ 0.1 μsec) was suitable for the application of the voltage pulse to the tube. The time between the application of the overvoltage and breakdown of the gap was observed by use of an oscilloscope. A resistance (100 KΩ to 10 MΩ) was connected in series with the electrodes and, on applying the voltage to the tube, a charging pulse flowed in the circuit. This pulse triggered the oscilloscope which was connected across the resistance. Breakdown of the gap caused a voltage to appear across the resistance and so the oscilloscope trace was of the form shown in figure 21(b), in which the formative time lag measurement is indicated.

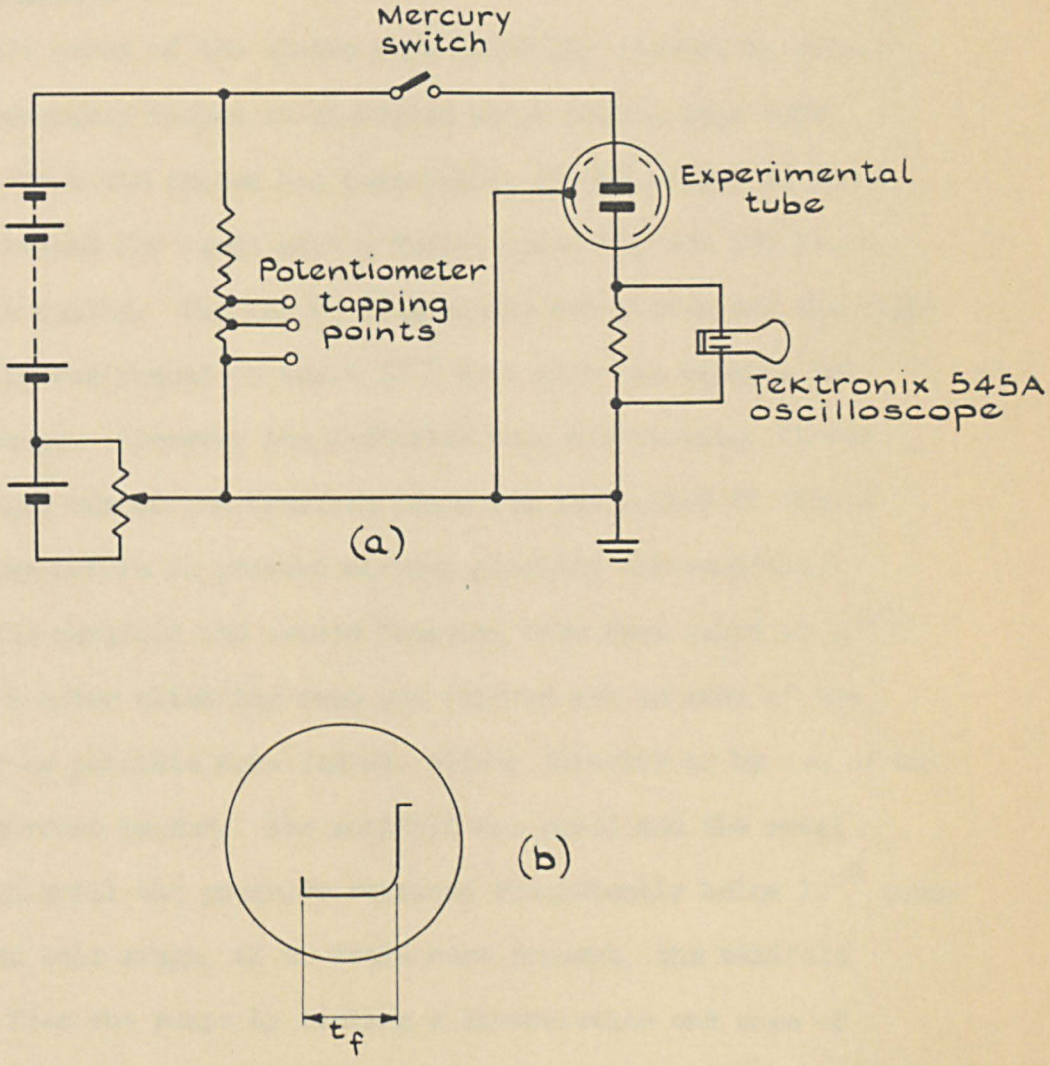

FIG. 21 FORMATIVE TIME LAG MEASUREMENT.
(a) ELECTRICAL CIRCUIT (b) OSCILLOSCOPE TRACE SHOWING THE FORMATIVE TIME LAG, t_f.

4.6 Experimental procedure

The experimental procedure can be conveniently described in two parts since two vacuum systems were used.

(a) System 1

All parts of the system were carefully cleaned in nitric acid and thoroughly washed in distilled water before they were assembled. Once the system had been built, it was pumped to about 10^{-1} torr, tested for leaks with a Tesla spark-coil and any leaks present were sealed. The tap T_3 (figure 16) was closed and the high vacuum system was pumped to about 10^{-6} torr with the backing and diffusion pumps. Whenever the diffusion pump was running, it was important that one of the freezing traps was maintained at liquid nitrogen temperature to prevent mercury reaching the manifold.

The manifold and second freezing trap were baked at 450°C for 12 hours after which the oven was removed and as many of the metal parts as possible were heated, either directly or by use of an r.f. eddy current heater. The manifold was baked and the metal parts heated until the pressure remained consistently below 10^{-6} torr.

At this stage, if no leaks were present, the manifold was closed from the pumps by sealing a constriction and some of the getters were fired. The pressure in the manifold was measured with the Alpert gauge and the system left for 24 hours. If no pressure rise ensued, the Alpert gauge was used as a pump and the pressure eventually fell to about 10^{-8} to 10^{-9} torr.

The gas system was prepared while the manifold was being pumped with the Alpert pump. Once the system had been freed of leaks, it was pumped to about 10^{-6} torr with the backing and diffusion pumps and the manometer oil was heated with a hand torch to drive off any dissolved gases. Also, as much of the glass-ware as possible was outgassed by heating with a hand torch. Liquid nitrogen was placed around the activated charcoal, taps T_2, T_4 and T_5 were closed and the helium flask was opened by use of the slug. The tap T_1 was then closed and T_2 opened, resulting in a low pressure of helium in the gas system. The helium was left over the charcoal for 24 hours, after which time the gas was ready for admittance to the manifold.

At this stage, the metal surfaces were deposited and a pressure rise usually ensued. The pressure was soon reduced to its original value by firing the remaining getters and further use of the Alpert pump. Measurements of the work function of the cathode surface were made soon after deposition.

A low pressure of helium was obtained in the manifold by opening the tap T_3 and a glow discharge was started in the cataphoresis tube. After the discharge had been running for two or more hours, formative time lag measurements were made, the cathode being illuminated with ultra-violet light from a high pressure mercury vapour discharge lamp. At a given pressure, the sparking potential was measured and the voltage setting calculated to give a particular value of percentage

overvoltage. The formative time lag was measured and was usually the average of some 20 readings. An interval of 10 seconds elapsed between successive voltage applications to allow the decay of charge which may have appeared on the electrodes.

(b) System 2

All the glass components were cleaned in nitric acid and washed in distilled water before assembly. The metal taps V_1, V_2 and V_3 (figure 17) were opened and the high vacuum system was processed in the same way as described for the first system. Before baking, however, the metal taps had to be prepared according to the manufacturer's instructions.

On sealing-off the manifold from the pumps, it was found that a low pressure could not be maintained. However, on closing V_1 and repeating the outgassing procedure, the system behaved satisfactorily. Further, on replacing the gas system by a sealed-off tube and repeating the procedure with V_1 open, low pressures could again be maintained in the manifold. When other helium bottles were added and the procedure repeated, the pressure rose at the same rate in each case. It was decided that the only possibilities were that the glass seals of the helium flasks were faulty or that helium was diffusing through the thin glass of the seals. It seemed unlikely that the seals should be faulty in each case, so the possibility of helium diffusion was considered in more detail (section 5.3). It was found that the observed and calculated rates of pressure

increase agreed sufficiently closely to lend weight to this hypothesis.

As a result, the experimental procedure was modified. The manifold was pumped to about 10^{-6} torr with V_1, V_2 and V_3 open. The taps were prepared for baking and the manifold was baked at 450°C for 12 hours. After the oven had been removed, the metal parts were outgassed. This cycle was repeated until the pressure did not rise above 10^{-6} torr at any stage, whereupon V_1 was closed. The usual procedure (described for system 1) was then followed and the pressure in the manifold could easily be reduced to about 10^{-9} to 10^{-10} torr.

The pressure measuring system was completely separate from the high vacuum and gas supply systems, so there was no need to attain very low pressures in this case, since 10^{-3} torr was quite adequate for the one arm of the manometer.

The helium flask was then opened and controlled amounts of the gas were let into the manifold by use of taps V_1 and V_2. Formative time lag measurements were carried out as described previously.

Chapter 5

RESULTS AND DISCUSSION

Formative time lag and other measurements were made using the four experimental tubes described in the previous chapter. These met with varying degrees of success and the most significant measurements came from experiments in which the fourth tube was used.

The experimental readings obtained from each tube are described in this chapter and, in general, the results will be interpreted as they are presented. The chapter ends with a summary of the conclusions reached, together with suggestions for further work.

5.1 Work function measurements

Of the four tubes constructed during the course of the investigation, tubes 1 and 2 contained facilities for the measurement of the work function of copper films deposited on glass substrates. Since the main emphasis of the work was on the time lag experiments, the work function measurements were of a preliminary nature only. Even so, it is of interest to describe the main trends observed.

In all cases the metal beads were thoroughly outgassed before evaporation. In practice this meant that a very thin film of the metal was deposited on the glass substrates before measurements

were made. The residual gas pressure in both tubes before deposition of the surfaces was 7×10^{-9} torr.

After the gold reference surface had been deposited on the vibrating electrode, evaporation of the copper bead on to the appropriate electrode was begun. This continued until the hot metal bead could no longer be seen through the glass substrate on which the film was being deposited. The thickness at which the copper film became opaque was taken to be of the order of 1700 Å[82]. Once this thickness had been achieved, evaporation was stopped and the contact potential between the film and the reference surface was measured.

On observing the variation of the work function of the copper film with time after deposition, a curve such as that given in figure 22 was obtained. It can be seen that the work function of the film rose from 4.94 to 5.62 eV over a period of about 40 minutes, after which time it remained essentially constant. In fact, some 13 days later the value of the work function was still 5.62 eV.

By comparison with these values, Riviere[81] obtained a figure of 4.52 eV for the work function of a freshly deposited copper film, which was in good agreement with values given by other workers. However, he suggested that care was needed in the attainment of a good vacuum before reproducible results could be obtained. Riviere deduced that the partial pressure of any

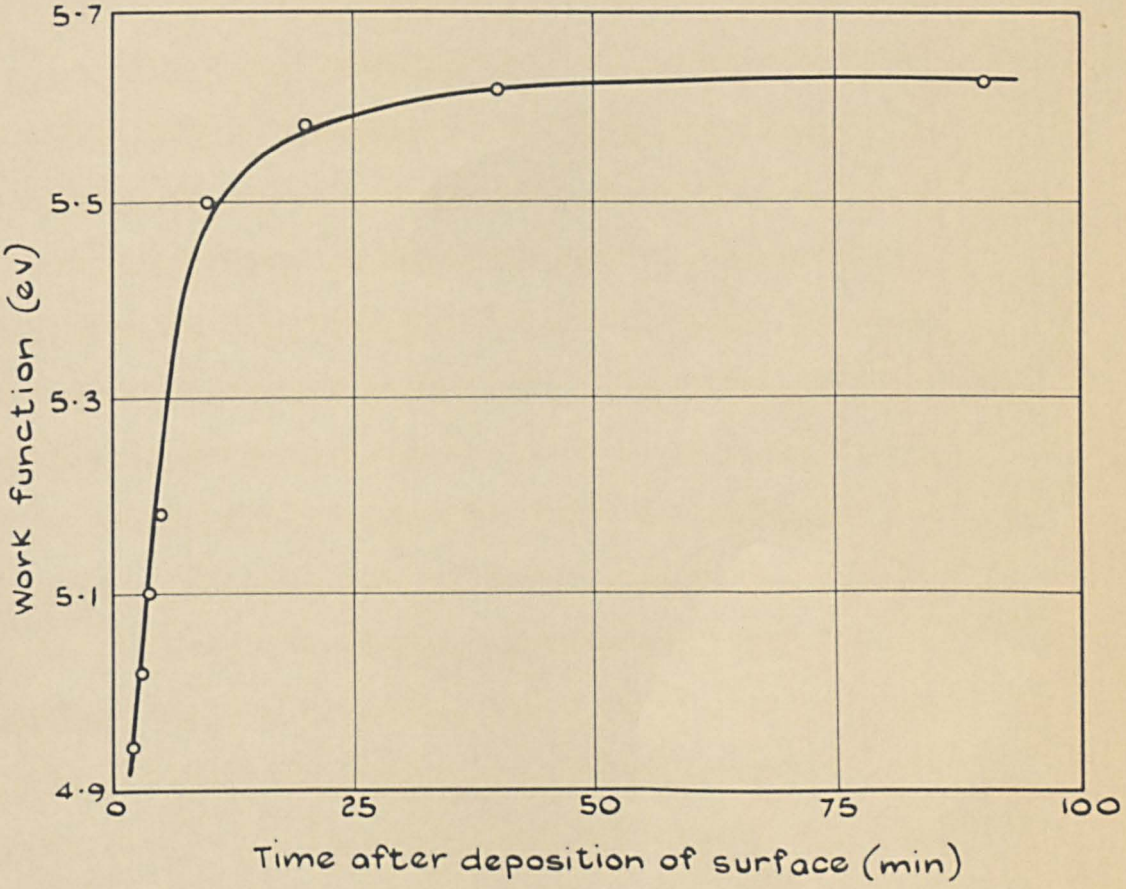

FIG. 22 VARIATION OF THE WORK FUNCTION OF A COPPER FILM WITH TIME. DEPOSITION OF THE SURFACE WAS COMPLETED AT TIME $t = 0$.

adsorbable gas in his tubes must have been less than 10^{-12} torr. By comparison, the pressure at which the present experiments were conducted was of the order of 10^{-8} torr. At pressures of this order and assuming a sticking coefficient of unity, a monolayer of gas would form on a surface in some tens of minutes. Thus it is probable that the work function change observed was due, at least in part, to the adsorption of residual gas.

One of the residual gases in the tube was likely to be oxygen and a monolayer of oxygen on the surface of the copper film would raise its work function[85]. Atoms of oxygen incident on a metal surface capture electrons from the metal on impact because of their electron affinity. They then set up a dipole layer with its negative charge outwards, so raising the work function of the surface. Changes in work function of more than 2 eV can be produced by ions adsorbed in this way. Thus the change of 1.1 eV (5.62 - 4.52 eV) can be satisfactorily explained by the adsorption of residual oxygen by the freshly deposited copper film.

From the relation $d\phi/q = \sigma M/\varepsilon_o$ [84] (where $d\phi$ = work function change, q = electronic charge, σ = number of aligned molecules per unit area, M = dipole moment of each molecule and ε_o = permittivity of free space), the average dipole moment of an adsorbed oxygen atom on the copper surface can be calculated to be approximately 0.38 debye unit.

It is unlikely that the observed work function change was due to a change in work function of the gold reference surface, since it has been shown[84] that gold does not adsorb oxygen at room temperature.

In passing, it may be noted that Farnsworth[85] observed that films evaporated on to surfaces at room temperature have work functions lower than the corresponding bulk metals. On annealing, the work functions of the films alter to those of the bulk metals and changes as great as 0.3 eV have been observed. This difference in work function was attributed to the presence of large densities of lattice defects in the films. Thus, it is possible that the change observed in the present experiments may have been partly due to an annealing effect.

On completion of these experiments, helium was admitted to the experimental tubes at a pressure of 6.7 torr and the work function of the copper surface was monitored. In each case, no significant variation in work function was detected over a period of 90 minutes. This is possibly not surprising since the films were already covered with a strongly adsorbed layer of oxygen. Moreover, from Weissler and Wilson's[86] experiments on the work functions of gas-covered surfaces, helium would be expected to have only a small effect on the work function of a clean surface. For example, Weissler and Wilson produced a change of only 0.2 eV

in the work function of a freshly deposited silver film by admitting helium and passing a glow discharge to the film.

5.2 Time lag measurements, tubes 1 and 2

Some time was spent in an attempt to obtain satisfactory formative time lag data from tubes 1 and 2. However, it was finally decided that there would have been little value in making a detailed analysis of the results obtained, so this section will contain only a brief account of this series of measurements.

Tubes 1 and 2 were used in conjunction with the first (figure 16) of the two vacuum systems described in section 4.2. Helium was admitted to the tubes after standing over activated charcoal at -192°C for 4 hours and was further purified by cataphoresis before experiments were carried out at various pressures. Both the copper and silver films were used as cathodes in these measurements.

On starting the measurements, it was immediately found that it was difficult to determine the true value of the sparking potential. As can be seen from the two curves given in figure 23, times greater than 1 minute could elapse between application of the voltage and breakdown of the gap. The reason for the difference between the two curves probably lies in the fact that the cathode in tube 1 had the higher work function by some 0.6 eV.

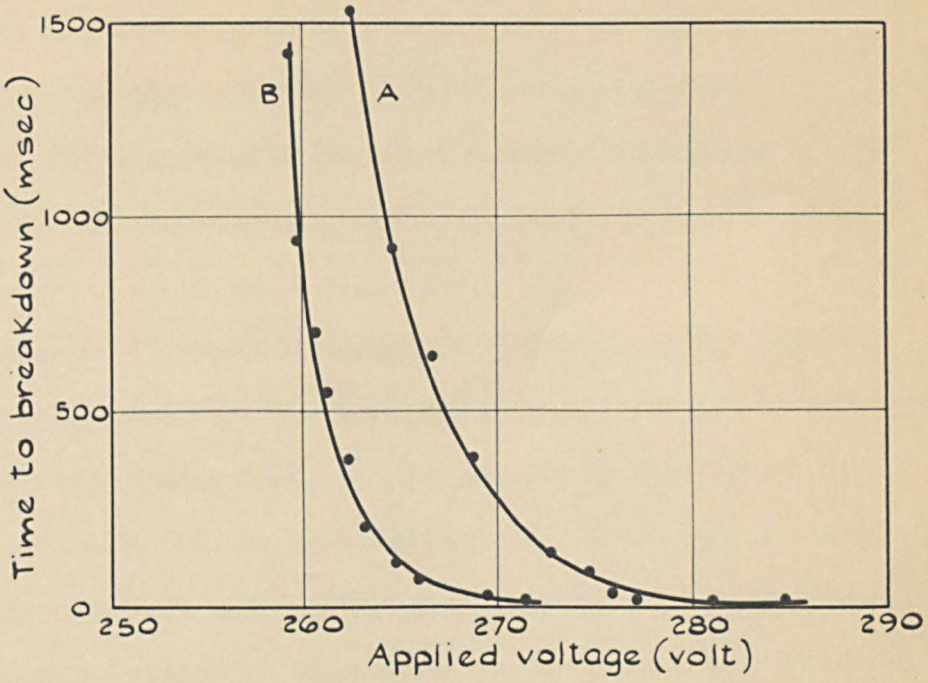

FIG. 23 TIME TO BREAKDOWN AS A FUNCTION OF APPLIED VOLTAGE. COPPER CATHODES IN HELIUM, p_o = 7·2 torr. A, TUBE 1 ; B, TUBE 2.

The long breakdown times observed were obviously not true formative time lags, since it has previously been indicated (section 3.3) that these should be of the order of tens of milliseconds only. Moreover, the statistical time lag had been eliminated in the measurements by the constant illumination of the cathode with ultra-violet light. Thus some other explanation must be provided.

Because of the ultra-violet illumination of the cathode, pre-breakdown currents were continuously passing between the electrodes during the voltage application. As seemed likely from the work function measurements of the previous section, it is possible that there was an insulating oxide film on the cathode. In fact, Davies, Fitch, Hopkins and Gozna[40] have postulated the existence of such an insulating layer on which positive ions could reside for some considerable time. So it could be that positively charged particles from the pre-breakdown current remained on the insulating layer, gradually increasing in number until the work function of the surface was reduced sufficiently for the secondary emission from the cathode to lead to breakdown.

Similar effects were observed[71] when determining the sparking potential in hydrogen using nickel cathodes coated with thermionic oxides.

In an attempt to obtain time lag curves, an arbitary method of determining the sparking potential was employed. The

voltage was applied to the tube at one minute intervals, gradually increasing the voltage until breakdown took place within 10 seconds of the voltage application. In this way, an apparent sparking potential was determined and two of the curves obtained giving the time lag as a function of percentage overvoltage are shown in figure 24. In view of the uncertainty involved in these measurements, no attempt will be made at interpreting these curves.

5.3 Measurements carried out with tube 3

The results obtained from tubes 1 and 2 were open to criticism because of the design of the vacuum system. This was such that the final admission of helium to the tubes took place through a greased stopcock which was an obvious source of gas contamination. A further source of contamination was the manometer oil with which the helium was in contact before admission to the tubes.

The fixed gap distance of the tubes placed a considerable limitation on the range of measurements which could be made. Furthermore, additional complications were introduced by the inclusion of facilities for work function measurements. The prime aim of subsequent experiments was the measurement of formative time lags, and it was with these considerations in mind that tube 3 and the second vacuum system were constructed.

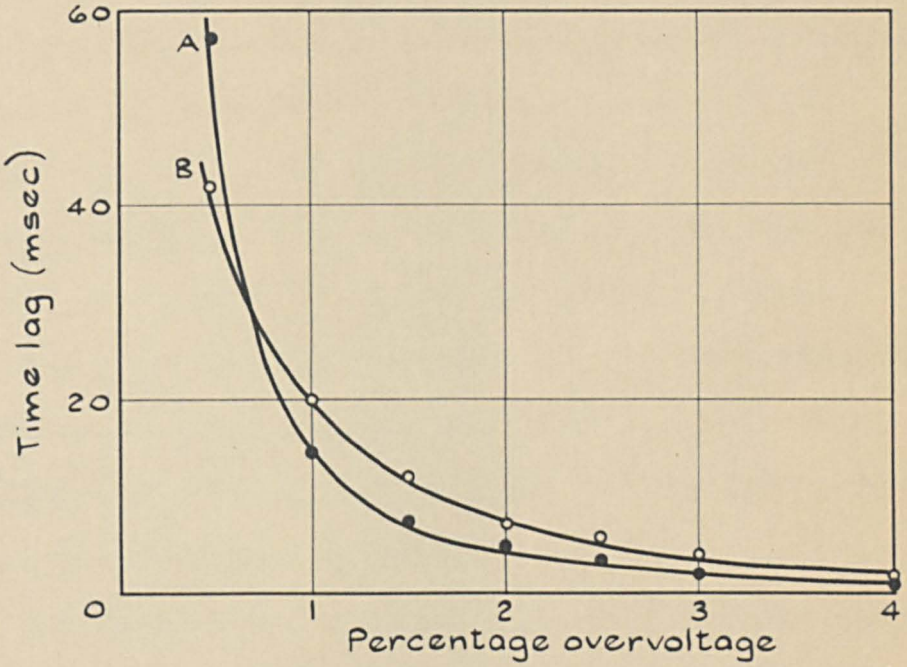

FIG. 24 TIME LAG AGAINST PERCENTAGE OVERVOLTAGE. COPPER CATHODES IN HELIUM, p_0 = 27·4 torr. A, d = 0·26 cm AND E_s/p_0 = 38·3 VOLT cm^{-1} $torr^{-1}$; B, d = 0·35 cm AND E_s/p_0 = 30·9 VOLT cm^{-1} $torr^{-1}$.

The main features of tube 3 (section 4.3, figure 19) were the variable gap distance and the increased electrode size which reduced distortion of the electric field between the electrodes. The improved design of the new vacuum system (section 4.2, figure 17) meant that the helium supply line could be reduced to pressures of the order of 10^{-9} torr and at no time did the helium come into contact with greased stopcocks, as bakeable metal taps were now employed. Further, the helium no longer came into contact with the manometer oil before admission to the tubes.

Because of the improved design of the vacuum system, it became apparent, for the reasons given in section 4.6(b), that the possibility of helium diffusion through the thin glass seal of the helium flask should be considered.

The quantity of gas q passing in time t through a plane membrane of area A and thickness d with a pressure gradient Δp is given by: $q = K A \Delta p \, t/d$. The permeation constant K for helium diffusing through Pyrex has been given by Altemose[87]. Making a number of assumptions and estimating the dimensions involved, the pressure resulting in the system after 20 hours was calculated to be of the order of 10^{-4} torr, compared with the measured value of 4×10^{-5} torr. This indicated that it was possible for helium to diffuse through the seal at a rate sufficient to account for the pressure rise observed (figure 25).

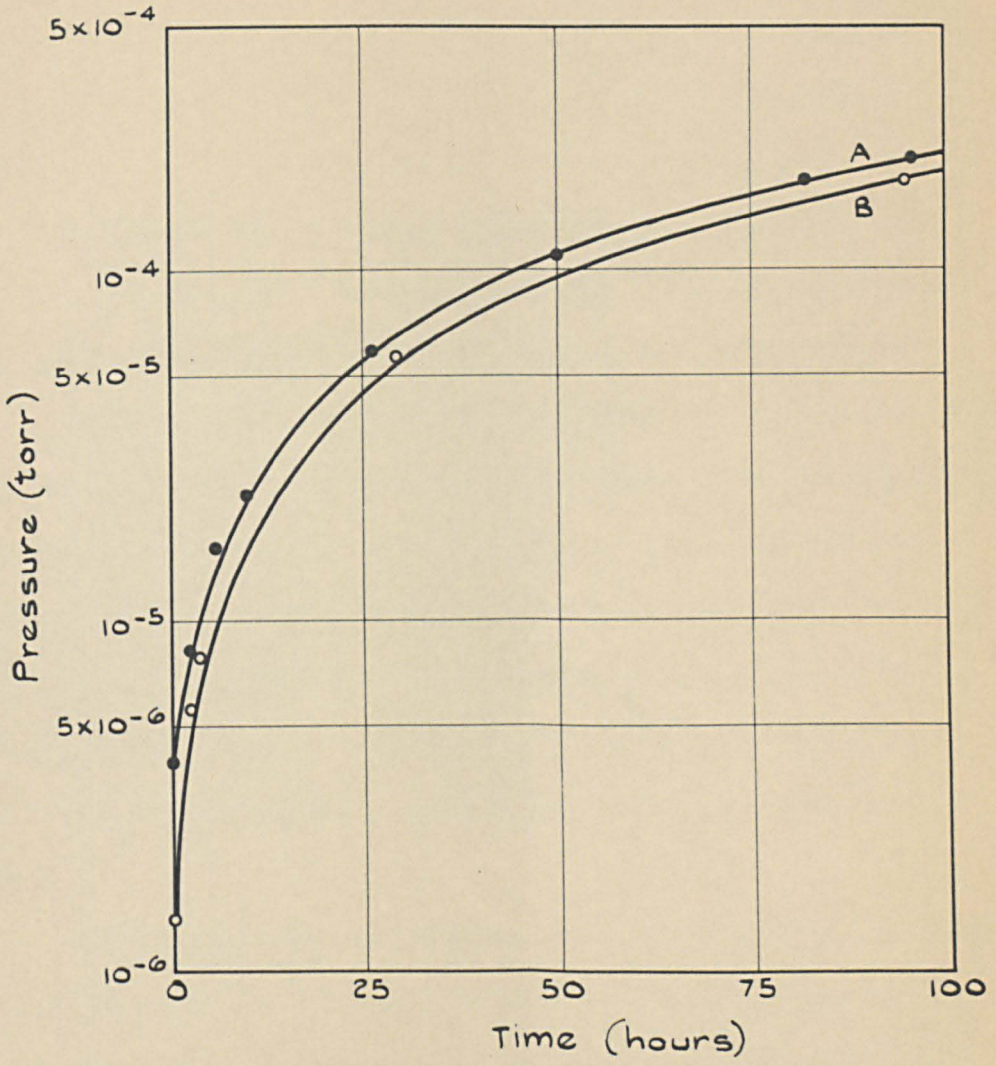

FIG. 25 RATE OF INCREASE OF PRESSURE.
A, FIRST CLOSURE; B, SECOND CLOSURE AFTER MORE RIGOROUS OUTGASSING.

The residual gas pressure in the experimental tube was successfully reduced to 4×10^{-10} torr by following the procedure described in section 4.6(b). Gold was then evaporated on to the glass substrates to form the electrodes. Helium was admitted to the tube and a series of measurements started.

Unfortunately, a similar difficulty was encountered as was met in tubes 1 and 2. Once again it was virtually impossible to obtain the true sparking potential and occasionally times as long as 7 seconds were observed before breakdown of the gap occurred. This was an improvement over the previous tubes, where the corresponding times could be as long as a minute. Even so, this was still not good enough to allow accurate measurement of the formative time lag from which a true indication of the secondary processes taking place could be obtained. A typical curve showing the dependence of these long breakdown times on applied voltage is given in figure 26.

On observing the discharge it was found that it was located at the Aquadag spots on the electrodes. One of the electrodes was then rotated so that the spots were no longer directly opposite each other, all other conditions remaining constant. As a result the discharge would no longer take place. So it seemed that the gold films were not sufficiently thick. This was borne out by subsequent examination of the electrodes when they were found to

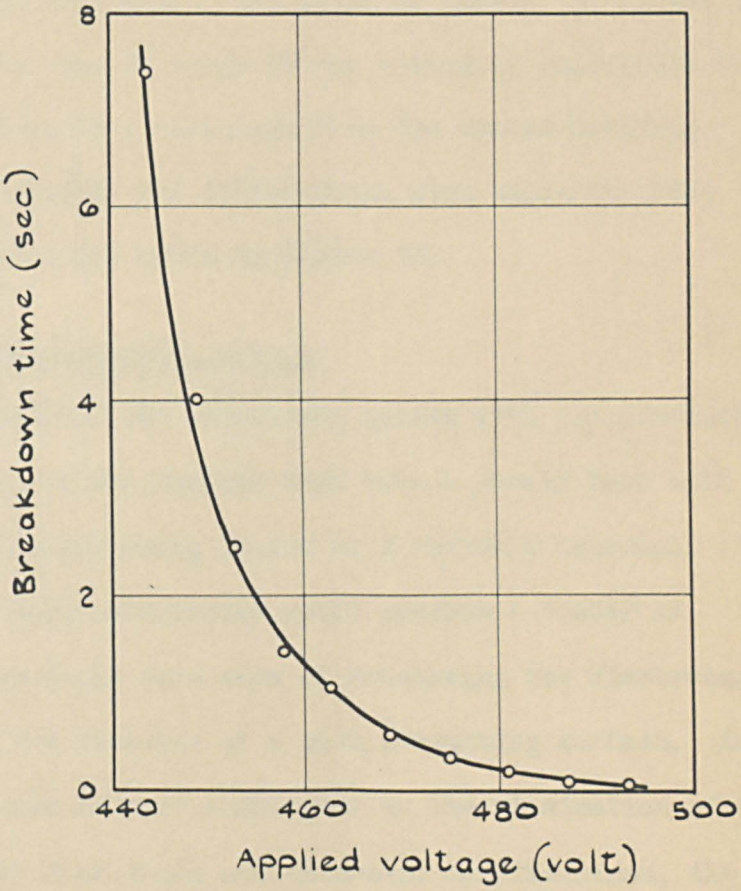

FIG. 26 TIME TO BREAKDOWN AS A FUNCTION OF APPLIED VOLTAGE. GOLD CATHODE IN HELIUM, p_o = 42 torr, d = 0·47 cm.

be transparent to visible light, one estimate of the film thickness being given as a few hundred angstrom units.

As before, curves giving the dependence of time lag on percentage overvoltage were obtained by using an arbitrary criterion to set the sparking potential. But, also as before, no weight could be attached to these curves since it was virtually impossible to divorce the true formative time lags from the charge build-up effects. For the record, two curves which were characteristic of these measurements are shown in figure 27.

5.4 Preliminary measurements, tube 4

As a result of the experience gained with the previous experimental tubes, it was decided that tube 4 should have bulk metal electrodes, nickel being chosen as a suitable material. It was expected that these electrodes would provide a number of advantages, amongst which were ease of outgassing the electrodes and confidence in the presence of a good, conducting surface. As a result the tube was further simplified by the elimination of the gold source. Apart from these and attendant modifications, the tube (section 4.3) was closely similar to tube 3, a common feature of both tubes being the variable inter-electrode spacing.

So that a quick check on the behaviour of the tube might be made, the residual gas pressure was reduced to 10^{-6} torr only and preliminary measurements carried out.

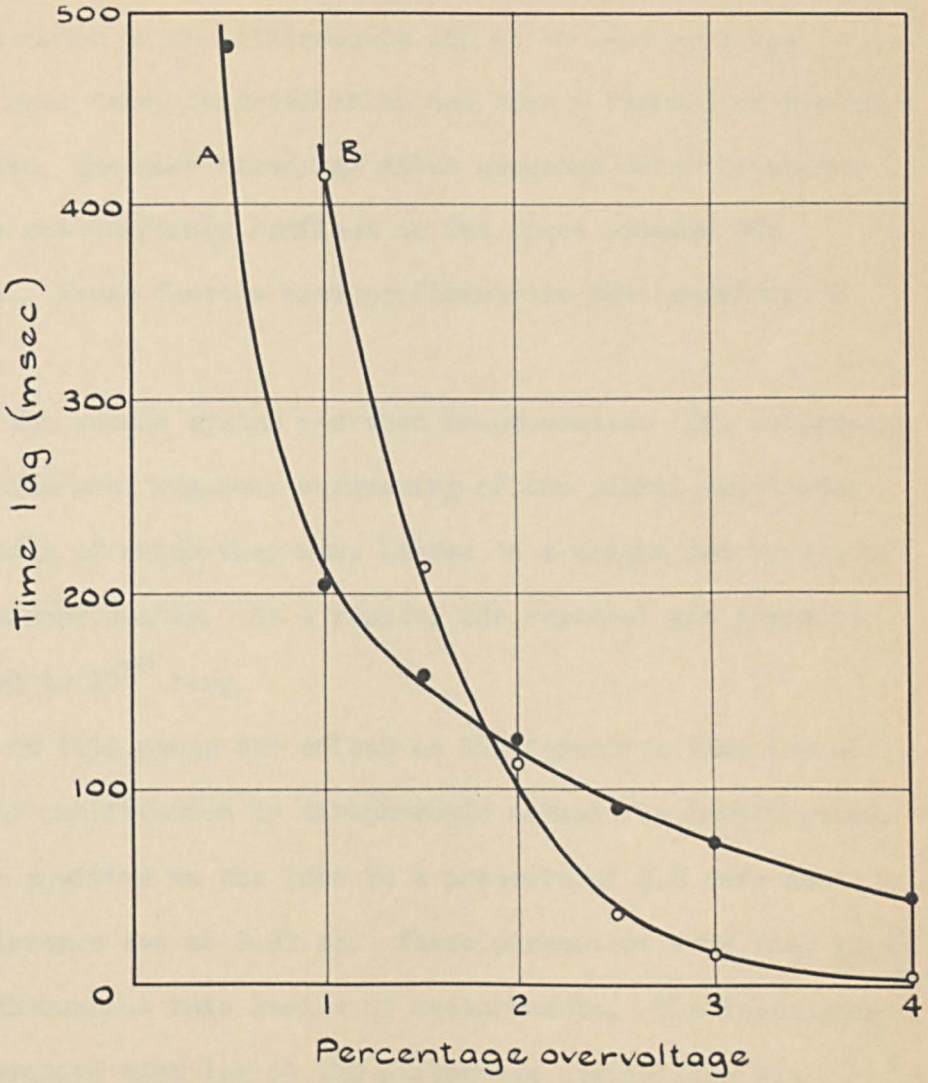

FIG. 27 TIME LAG AS A FUNCTION OF PERCENTAGE OVERVOLTAGE. GOLD CATHODE IN HELIUM AT 42·0 torr. A, d = 0·53 cm AND E_s/p_o = 17·6 volt cm^{-1} $torr^{-1}$; B, d = 0·19 cm AND E_s/p_o = 39·2 volt cm^{-1} $torr^{-1}$.

On admitting helium to the tube to a pressure of 46 torr, the longest time to breakdown that could be obtained was of the order of 20 milliseconds and at no time were the long breakdown times observed which had been a feature of previous tubes. Also, the glow discharge which occurred after breakdown of the gap was uniformly confined to the space between the electrodes. These factors bred confidence in the behaviour of this tube.

The vacuum system was then re-processed. The outgassing procedure included rigorous outgassing of the nickel electrodes in the course of which they were heated to a bright red by use of an eddy current heater. As a result, the residual gas pressure was reduced to 10^{-8} torr.

At this stage the effect on the formative time lag of further gas purification by cataphoretic action was investigated. Helium was admitted to the tube to a pressure of 6.8 torr and the gap distance set at 0.92 cm. These parameters were then kept constant throughout this series of measurements. The dependence of the formative time lag on the percentage overvoltage was measured without use of the cataphoresis tube and the smooth curve which resulted is shown in figure 28 (curve A).

Immediately these readings had been completed, a glow discharge was started in the cataphoresis tube, when a current of 15 mA passed between the electrodes at a potential difference of 500 volts.

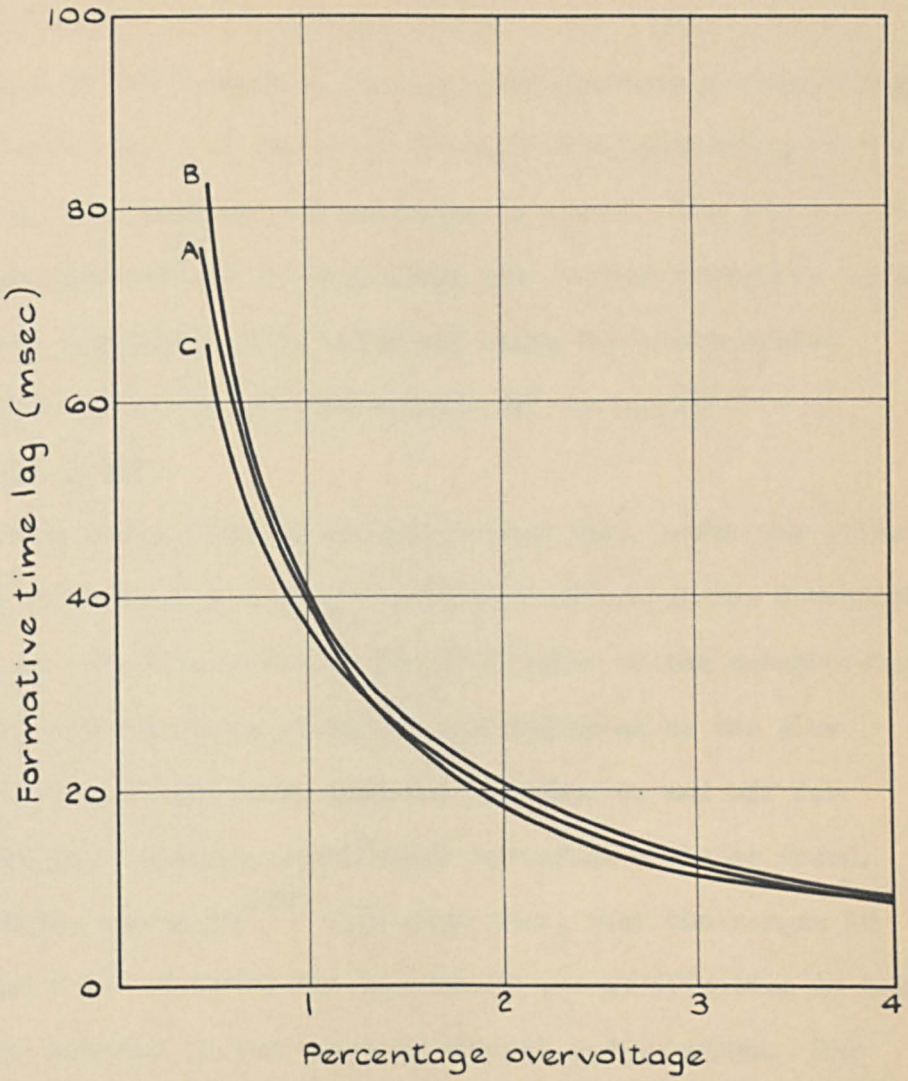

FIG. 28 THE EFFECT OF CATAPHORESIS ON THE FORMATIVE TIME LAG IN HELIUM. $p_0 = 6{\cdot}8$ torr, $d = 0{\cdot}92$ cm AND $E_s/p_0 = 32{\cdot}4$ volt cm^{-1} $torr^{-1}$. A, BEFORE USE OF CATAPHORESIS; B, 4 HOURS AFTER SWITCHING ON THE CATAPHORESIS DISCHARGE; C, 66 HOURS AFTER CURVE B WAS OBTAINED.

After the cataphoretic action had been taking place for 4 hours, a second curve (figure 28, curve B) was obtained showing the variation of the formative time lag with percentage overvoltage. A similar curve (curve C) was also obtained after the cataphoretic discharge had been running for a further 66 hours. The discharge was then switched off and 5 hours later yet another formative time lag curve was measured. This curve lay among the three curves already given and is not plotted because of the possibility of confusing the graph.

From these readings it can be seen that, under the given conditions, cataphoresis had no significant effect on the formative time lag. As a further check on the efficiency of the cataphoretic purification, the sparking potential was monitored as the glow discharge in the cataphoresis tube was switched on and off for varying periods. Again no significant variation could be found.

Riesz and Dieke[77] indicated that, over the ranges 10 to 25 mA and 10 to 20 torr, the process of gas purification in helium was greatly enhanced by increases in current and pressure. The present experiments were carried out at 15 mA and 6.8 torr which roughly corresponded to the lower ranges used by Riesz and Dieke. Even so, it would have been expected that some clean-up should have taken place. In the same way that a limit was set on Riesz and Dieke's values of current and pressure, these parameters were limited in the present experiments by the nature of the available power supply.

A further possibility for the apparent lack of purifying action is that the helium used was relatively pure. Every precaution had been taken not to introduce impurities other than those trace impurities which may have already been present in the spectroscopically pure helium. It is probable that these two factors in combination meant that the cataphoretic action had no significant effect on the discharge parameters investigated.

5.5 Formative time lag measurements, tube 4

The vacuum system was re-processed after the preliminary measurements of the previous section. A residual gas pressure of the order of 10^{-9} torr was achieved after the system had been baked a number of times, each bake being followed by outgassing of the metal components. The electrical measuring circuits were then set up, helium was admitted to the tube and the final series of formative time lag measurements were begun.

At a given value of pressure a suitable gap distance was set and the corresponding sparking potential measured. The required voltage to be applied to the tube to give a convenient value of percentage overvoltage was then calculated. The same values of percentage overvoltage were used for each curve so that the data was readily acceptable to a computer. The formative time lag was the average of some ten measurements at each value of percentage overvoltage, ten seconds elapsing between each measurement. The gap

distance was then altered and in this way a number of curves of formative time lag against percentage overvoltage were obtained at a given pressure.

The helium pressure was then increased by admitting more helium to the tube and another set of time lag curves obtained. In this way 25 curves were obtained at 5 different pressures in the range 14.9 to 62.2 torr at gap distances varying from 0.18 to 0.82 cm. These curves are shown in figures 29 to 33, the same co-ordinates being used in each case for ease of comparison.

As is common practice, the pressure given is the reduced pressure corresponding to that at 273°K. The resistance in series with the tube was 470 kΩ throughout the measurements. Other conditions prevailing during the experiments included continuous ultra-violet illumination of the cathode and earthing of the electrostatic screen. The cataphoresis effect was not used for the reasons already given.

Since sparking potentials and gap distanceshad been measured, the necessary data was available for the production of Paschen curves. Five of these curves (figure 34) were obtained, each at constant pressure and varying inter-electrode distance.

It was also possible to obtain curves (figure 35) of the generalized secondary coefficient from the sparking potential by use of the breakdown criterion (equation 7). These secondary emission curves were calculated using Davies, Llewellyn Jones and Morgan's

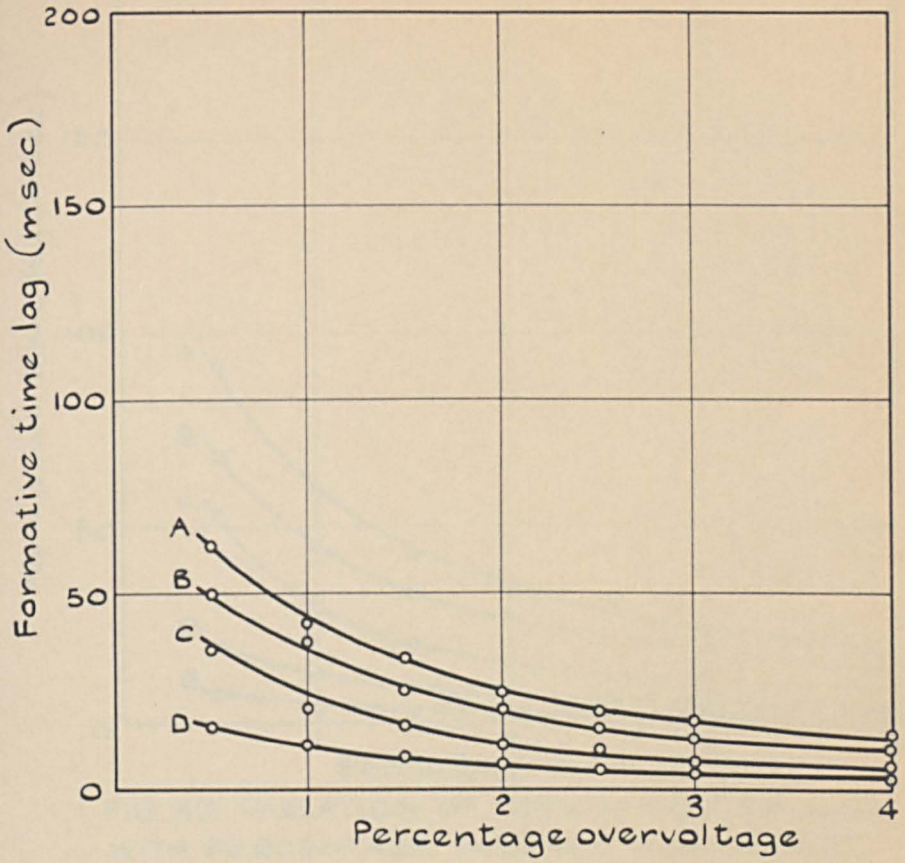

FIG. 29 VARIATION OF FORMATIVE TIME LAG WITH PERCENTAGE OVERVOLTAGE. NICKEL ELECTRODES IN HELIUM AT CONSTANT PRESSURE, p_0 = 14·9 torr.

Curve	d (cm)	E_s / p_0 (volt cm^{-1} torr^{-1})
A	0·78	22·0
B	0·68	23·7
C	0·53	27·4
D	0·34	38·7

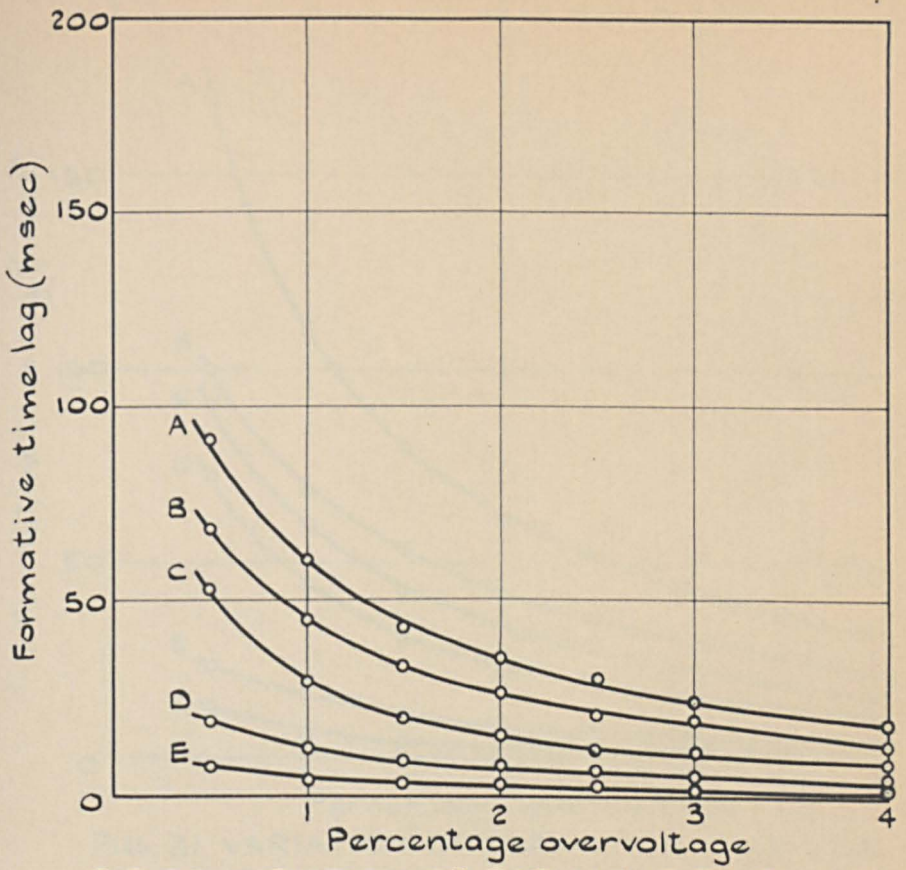

FIG. 30 VARIATION OF FORMATIVE TIME LAG WITH PERCENTAGE OVERVOLTAGE. NICKEL ELECTRODES IN HELIUM AT CONSTANT PRESSURE, $p_0 = 22 \cdot 1$ torr.

curve	d (cm)	E_s / p_0 (volt cm^{-1} $torr^{-1}$)
A	0·80	16·8
B	0·70	18·0
C	0·51	21·1
D	0·36	25·7
E	0·27	33·2

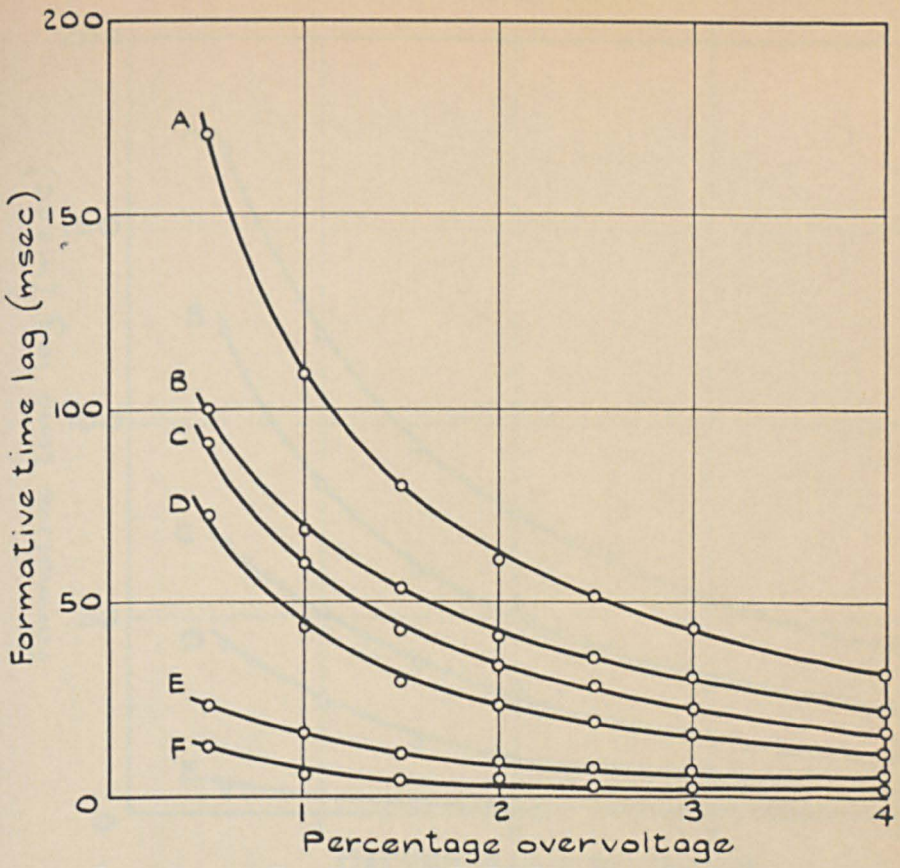

FIG. 31 VARIATION OF FORMATIVE TIME LAG WITH PERCENTAGE OVERVOLTAGE. NICKEL ELECTRODES IN HELIUM AT CONSTANT PRESSURE, $p_0 = 34 \cdot 2$ torr.

curve	d (cm)	E_s/p_0 (volt cm^{-1} $torr^{-1}$)
A	0·82	13·5
B	0·71	14·2
C	0·61	15·2
D	0·52	16·2
E	0·36	19·0
F	0·19	29·1

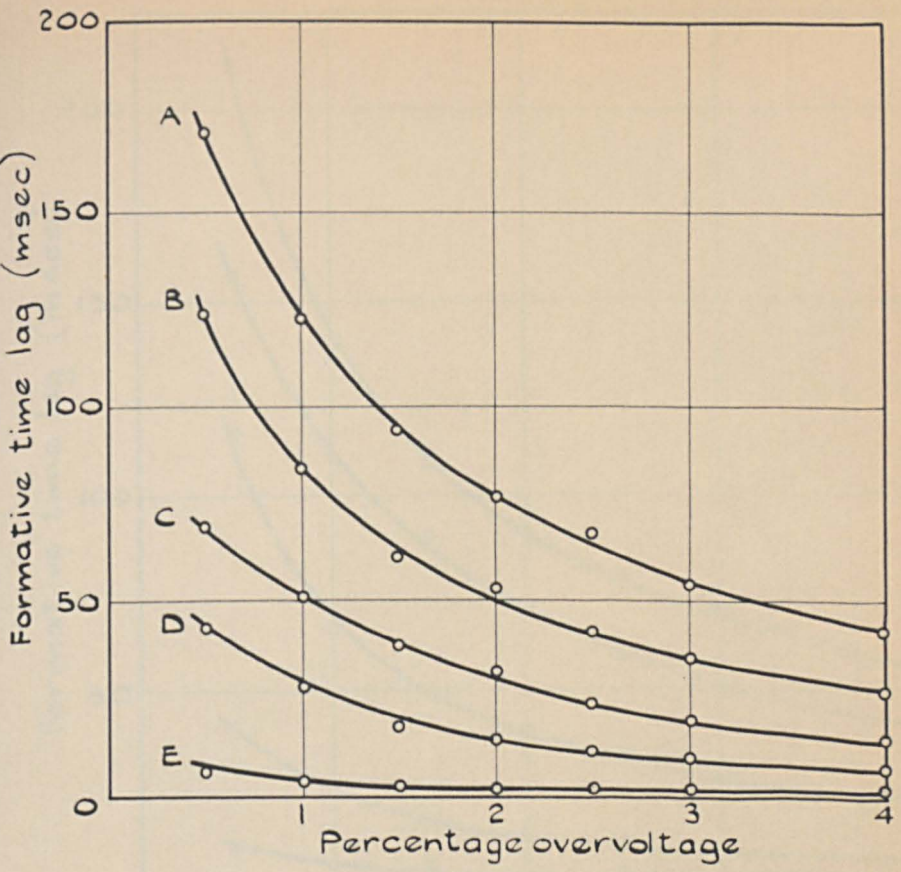

FIG. 32 VARIATION OF FORMATIVE TIME LAG WITH PERCENTAGE OVERVOLTAGE. NICKEL ELECTRODES IN HELIUM AT CONSTANT PRESSURE, P_o = 44·4 torr.

curve	d (cm)	E_s/P_o (volt cm^{-1} $torr^{-1}$)
A	0·82	11·6
B	0·69	12·5
C	0·54	13·7
D	0·42	15·1
E	0·18	23·8

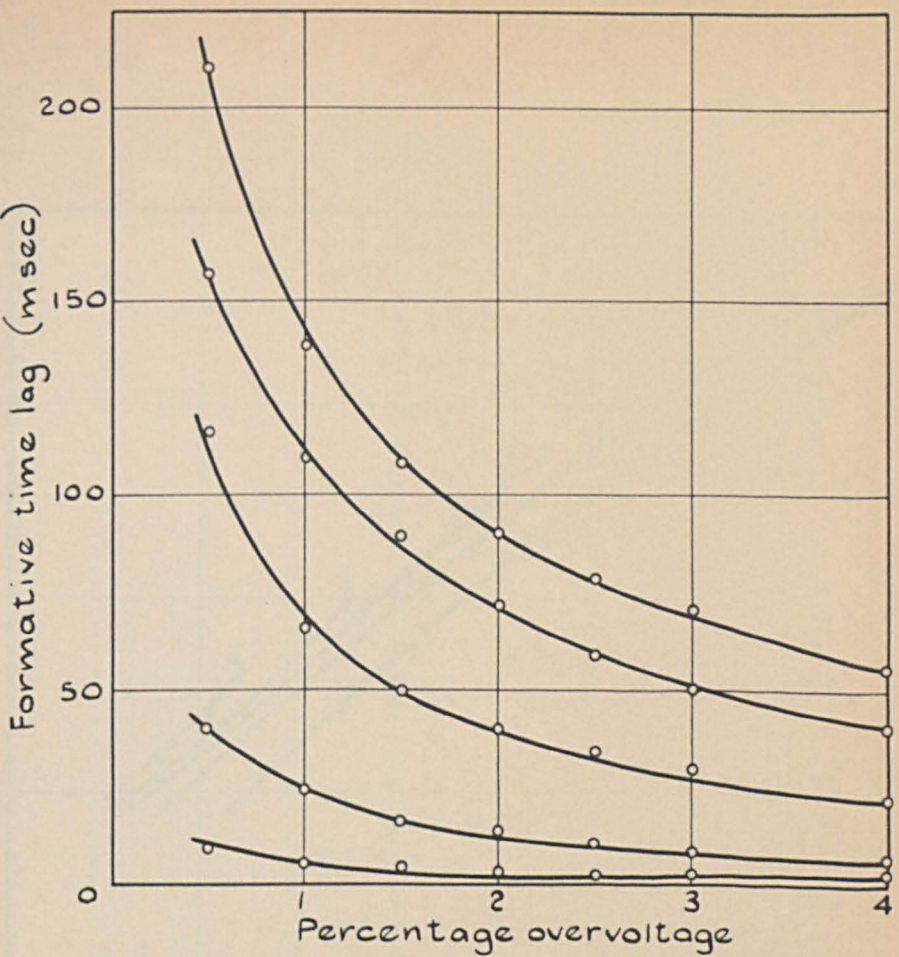

FIG. 33 VARIATION OF FORMATIVE TIME LAG WITH PERCENTAGE OVERVOLTAGE., NICKEL ELECTRODES IN HELIUM AT CONSTANT PRESSURE, $p_0 = 62 \cdot 2$ torr.

curve	d (cm)	E_s/p_0 (volt cm^{-1} torr^{-1})
A	0·82	9·8
B	0·72	10·3
C	0·53	11·4
D	0·34	13·3
E	0·19	16·2

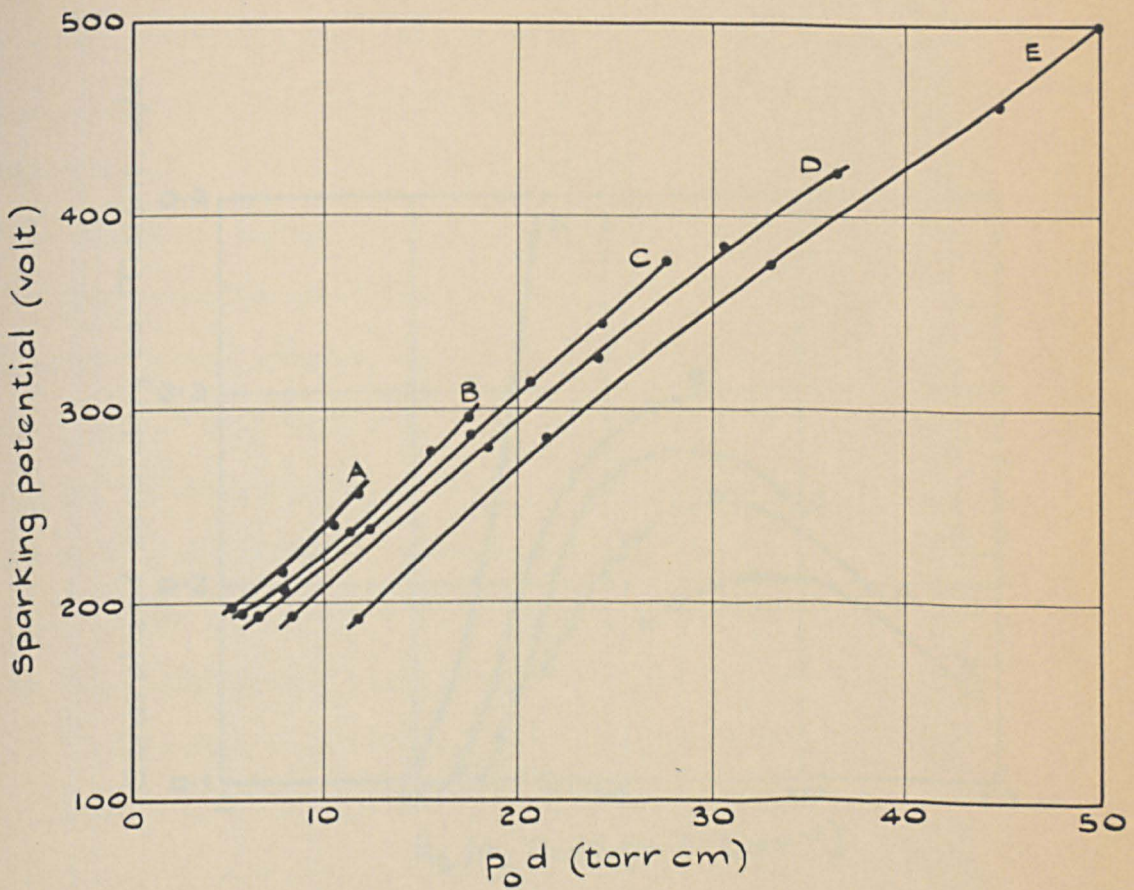

FIG. 34 PASCHEN CURVES IN HELIUM.
A, 14·9 torr; B, 22·1 torr; C, 34·2 torr;
D, 44·4 torr; E, 62·2 torr.

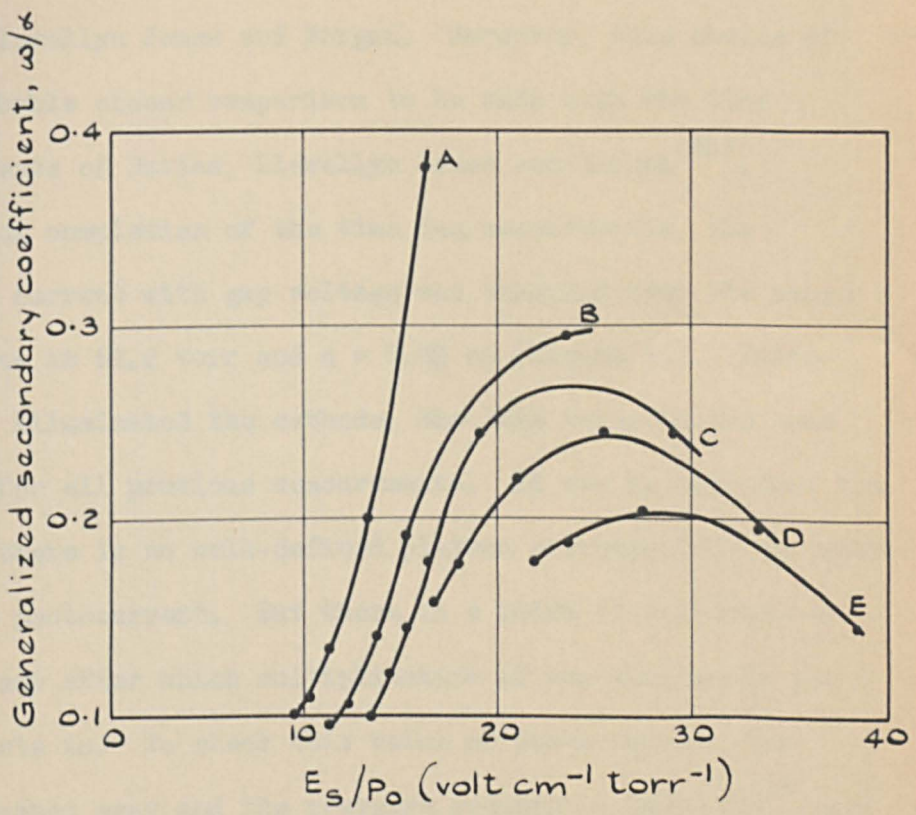

FIG. 35 VARIATION OF THE GENERALIZED SECONDAR COEFFICIENT IN HELIUM WITH E_s/P_o. A, 62·2 torr; B, 44·4 torr; C, 34·2 torr; D, 22·1 torr; E, 14·9 torr.

values[27] of α/p_o. These values were chosen in preference to Fletcher's[28] because it was felt that the conditions under which the present experiments were carried out were closer to those used by Davies, Llewellyn Jones and Morgan. Moreover, this choice of α/p_o would enable closer comparison to be made with the time lag measurements of Davies, Llewellyn Jones and Morgan[64].

Upon completion of the time lag measurements, the variation of current with gap voltage was examined over the range 0 to 300 volts at 62.2 torr and d = 0.82 cm (figure 36). Ultraviolet light illuminated the cathode, the lamp being in the same position as for all previous measurements. It can be seen from the figure that there is no well-defined plateau corresponding to saturation of the photocurrent. But there is a point of inflexion at 4.5×10^{-11} amp after which multiplication of the current by gas ionization sets in. To check this value of photocurrent, the helium was pumped away and the pressure reduced to below 10^{-6} torr when the photocurrent was measured as 4.7×10^{-11} amp at 125 volts.

The possibility of the photocurrent varying with gap distance was then investigated. The current was measured at the electrode spacings used in the time lag experiments and figure 37 was obtained. There was no significant variation in photocurrent indicating that the anode was not masking the cathode from the ultraviolet source at the smaller gap distances. There was, however, a

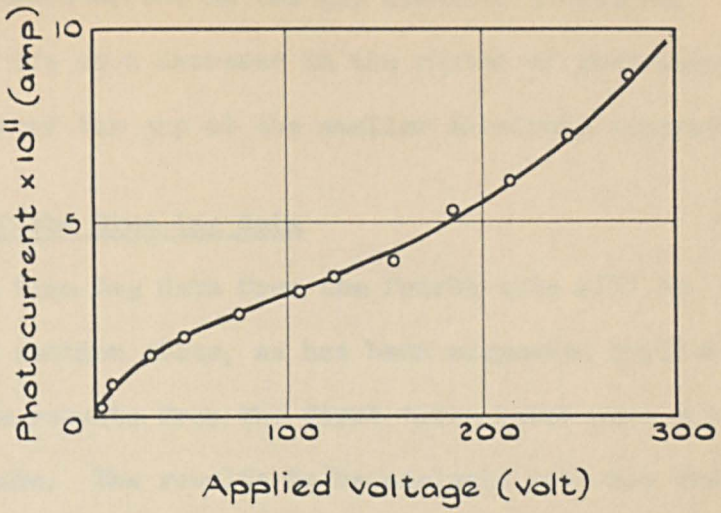

FIG. 36 VARIATION OF PHOTOCURRENT WITH APPLIED VOLTAGE, IN HELIUM AT 62·2 torr.

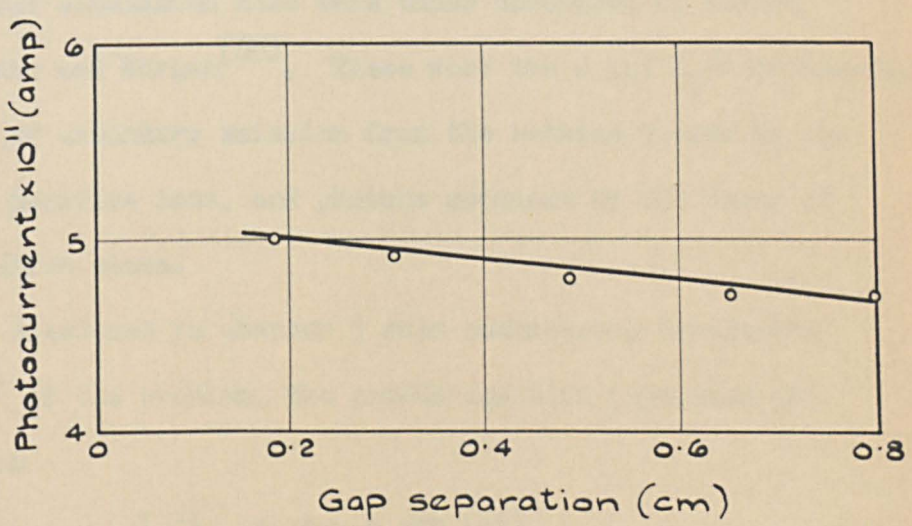

FIG. 37 VARIATION OF PHOTOCURRENT WITH GAP DISTANCE, IN VACUUM.

small increase in photocurrent as the gap distance shortened. This may have been due to a decrease in the number of photoelectrons lost from the sides of the gap at the smaller electrode separations.

5.6 Computation of the time lag data

Only the time lag data from the fourth tube will be considered in this section since, as has been suggested earlier in the chapter, the results from the first three tubes were not sufficiently accurate. The results to be analysed here are the 25 curves of figures 29 to 33.

Davies, Llewellyn Jones and Morgan[64] have shown that the secondary processes due to the incidence at the cathode of undelayed photons, positive ions and metastable atoms were not sufficient to account for the time lags observed by them in helium. So the processes first considered here were those described by Davies, Llewellyn Jones and Morgan[65]. These were the γ and δ_1/α processes, namely those of secondary emission from the cathode caused by the incidence of positive ions, and photons produced by the decay of metastable helium atoms.

As discussed in chapter 3 when considering Davidson's treatment[61] of the problem, the growth equation (equation 42) may be written

$$i_-/i_o = A - B \exp(\lambda t),$$

where $A = 1/F(0)$,

$$B = -\frac{1}{\lambda\left[\frac{\partial F(p)}{\partial p}\right]_{p=\lambda}}$$

and the growth constant λ is the real root of $F(p) = 0$. Here the symbols have the meanings given in chapter 3.

The secondary processes are introduced by the function $F(p)$ which is determined by the nature of the processes considered. For the action of positive ions and non-resonance photons produced by the decay of metastable atoms, when $\gamma + \delta_1/\alpha = \omega/\alpha$, the function becomes:

$$F(p) = 1 - \frac{\delta_1}{\psi}\left[\frac{\exp(\psi d)-1}{1 + p\,\tau_1}\right] - \frac{\alpha\gamma}{\phi}\left[\exp(\phi d) - 1\right],$$

where $\psi = \alpha - p/W_-$, $\phi = \alpha - p/W$ and the delay time $\tau_1 = 1/(192\ p_o)$. The equations may be simplified at sufficiently large t, since A may then be omitted and $\psi \simeq \phi \simeq \alpha$.

The first calculations using these equations were done by hand, but it soon became obvious that it would have taken a considerable time to analyse all the curves by this method with any degree of completeness. Since an Elliott 503 computer was available, suitable programmes were written by the author to carry out the necessary calculations. The language in which the programmes were written was Algol 60[88] adapted for use with the 503 computer.

The fundamental calculation carried out was the computation of the theoretical time lag at a given overvoltage for a chosen ratio of the secondary coefficients δ_1/α and γ. This entailed solution of the equation $F(p) = 0$ to give the growth constant λ from which the constant B could be evaluated. On substitution of these values of λ and B in the current growth equation $i_-/i_o = - B \exp(\lambda t)$, the formative time lag could be readily obtained since this was defined as the time t for the current to grow from i_o to i_- (from 4.5×10^{-11} to 10^{-6} amp in the present case).

The procedure followed by the computer to obtain the theoretical curve giving the best fit to a chosen experimental curve can now be described. Associated with each curve were characteristic values of pressure, gap distance, generalized secondary coefficient and current ratio i_-/i_o. Also each of the seven points of the curve had its own values of formative time lag, percentage overvoltage and primary ionization coefficient α/p_o. These were the parameters presented to the computer.

The percentage x of the total secondary action for which the δ_1/α process was responsible set the values of δ_1/α and γ at $0.01x\ \omega/\alpha$ and $(1 - 0.01x)\omega/\alpha$ respectively.

Seven values of formative time lag were then calculated for each value of overvoltage for a given value of x. This was repeated for each value of $x = 0, 1, 2, \ldots, 100$ and so 101 theoretical curves

were obtained. The curve giving the closest fit to the experimental curve was selected from these 101 curves by the method of least squares. The value of x corresponding to the best theoretical curve then gave the required percentage action of the δ_1/α and γ processes. The computer output gave this value of x and the seven related values of formative time lag enabling a theoretical curve to be plotted.

The calculation was carried out for the δ_1/α and γ processes for each of the 25 experimental curves. As a result it was found that reasonable agreement between the experimental and computed curves was obtained in only five cases.

The possibility of another process giving a fit to the curves was suggested at Swansea to the author by Griffiths[89]. This process is closely similar to the δ_1/α process, but involves the production of delayed radiation from the decay of metastable helium molecules instead of atoms. This process is designated the δ_2/α process.

Phelps[66] has described a process whereby atoms excited to the 2^3S triplet metastable state are converted to metastable molecules in the $2^3\Sigma$ state in three-body collisions with normal gas atoms. The mean lifetime of the 2^3S state before destruction to the $2^3\Sigma$ state is $(0.26\ p_o^2)^{-1}$ sec. These metastable molecules can then decay with the production of non-resonance radiation to the ground state of He_2 leading to immediate dissociation[90].

No experimental data could be discovered which gave the collisional cross-sections or destruction frequency of these molecular metastable states. As a result it was assumed that the molecular metastables had a lifetime much shorter than that of the 2^3S atoms which were concerned in the production of the molecular metastables. So the delay time τ_2 associated with this particular non-resonance radiation was assumed to be $(0.26\ p_o^2)^{-1}$ sec.

Besides the δ_1/α and γ combination already considered, there were now two further combinations of processes to be taken into account, namely δ_2/α and γ, and δ_1/α and δ_2/α.

Since the δ_1/α and δ_2/α processes are by nature essentially similar, the computer programme for the δ_2/α and γ combination was readily obtained from the δ_1/α and γ programme. The major difference introduced was the change in delay times from τ_1 to τ_2. The function F(p) now became

$$F(p) = 1 - \frac{\delta_2}{\psi}\left[\frac{\exp(\psi d)-1}{1 + p\,\tau_2}\right] - \frac{\alpha\gamma}{\phi}\left[\exp(\phi d) - 1\right],$$

where $\tau_2 = (0.26\ p_o^2)^{-1}$ sec.

The programme for the δ_1/α and δ_2/α combination proved more difficult, since the function F(p) was considerably modified to

$$F(p) = 1 - \frac{\delta_1}{\psi}\left[\frac{\exp(\psi d)-1}{1 + p\,\tau_1}\right] - \frac{\delta_2}{\psi}\left[\frac{\exp(\psi d)-1}{1 + p\,\tau_2}\right].$$

Apart from the changes introduced by this modification, the programme was similar to the two already described.

These two programmes were then used to calculate theoretical curves for each of the 25 experimental curves in addition to those already computed. The calculated curves giving the best fit with the experimental data out of the three combinations of processes considered are given in the appendix. An example of the fit obtained is given in figure 38 which, although giving excellent agreement, was by no means the best achieved.

5.7 Discussion of the results

When an attempt was made to look for trends in the variation of the secondary coefficients, the clearest picture emerged from consideration of the family of curves obtained at 22.1 torr. The percentage contribution of each secondary process to the generalized secondary coefficient is given as a function of E_s/p_o in figure 39.

Similar results were also obtained from the calculations at 14.9, 34.2 and 44.4 torr (figures 40 to 42). In each of these three cases, only one set of measurements was made at a sufficiently high value of E_s/p_o to give appreciable positive ion action. Thus the γ contribution is tentatively given as a dashed line based on the curve obtained at 22.1 torr.

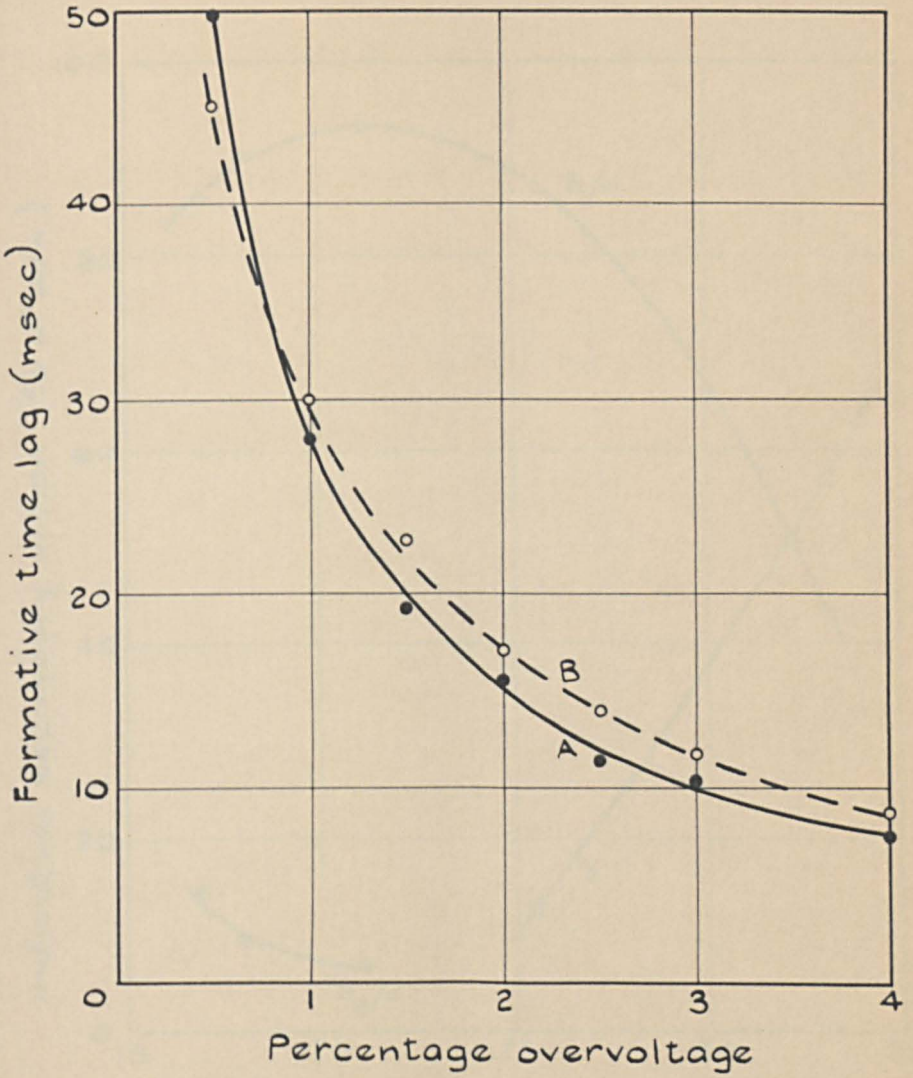

FIG. 38 VARIATION OF THE FORMATIVE TIME LAG IN HELIUM WITH PERCENTAGE OVERVOLTAGE. p_0 = 22·1 torr, d = 0·51 cm. A, MEASURED; B, CALCULATED WHEN $\delta_1/\alpha = 0{\cdot}93\,\omega/\alpha$ AND $\delta_2/\alpha = 0{\cdot}07\,\omega/\alpha$.

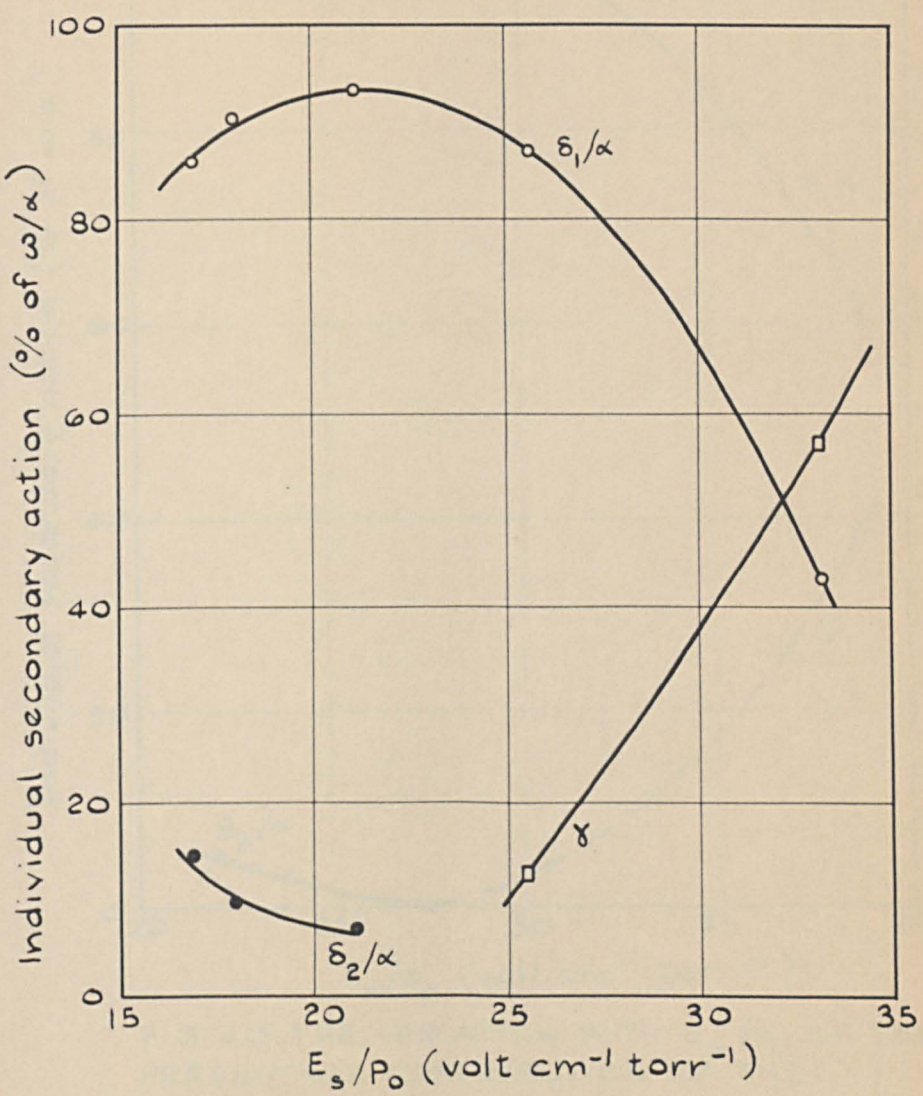

FIG. 39 THE VARIATION WITH E_s/p_o OF THE PERCENTAGE CONTRIBUTION OF THE SECONDARY PROCESSES IN HELIUM TO ω/α AT CONSTANT PRESSURE, $p_o = 22.1$ torr.

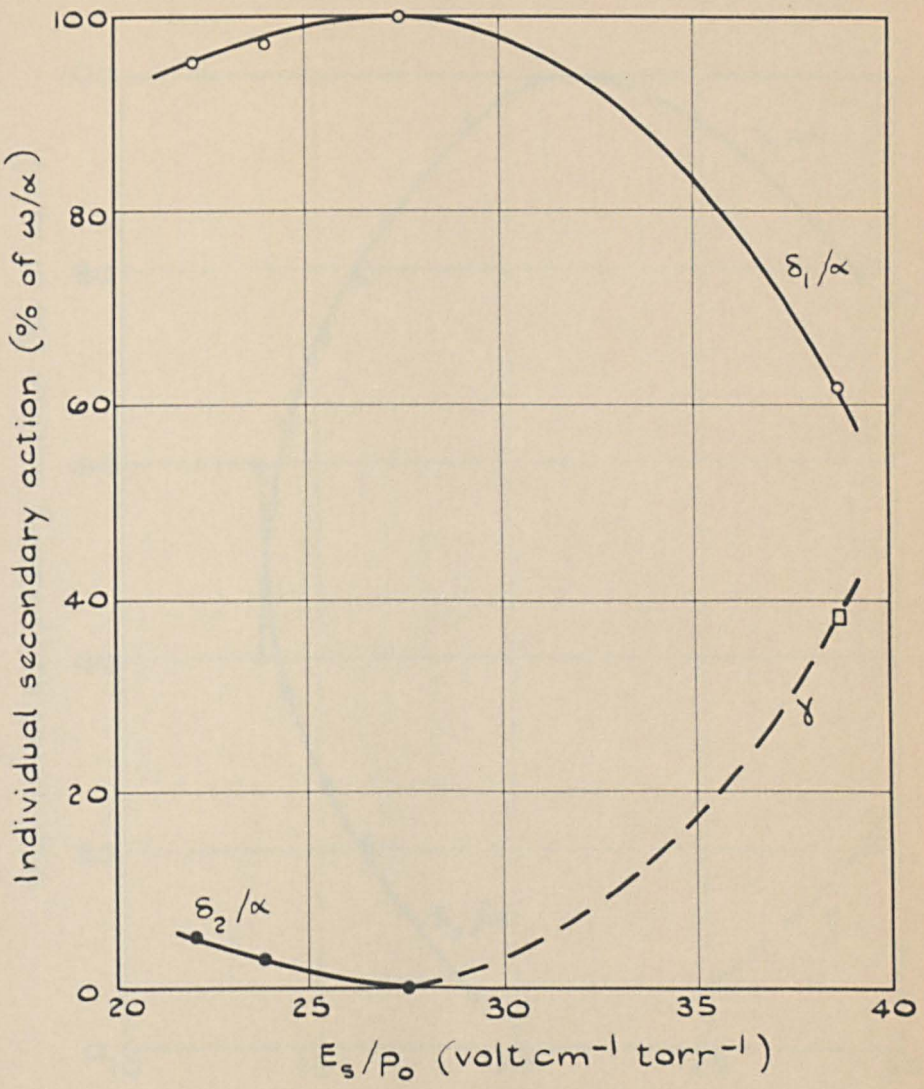

FIG. 40 THE VARIATION WITH E_s/p_o OF THE PERCENTAGE CONTRIBUTION OF THE SECONDARY PROCESSES IN HELIUM TO ω/α AT CONSTANT PRESSURE, $p_o = 14 \cdot 9$ torr.

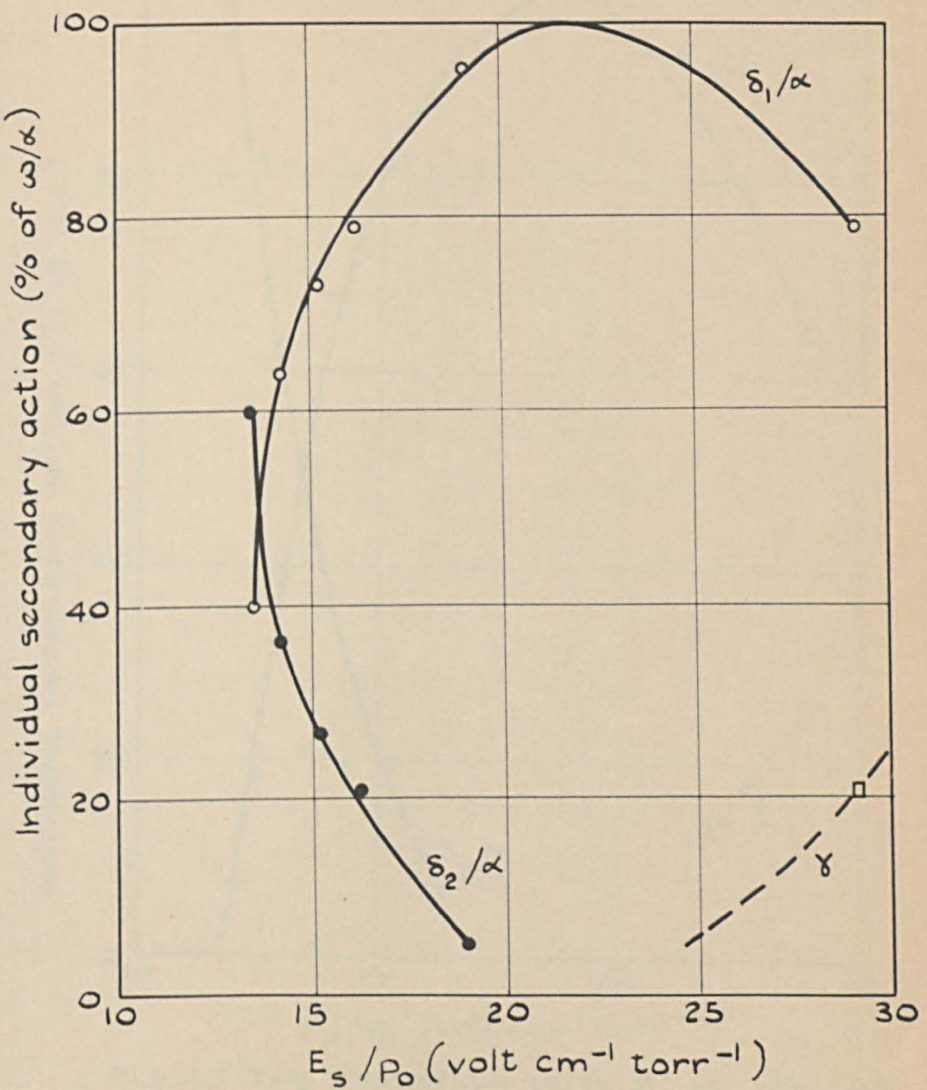

FIG. 41 THE VARIATION WITH E_s/p_o OF THE PERCENTAGE CONTRIBUTION OF THE SECONDARY PROCESSES IN HELIUM TO ω/α AT CONSTANT PRESSURE, $p_o = 34 \cdot 2$ torr.

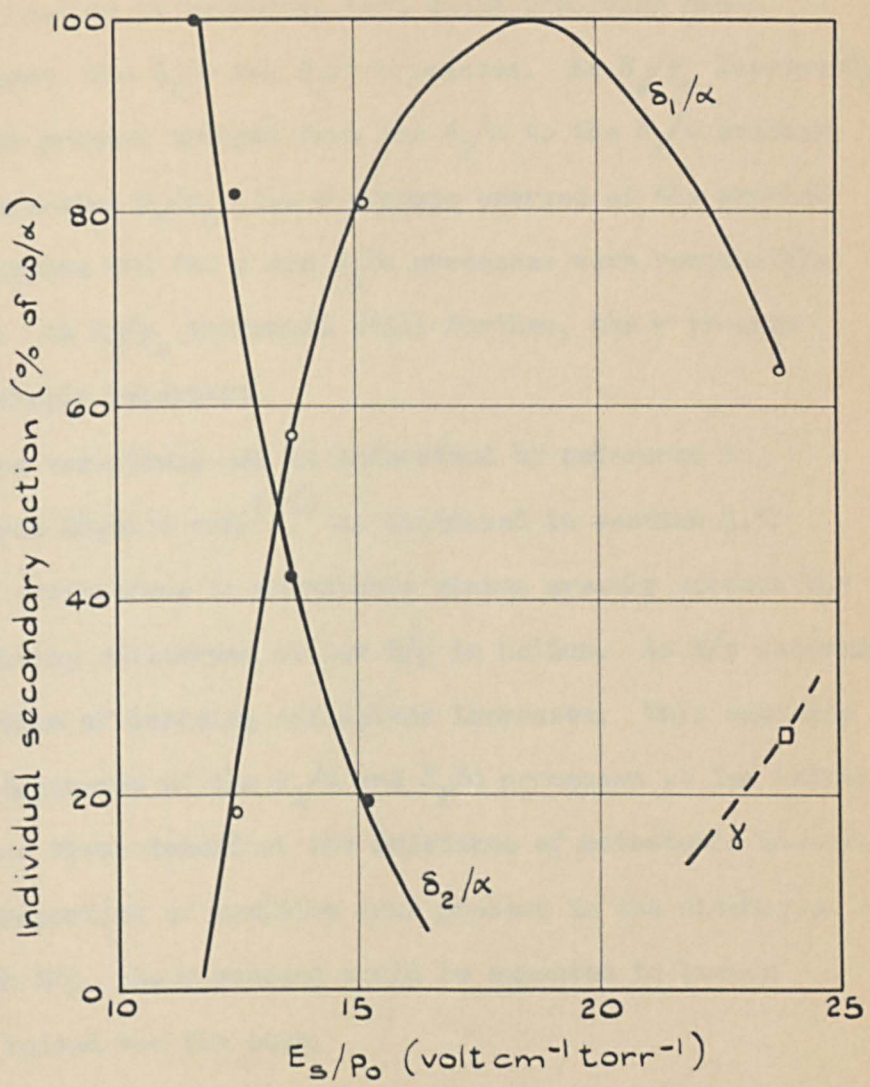

FIG. 42 THE VARIATION WITH E_s/p_o OF THE PERCENTAGE CONTRIBUTION OF THE SECONDARY PROCESSES IN HELIUM TO ω/α AT CONSTANT PRESSURE, $p_o = 44 \cdot 4$ torr.

At the lower ranges of E_s/p_o considered in these figures, the processes leading to breakdown were those involving non-resonance photons, the δ_1/α and δ_2/α processes. As E_s/p_o increased, so the dominant process changed from the δ_2/α to the δ_1/α process. On further increasing E_s/p_o, the γ process emerged at the expense of the δ_2/α process and the γ and δ_1/α processes were responsible for breakdown. As E_s/p_o increased still further, the γ process became increasingly important.

These variations can be understood by reference to Corrigan and von Engel's work[70] as discussed in section 3.3. The number of excitations to metastable states greatly exceeds the number of ionizing collisions at low E/p in helium. As E/p increases so the proportion of ionizing collisions increases. This explains the observed dominance of the δ_1/α and δ_2/α processes at low values of E_s/p_o, since these depend on the existence of metastable states. Because the proportion of positive ions present in the discharge increases with E/p, the γ process would be expected to become important as indeed was the case.

The time lags obtained became shorter as E_s/p_o increased at constant pressure, as is shown in figure 43. This was to be expected since the fastest of the three processes, the γ process, became increasingly important as E_s/p_o increased. Moreover, as E_s/p_o increased the γ process itself became faster, since the drift velocity of positive ions in helium has been shown[21] to be directly proportional to E/p.

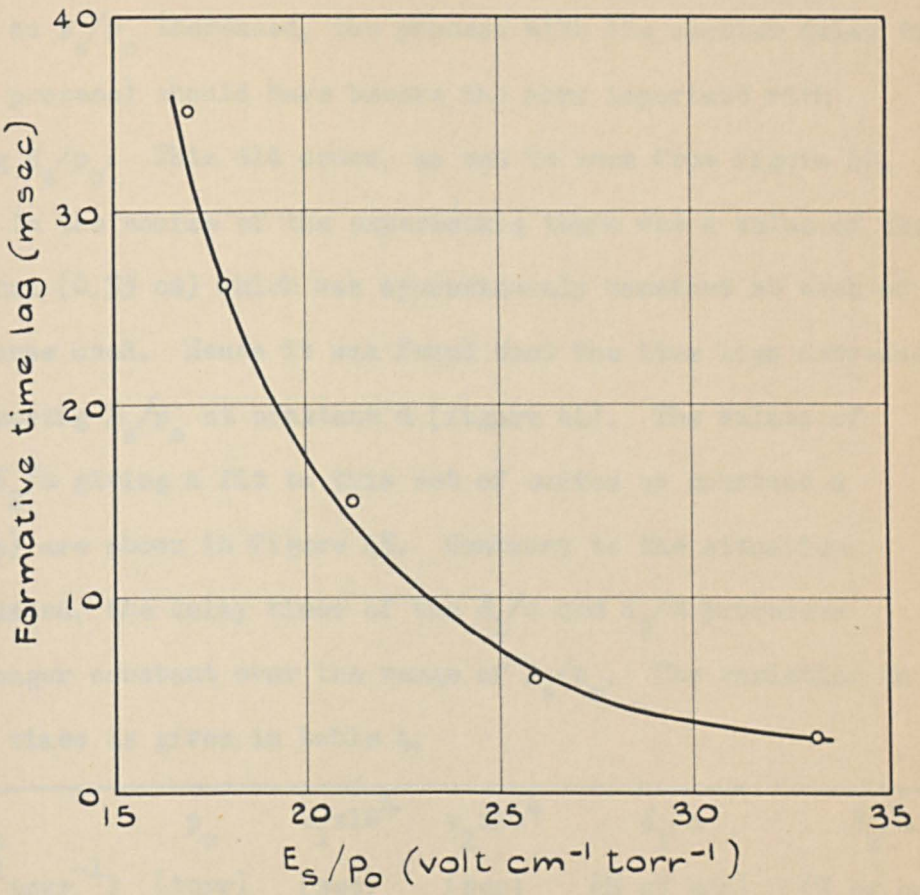

FIG. 43 VARIATION OF FORMATIVE TIME LAG WITH E_s/p_o AT CONSTANT PERCENTAGE OVERVOLTAGE AND GAS PRESSURE.
$\Delta V = 2\%$, $p_o = 22 \cdot 1$ torr.

The δ_2/α process had a longer delay time than the δ_1/α process at the pressures considered. At 22.1 torr for example, $\tau_1 \simeq 2.4 \times 10^{-4}$ sec and $\tau_2 \simeq 79 \times 10^{-4}$ sec. Since the time lags decreased as E_s/p_o increased, the process with the shorter delay time (the δ_1/α process) should have become the more important with increasing E_s/p_o. This did occur, as can be seen from figure 40.

In the course of the experiments there was a value of the gap distance (0.53 cm) which was approximately constant at each of the pressures used. Hence it was found that the time lags decreased with increasing E_s/p_o at constant d (figure 44). The values of δ_1/α and δ_2/α giving a fit to this set of curves at constant d (varying p) are shown in figure 45. Contrary to the situation just discussed, the delay times of the δ_1/α and δ_2/α processes were no longer constant over the range of E_s/p_o. The variation in the delay times is given in table 4.

E_s/p_o (volt $cm^{-1}torr^{-1}$)	p_o (torr)	$\tau_1 x10^4$ (sec)	$\tau_2 x10^4$ (sec)	δ_1/α (% of ω/α)	δ_2/α (% of ω/α)
11.4	62.2	0.8	9.9	0	100
12.5	44.4	1.2	19	57	43
16.2	34.2	1.5	33	79	21
21.1	22.1	2.4	79	93	7
27.4	14.9	3.5	173	100	0

Table 4. Variation of delay times with E_s/p_o.

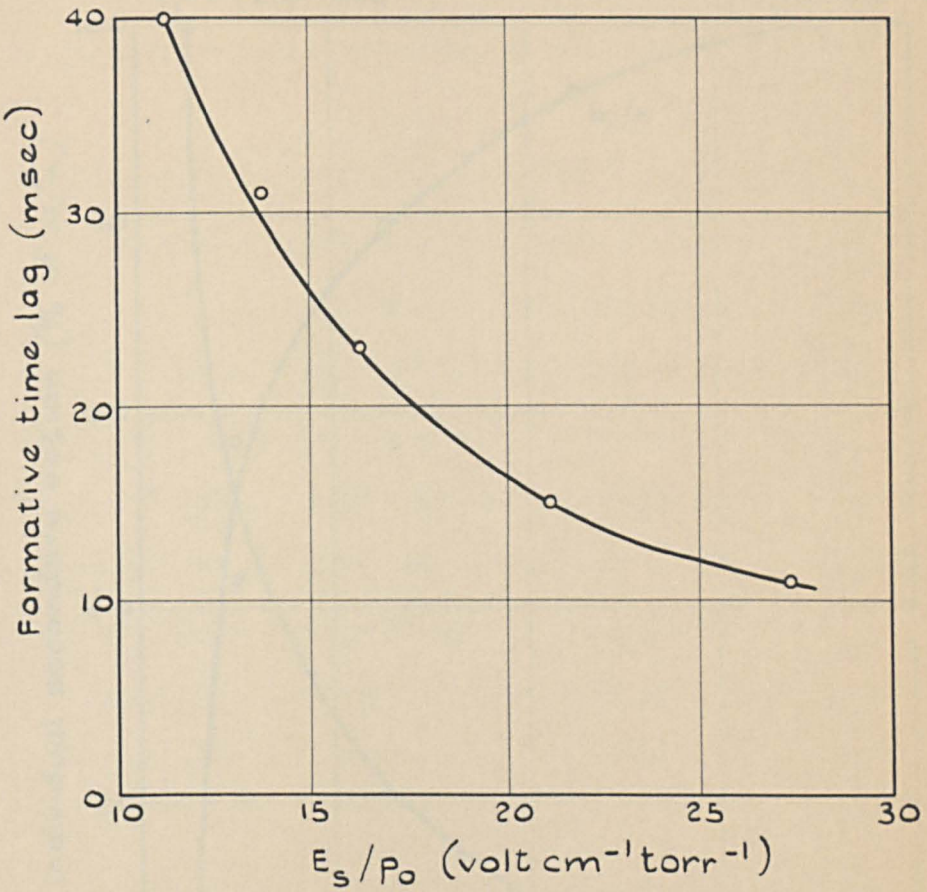

FIG. 44 VARIATION OF FORMATIVE TIME LAG WITH E_s/p_o AT CONSTANT PERCENTAGE OVERVOLTAGE AND GAP DISTANCE.
$\Delta V = 2\%$, $d = 0{\cdot}53$ cm.

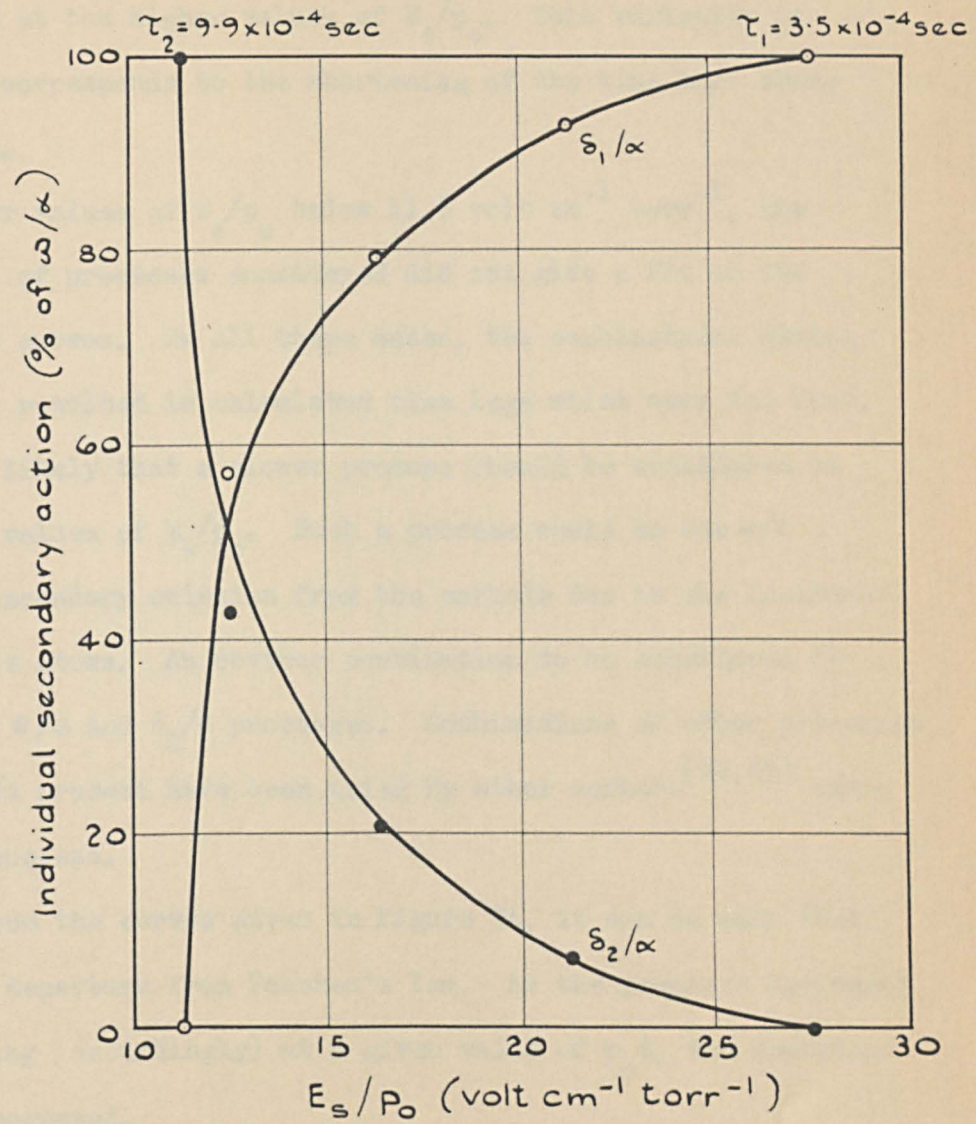

FIG. 45 THE VARIATION WITH E_s/p_o OF THE PERCENTAGE CONTRIBUTION OF THE SECONDARY PROCESSES IN HELIUM TO ω/α AT CONSTANT GAP DISTANCE, $d = 0{\cdot}53$ cm.

The delay time decreased from 9.9×10^{-4} sec when the δ_2/α process was acting alone to 3.5×10^{-4} sec when δ_1/α was acting alone at the higher values of E_s/p_o. This variation in delay times corresponds to the shortening of the time lags shown in figure 44.

For values of E_s/p_o below 11.6 volt cm^{-1} $torr^{-1}$, the combinations of processes considered did not give a fit to the experimental curves. In all these cases, the combinations giving the best fit resulted in calculated time lags which were too fast. So it seems likely that a slower process should be considered at these lower values of E_s/p_o. Such a process would be the ε/α process of secondary emission from the cathode due to the incidence of metastable atoms. An obvious combination to be considered is that of the ε/α and δ_2/α processes. Combinations of other processes with the ε/α process have been tried by other workers[64,65] without marked success.

From the curves given in figure 34, it can be seen that there was a departure from Paschen's law. As the pressure decreased (d increasing accordingly) at a given value of $p_o d$, the sparking potential increased.

It is possible that this deviation from the law was due to the loss of increasing numbers of the active species from the discharge region as the electrode spacing increased. Such an effect was suggested by McCallum and Klatzow[37] when they observed

departures from Paschen's law in argon and neon. However, they did not observe such an effect in helium. In contradiction to this, and in agreement with the present results, Fletcher[28] observed such a deviation from Paschen's law which was reflected in his values of ω/α (figure 10(b)).

Davies, Llewellyn Jones and Morgan[65] suggested that the similarity relationships should be violated in helium because of the pressure dependence of the δ_1/α process. Such a violation would then be observed through departures from Paschen's law. In the present work, two of the processes (δ_1/α and δ_2/α) were pressure dependent. Thus the observed departures from Paschen's law could be due to one or both of the reasons discussed.

It was suggested in section 1.4 that ω/α should decrease as d increased at constant E/p_o if metastable action was important. Readings obtained at two closely related values of E_s/p_o are given in table 5.

E_s/p_o (volt cm^{-1} $torr^{-1}$)	d (cm)	ω/α
23.8	0.18	0.295
23.7	0.68	0.188

Table 5. Values of ω/α and d.

From the table it can be seen that as d increases ω/α indeed decreases, so giving additional evidence of the importance of metastable action in helium.

5.8 Conclusions and suggestions for further work

The formative time lags measured with nickel cathodes in helium decreased with increasing E_s/p_o. This trend was observed for varying gap distance at constant pressure and for varying pressure at constant gap distance.

When Davidson's theory was used to compute theoretical time lag curves, good agreement was obtained with the experimental curves at values of E_s/p_o greater than 11.6 volt cm^{-1} $torr^{-1}$. This agreement was obtained by use of the secondary processes due to non-resonance photons (δ_1/α and δ_2/α processes) and positive ions (γ process). The combination of the δ_1/α and δ_2/α processes gave satisfactory agreement over the lower range of E_s/p_o. As E_s/p_o increased, so the γ process became more important than the δ_2/α process and agreement was obtained using the δ_1/α and γ combination.

It would be instructive to extend the investigation of the range of E_s/p_o less than 11.6 volt cm^{-1} $torr^{-1}$ and to consider the effect of metastable atom action at the cathode (ε/α process) in combination with the δ_2/α process. Also the effect of helium purity could be rigorously examined if a mass spectrometer were available

to monitor the presence of impurity atoms. If necessary the Biondi super-leak method[91] of purifying helium could be used in an effort to obtain the gas in a high state of purity.

Appendix

COMPUTED TIME LAG CURVES

All twenty-five figures contained in this appendix give the variation of the formative time lag with percentage overvoltage at particular values of helium pressure and inter-electrode distance. The dashed curves were computed by the methods described in section 5.6 and are compared with the experimental curves which are drawn as continuous lines.

The value of the coefficients δ_1/α, δ_2/α and γ which gave the best fit to the experimental data are given in each case.

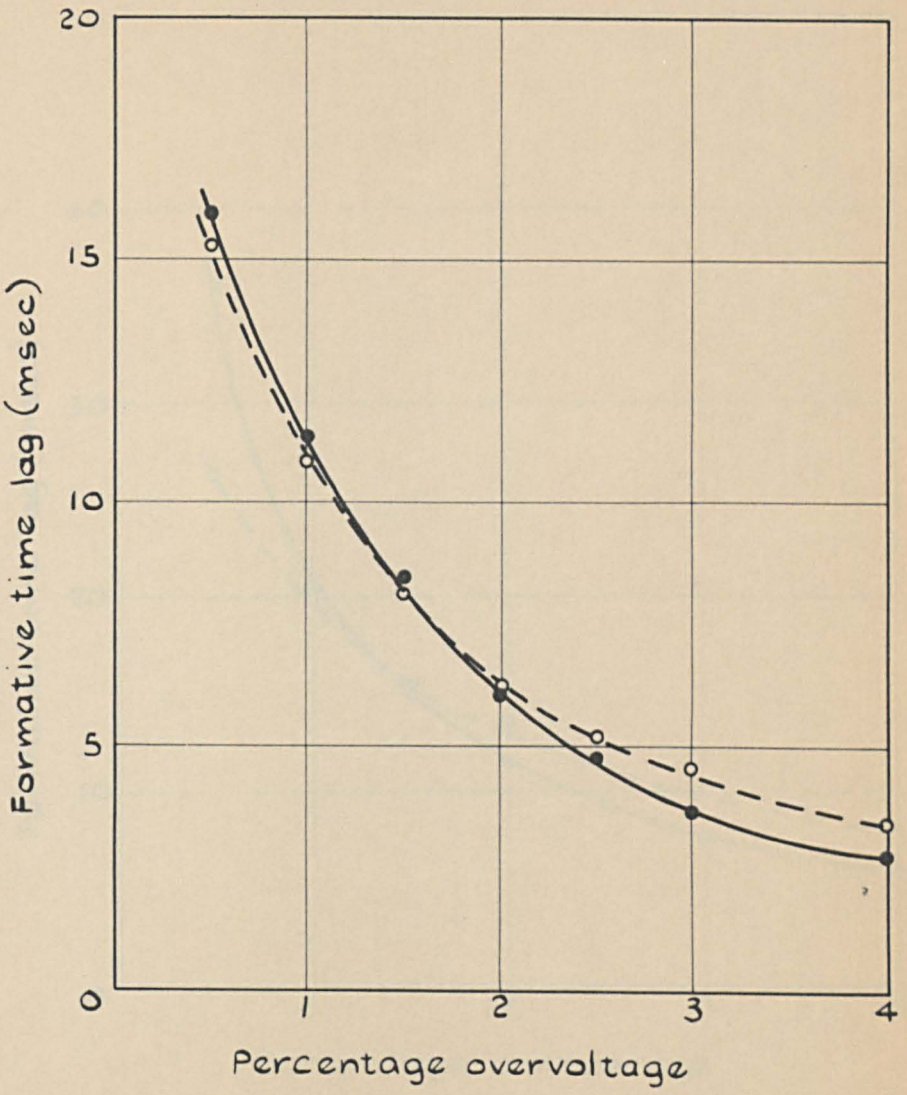

FIG. 46 $p_0 = 14 \cdot 9$ torr, $d = 0 \cdot 34$ cm

$\delta_1 / \alpha = 0 \cdot 62\ \omega/\alpha$, $\gamma = 0 \cdot 38\ \omega/\alpha$

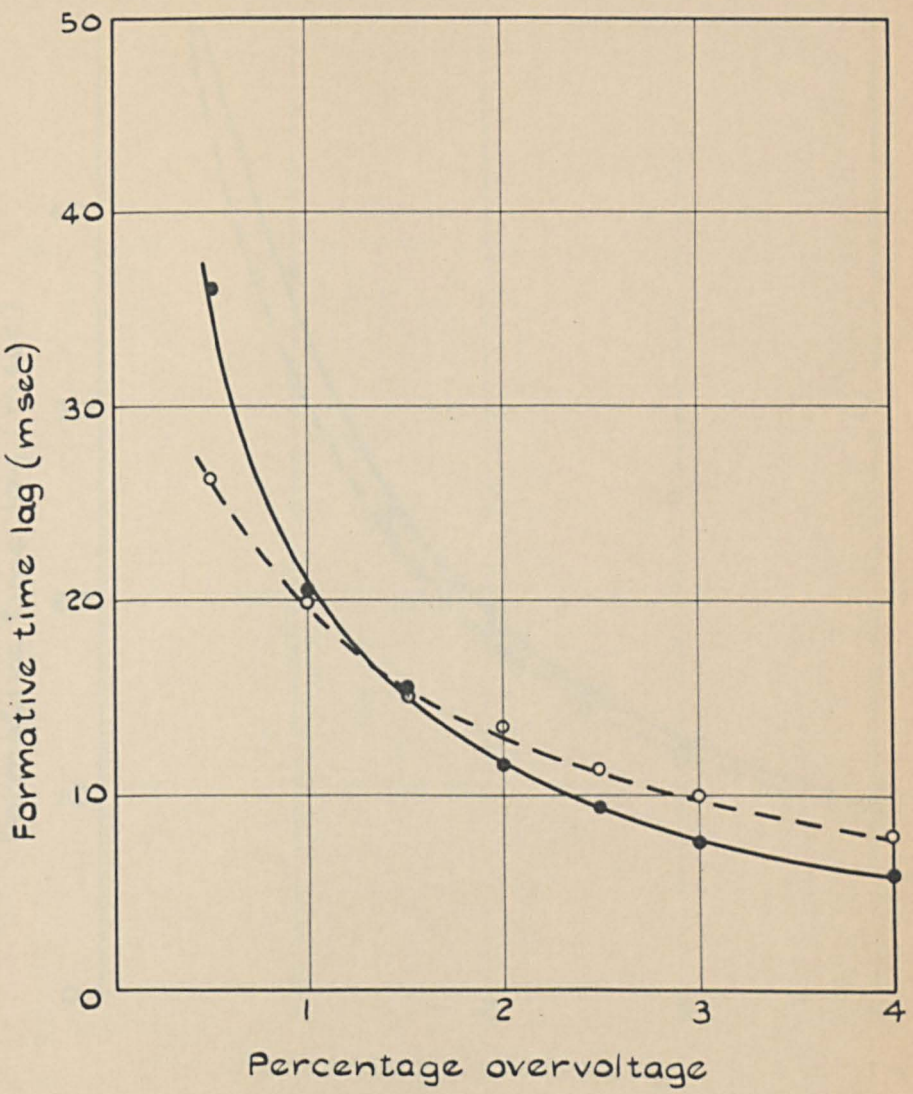

FIG. 47 $p_0 = 14{\cdot}9$ torr, $d = 0{\cdot}53$ cm

$\delta_1/\alpha = \omega/\alpha$

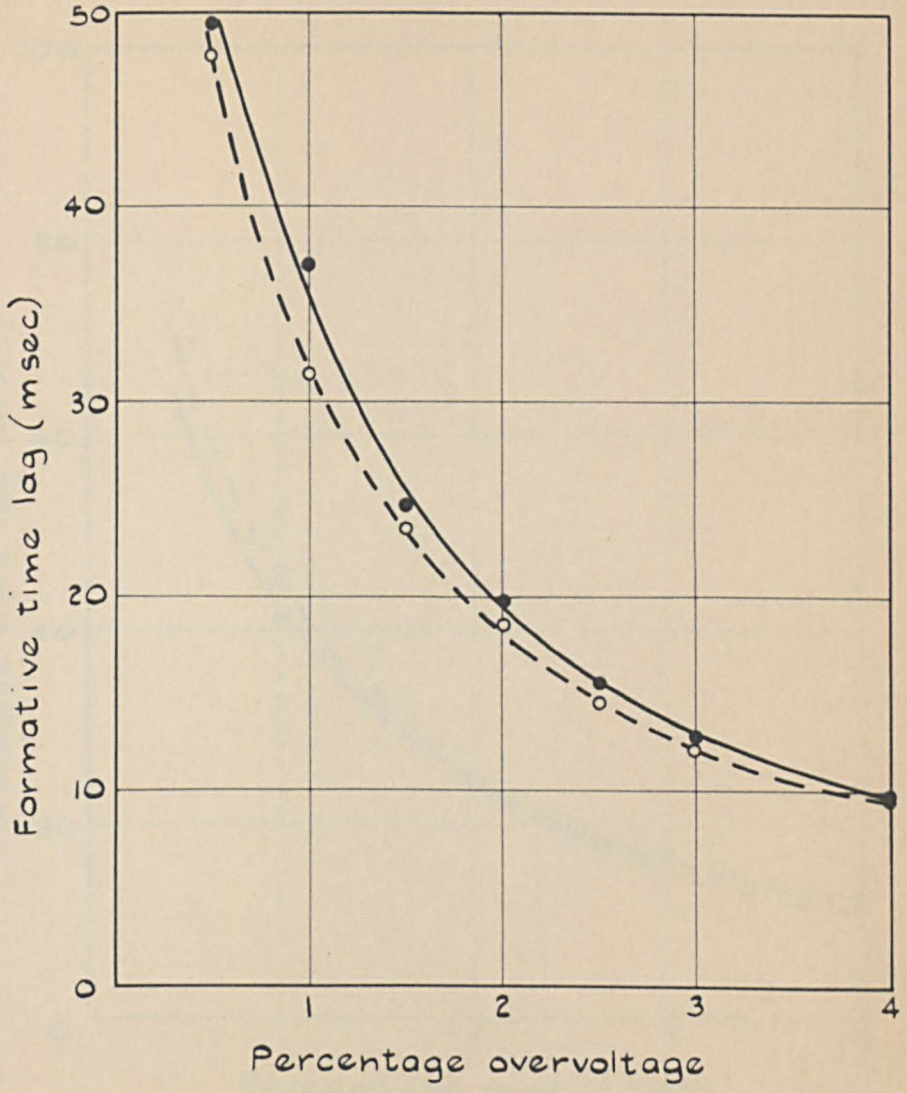

FIG. 48 $P_0 = 14{\cdot}9$ torr, $d = 0{\cdot}68$ cm

$\delta_1/\alpha = 0{\cdot}97\ \omega/\alpha$, $\delta_2/\alpha = 0{\cdot}03\ \omega/\alpha$

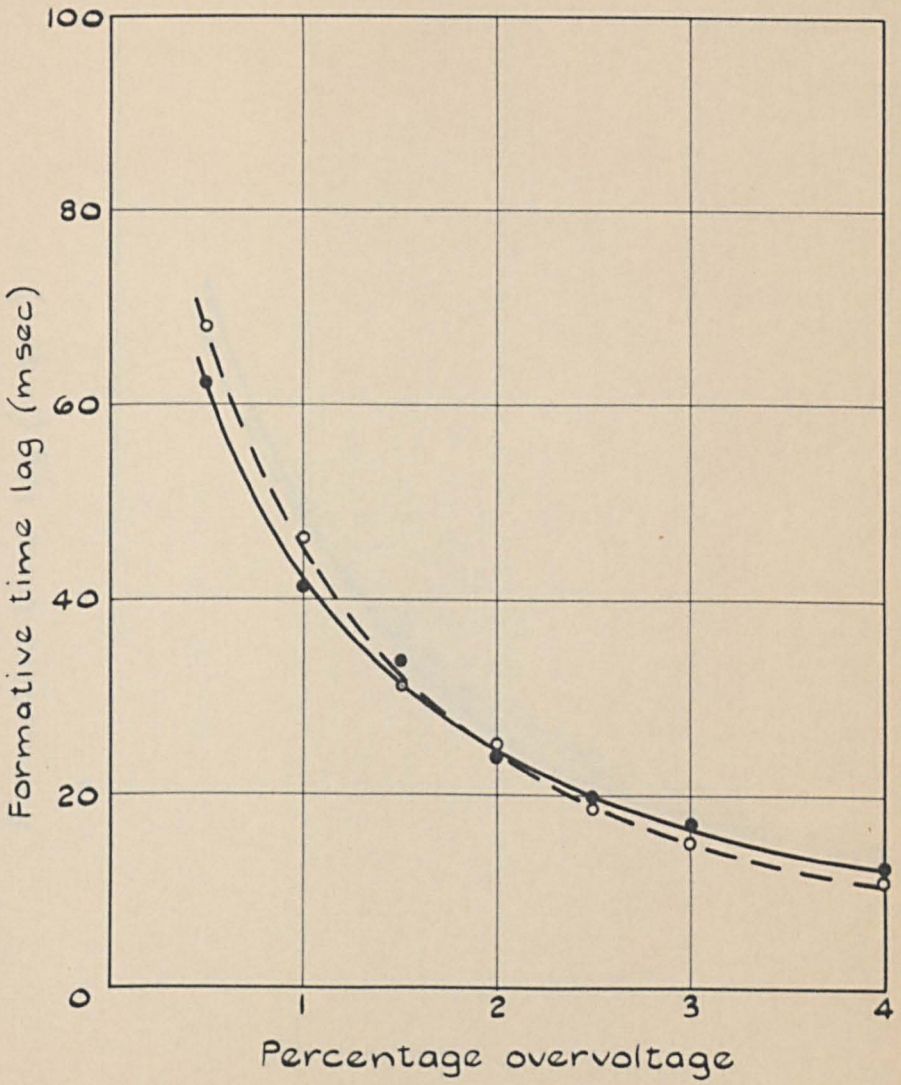

FIG. 49 $p_0 = 14{\cdot}9$ torr, $d = 0{\cdot}78$ cm

$\delta_1/\alpha = 0{\cdot}95\omega/\alpha$, $\delta_2/\alpha = 0{\cdot}05\omega/\alpha$

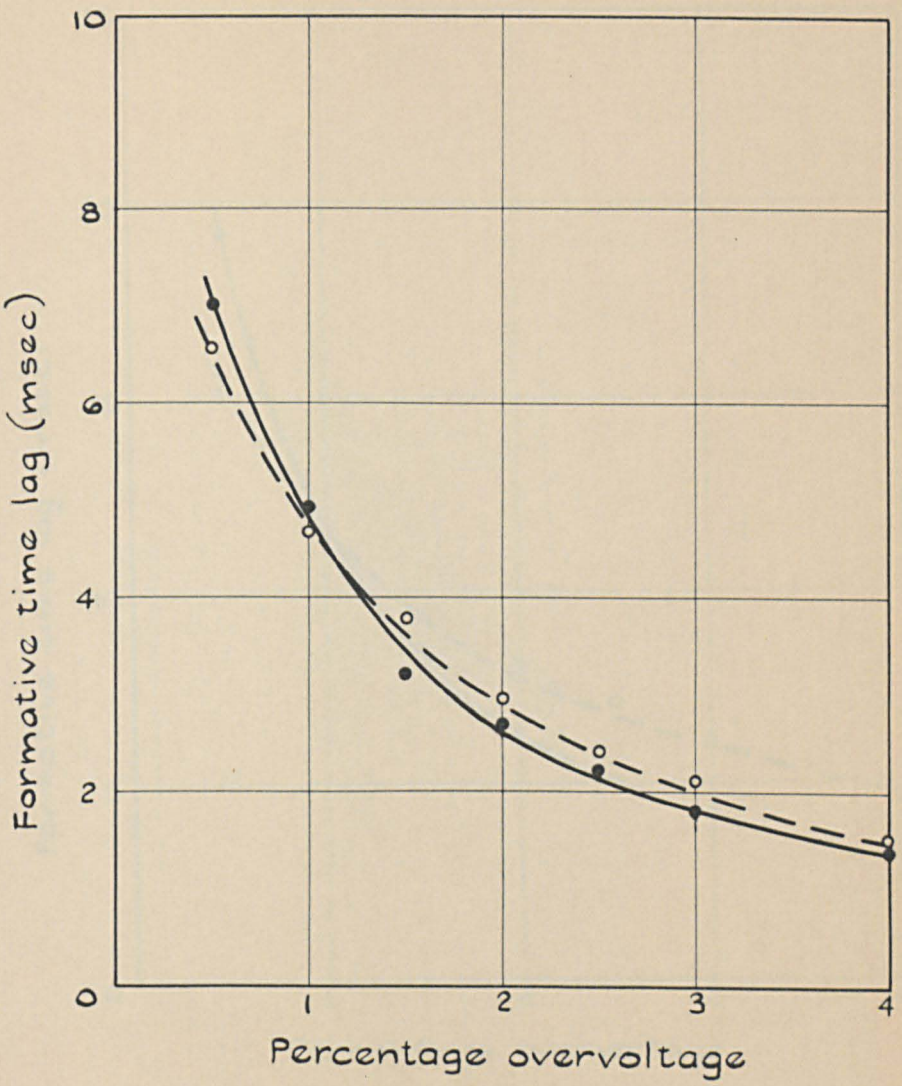

FIG. 50 $p_0 = 22{\cdot}1$ torr, $d = 0{\cdot}27$ cm

$\delta_1/\alpha = 0{\cdot}43\,\omega/\alpha$, $\gamma = 0{\cdot}57\,\omega/\alpha$

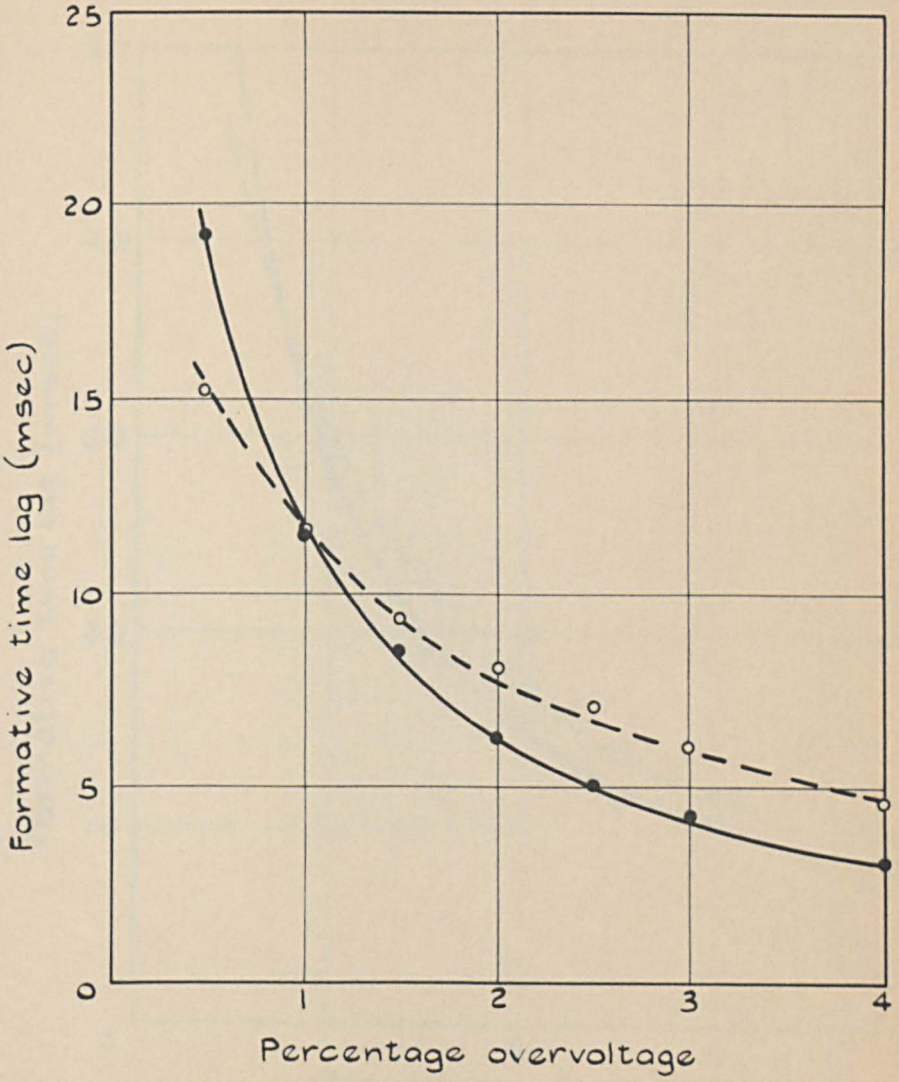

FIG. 51 $p_0 = 22{\cdot}1$ torr; $d = 0{\cdot}36$ cm
$\delta_1/\alpha = 0{\cdot}87\,\omega/\alpha$, $\gamma = 0{\cdot}13\,\omega/\alpha$

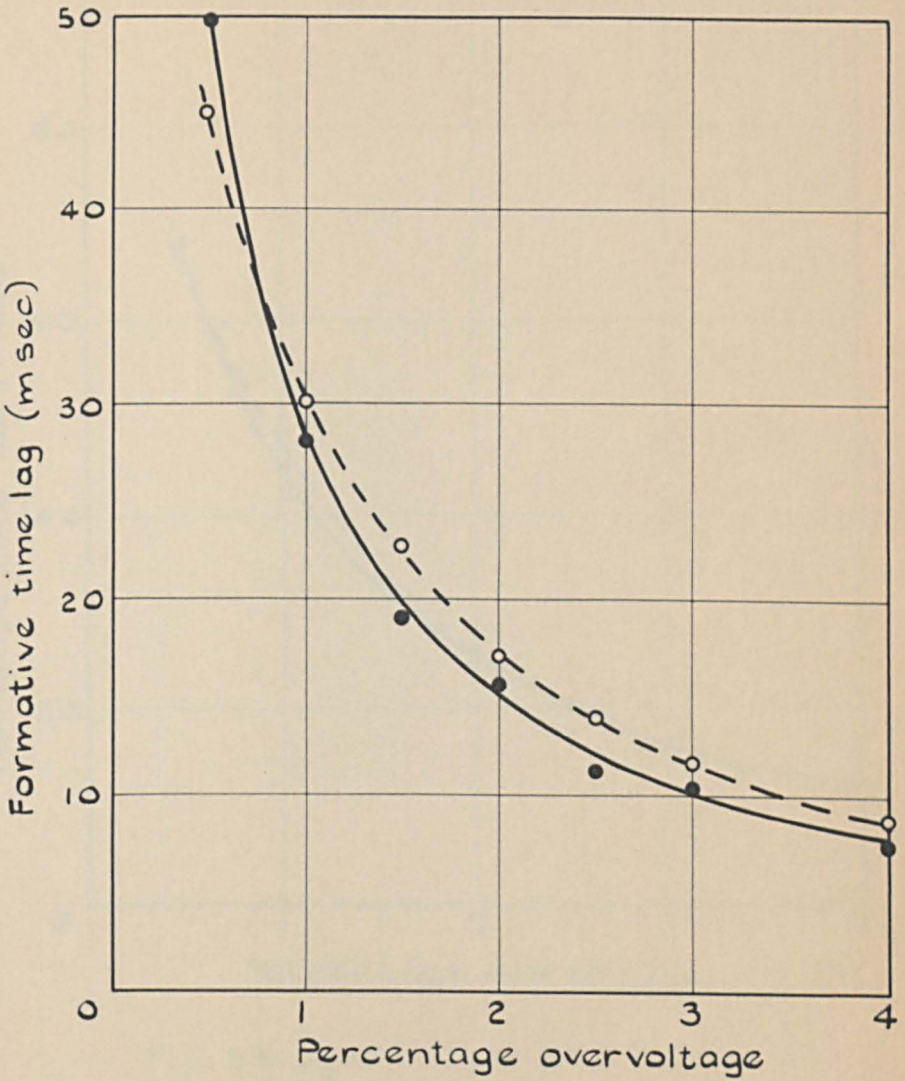

FIG. 52 $P_0 = 22{\cdot}1$ torr, $d = 0{\cdot}51$ cm.
$\delta_1/\alpha = 0{\cdot}93\,\omega/\alpha$, $\delta_2/\alpha = 0{\cdot}07\,\omega/\alpha$.

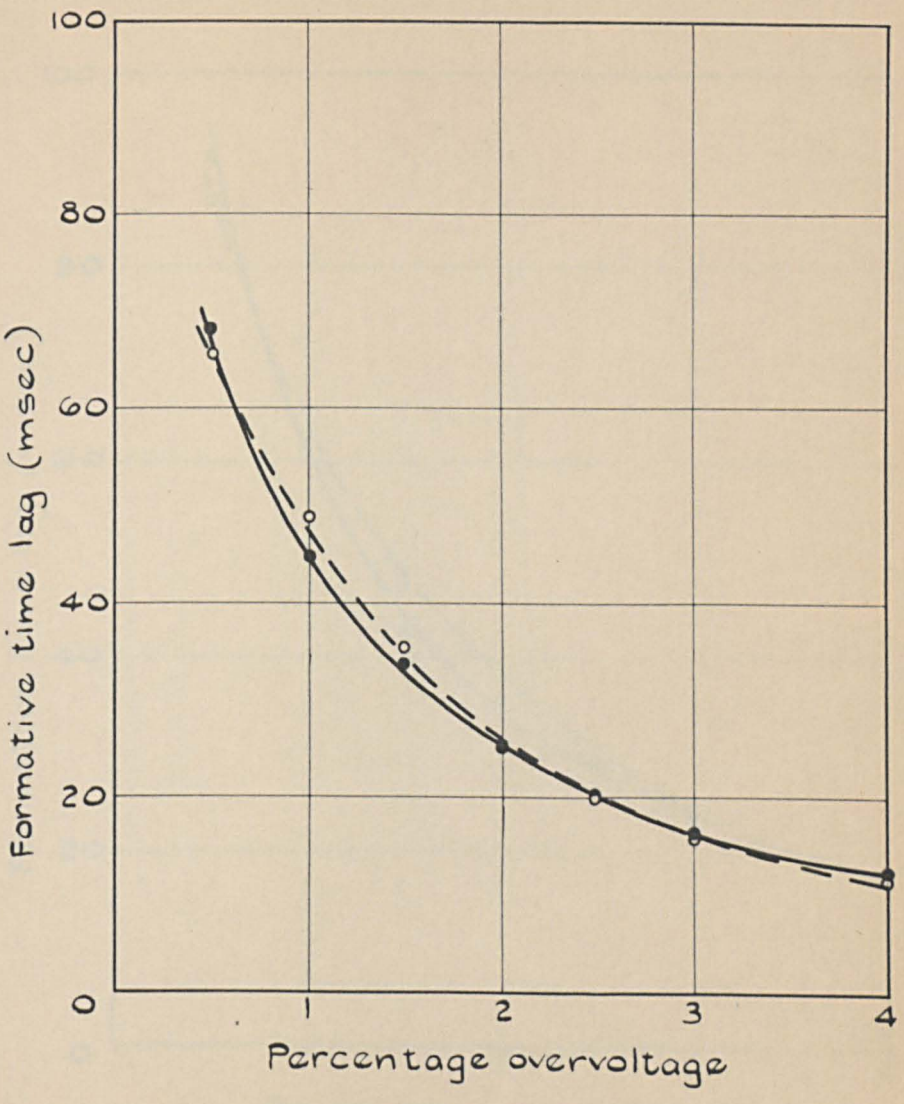

FIG. 53 $p_0 = 22{\cdot}1$ torr, $d = 0{\cdot}70$ cm

$\delta_1/\alpha = 0{\cdot}90\,\omega/\alpha$, $\delta_2/\alpha = 0{\cdot}10\,\omega/\alpha$

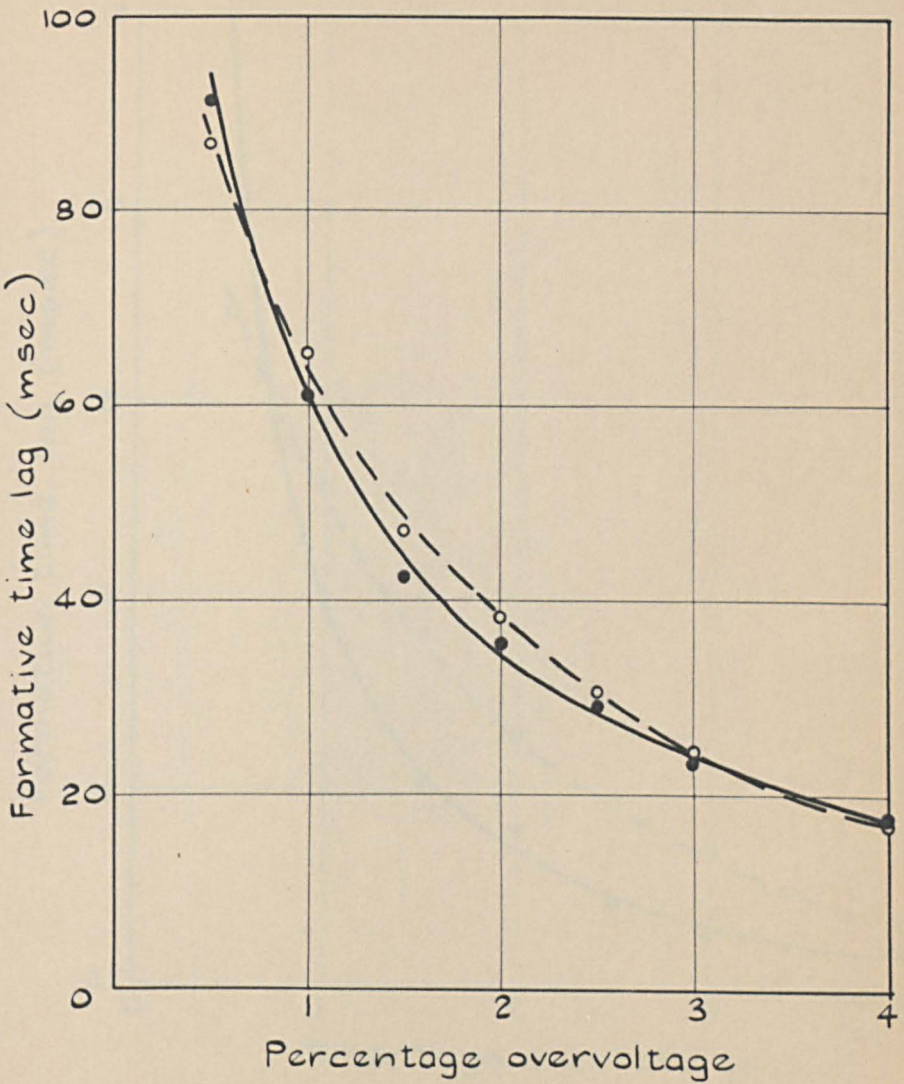

FIG. 54 $P_0 = 22{\cdot}1$ torr, $d = 0{\cdot}80$ cm

$\delta_1/\alpha = 0{\cdot}86\,\omega/\alpha$, $\delta_2/\alpha = 0{\cdot}14\,\omega/\alpha$

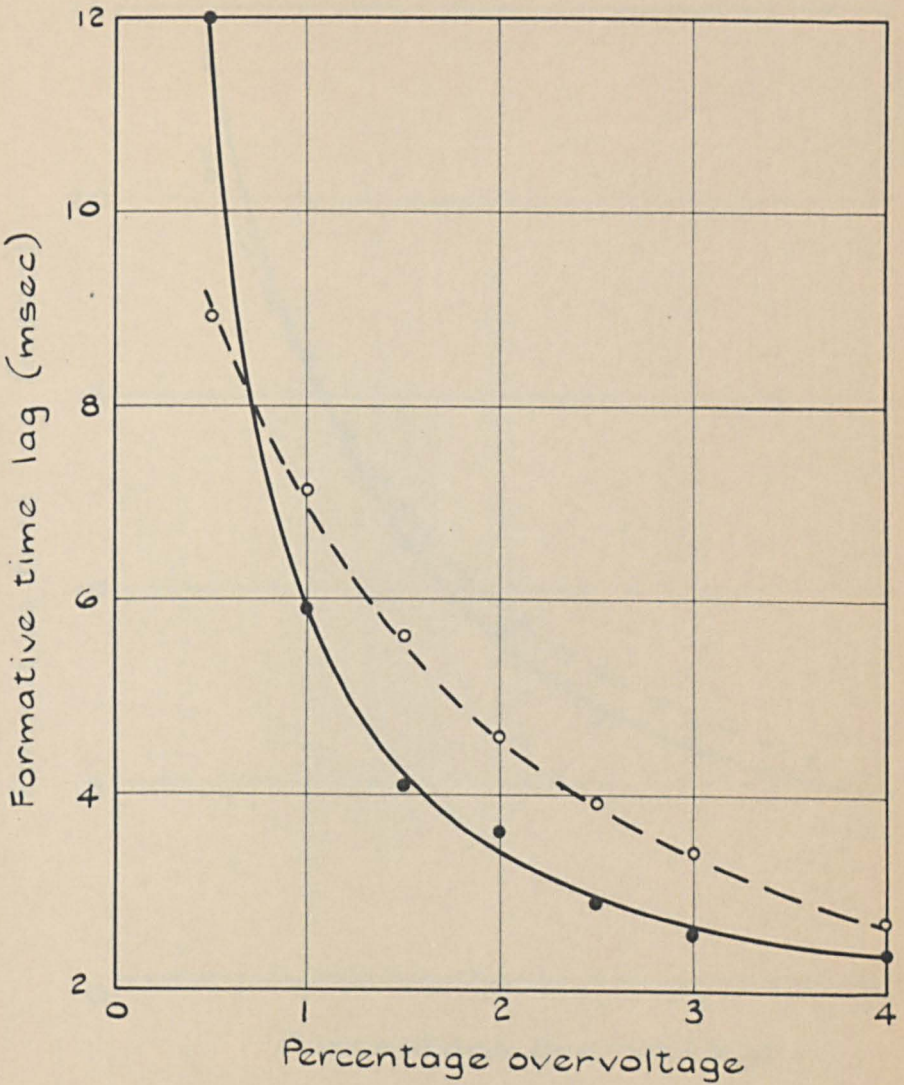

FIG. 55 $p_0 = 34{\cdot}2$ torr, $d = 0{\cdot}19$ cm

$\delta_1/\alpha = 0{\cdot}79\,\omega/\alpha$, $\gamma = 0{\cdot}21\,\omega/\alpha$

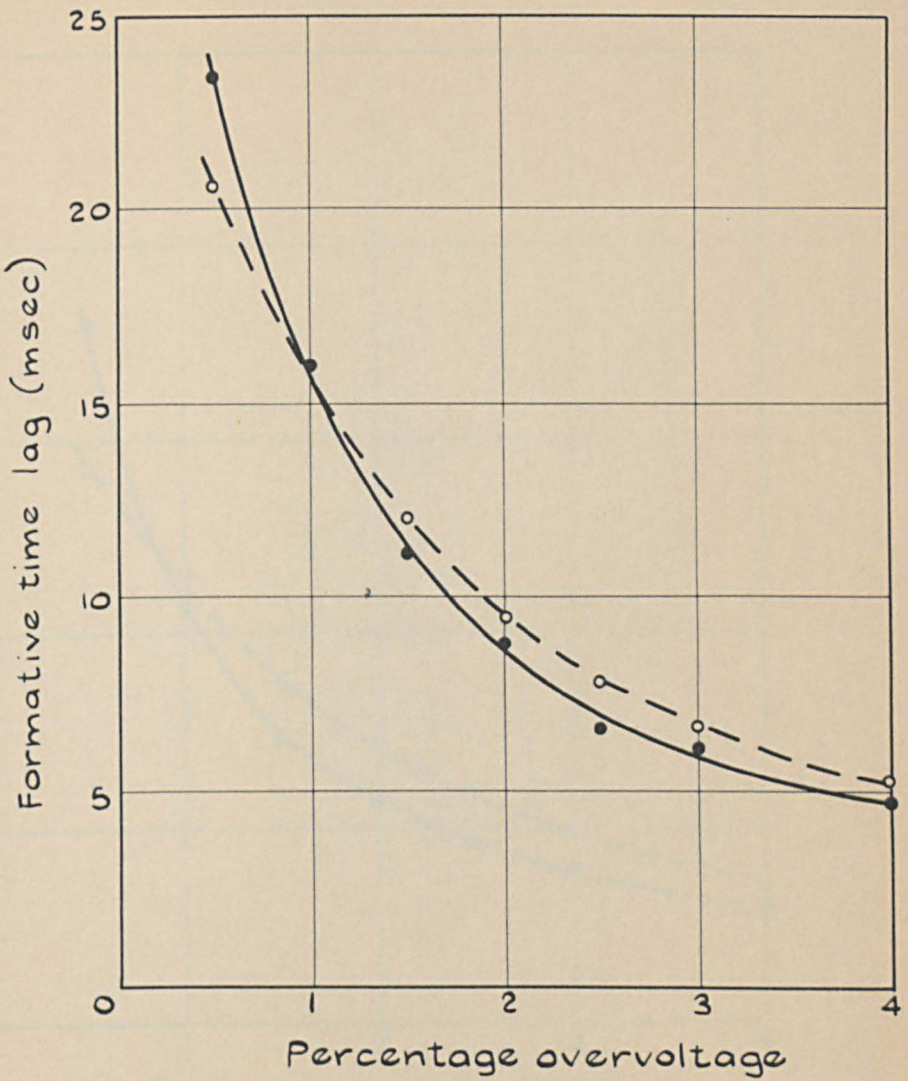

FIG. 56 $p_0 = 34 \cdot 2$ torr, $d = 0 \cdot 36$ cm
$\delta_1/\alpha = 0 \cdot 95\,\omega/\alpha$, $\delta_2/\alpha = 0 \cdot 05\,\omega/\alpha$

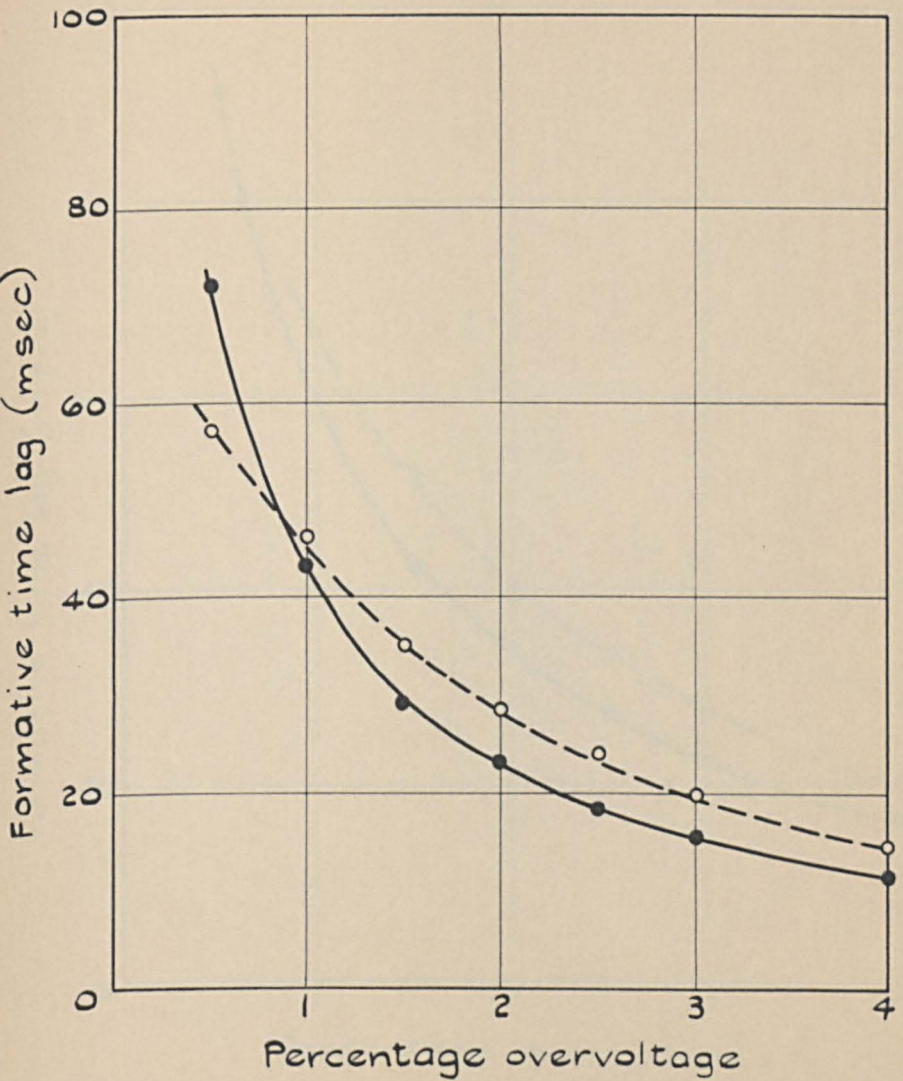

FIG. 57 $p_0 = 34{\cdot}2$ torr, $d = 0{\cdot}52$cm.

$\delta_1/\alpha = 0{\cdot}79\,\omega/\alpha$, $\delta_2/\alpha = 0{\cdot}21\,\omega/\alpha$

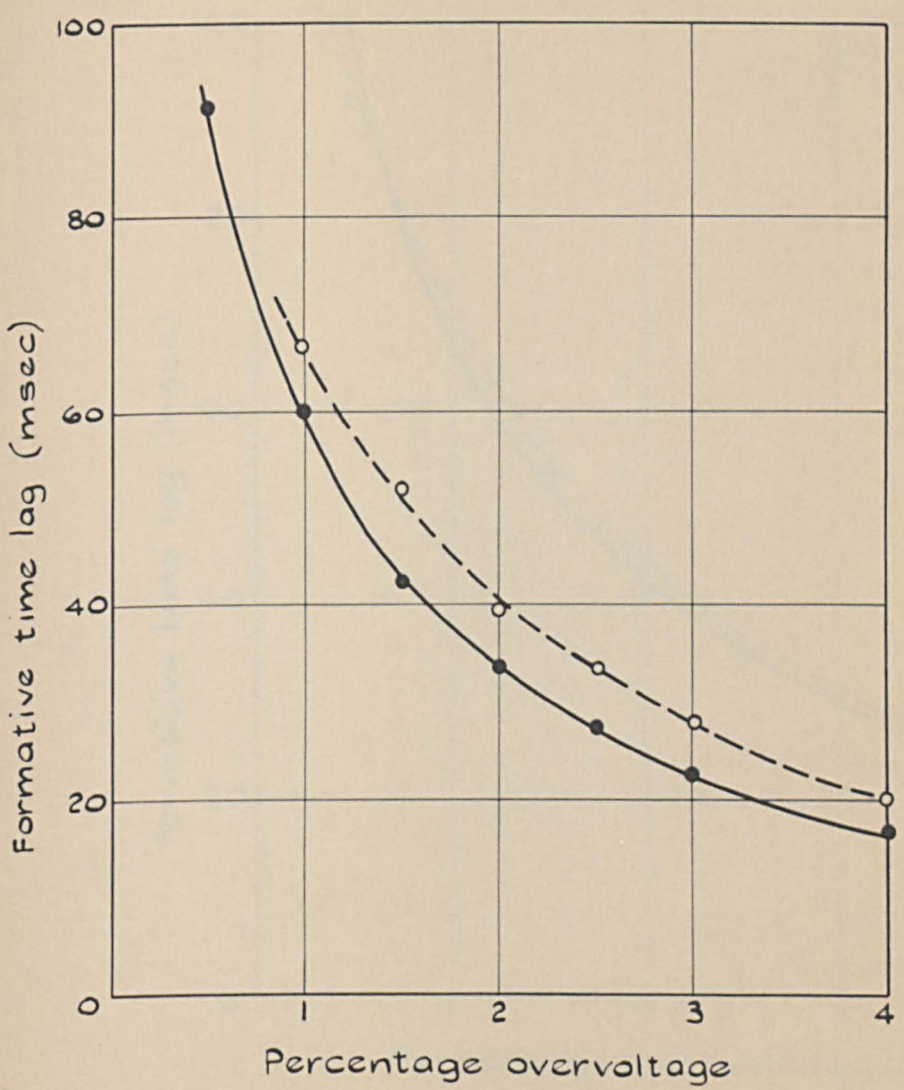

FIG. 58 $P_0 = 34{\cdot}2$ torr, $d = 0{\cdot}61$ cm
$\delta_1/\alpha = 0{\cdot}73\,\omega/\alpha$, $\delta_2/\alpha = 0{\cdot}27\,\omega/\alpha$

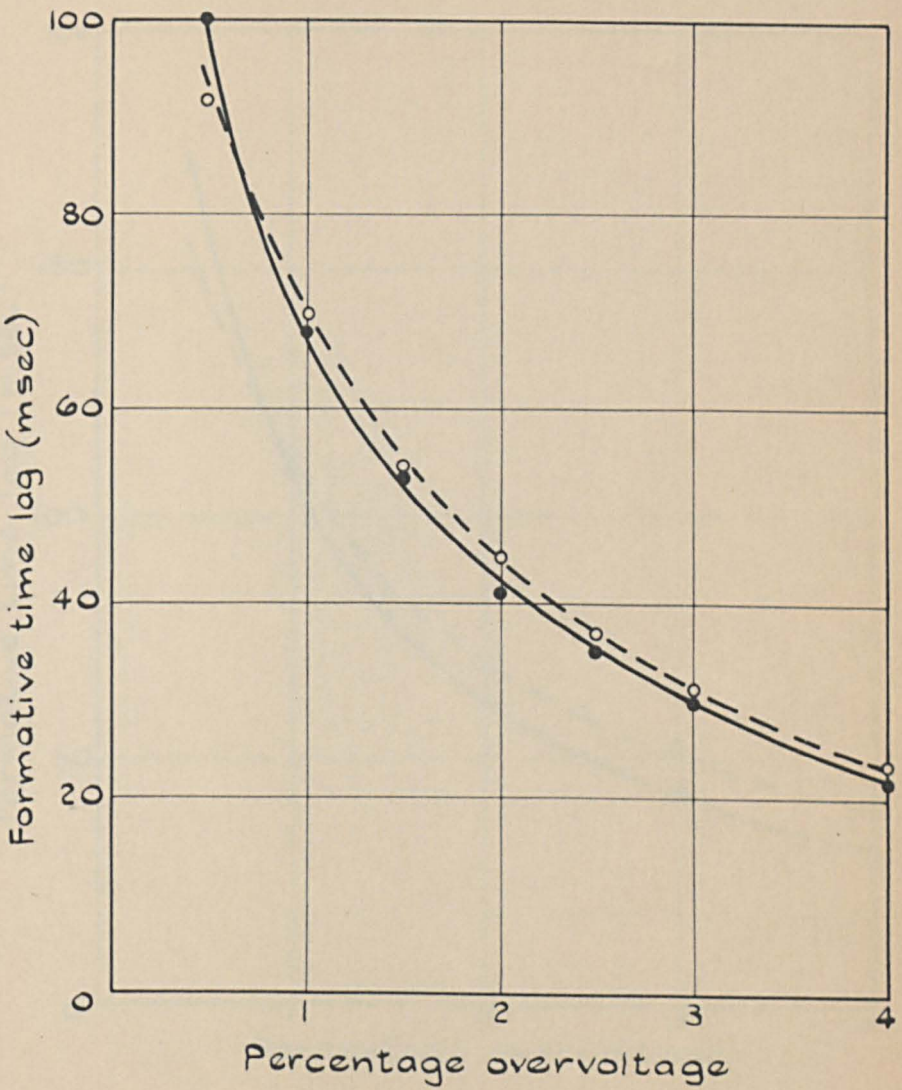

FIG. 59 $P_0 = 34{\cdot}2$ torr; $d = 0{\cdot}71$ cm

$\delta_1/\alpha = 0{\cdot}64\,\omega/\alpha$, $\delta_2/\alpha = 0{\cdot}36\,\omega/\alpha$

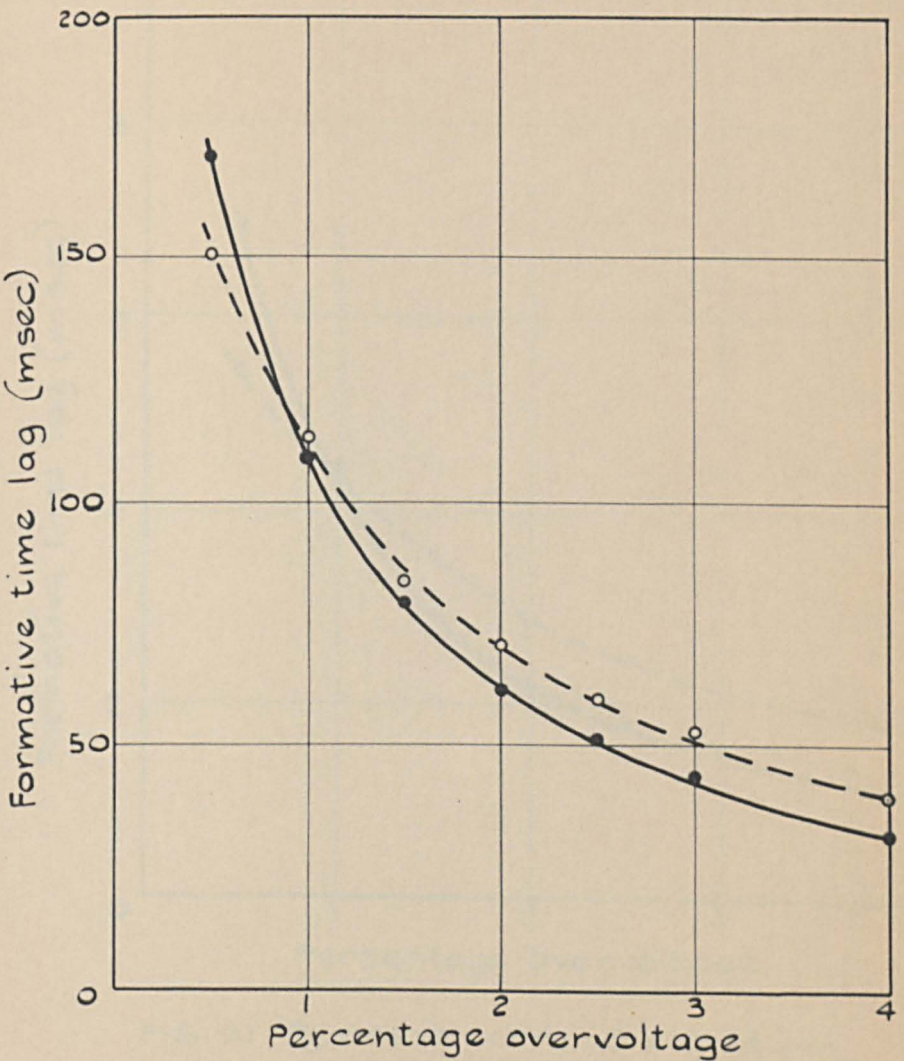

FIG. 60 $p_0 = 34{\cdot}2$ torr, $d = 0{\cdot}82$ cm

$\delta_1/\alpha = 0{\cdot}40\,\omega/\alpha$, $\delta_2/\alpha = 0{\cdot}60\,\omega/\alpha$

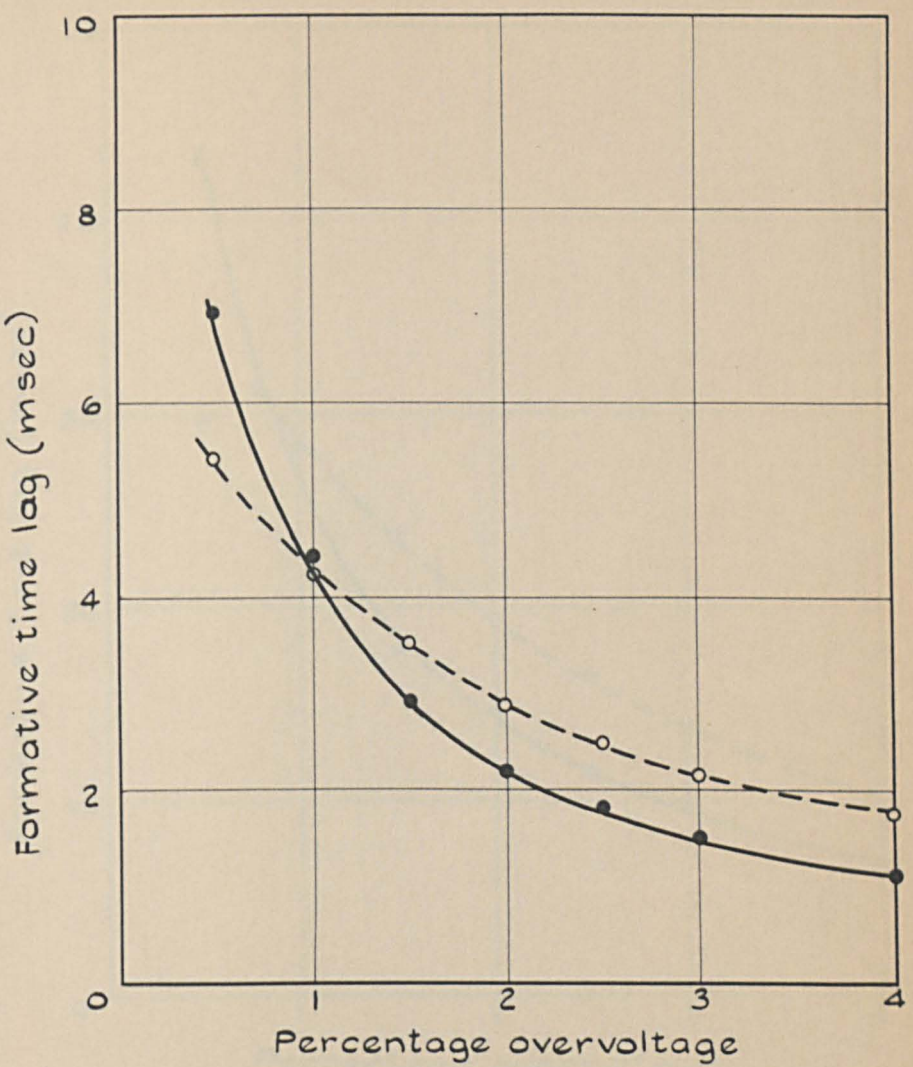

FIG. 61 $P_0 = 44{\cdot}4$ torr, $d = 0{\cdot}18$ cm

$\delta_1/\alpha = 0{\cdot}64\,\omega/\alpha$, $\gamma = 0{\cdot}36\,\omega/\alpha$

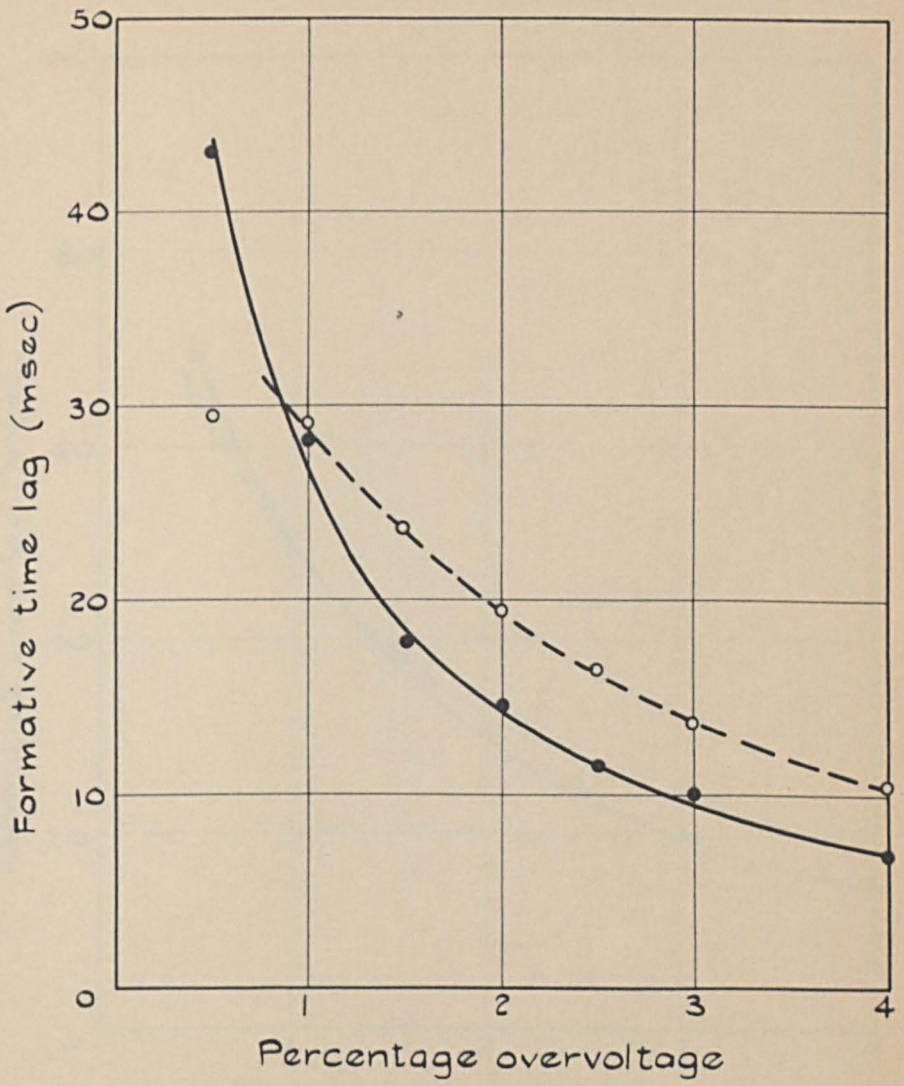

FIG. 62 $p_0 = 44{\cdot}4$ torr, $d = 0{\cdot}42$ cm

$\delta_1/\alpha = 0{\cdot}81\omega/\alpha$, $\delta_2/\alpha = 0{\cdot}19\omega/\alpha$

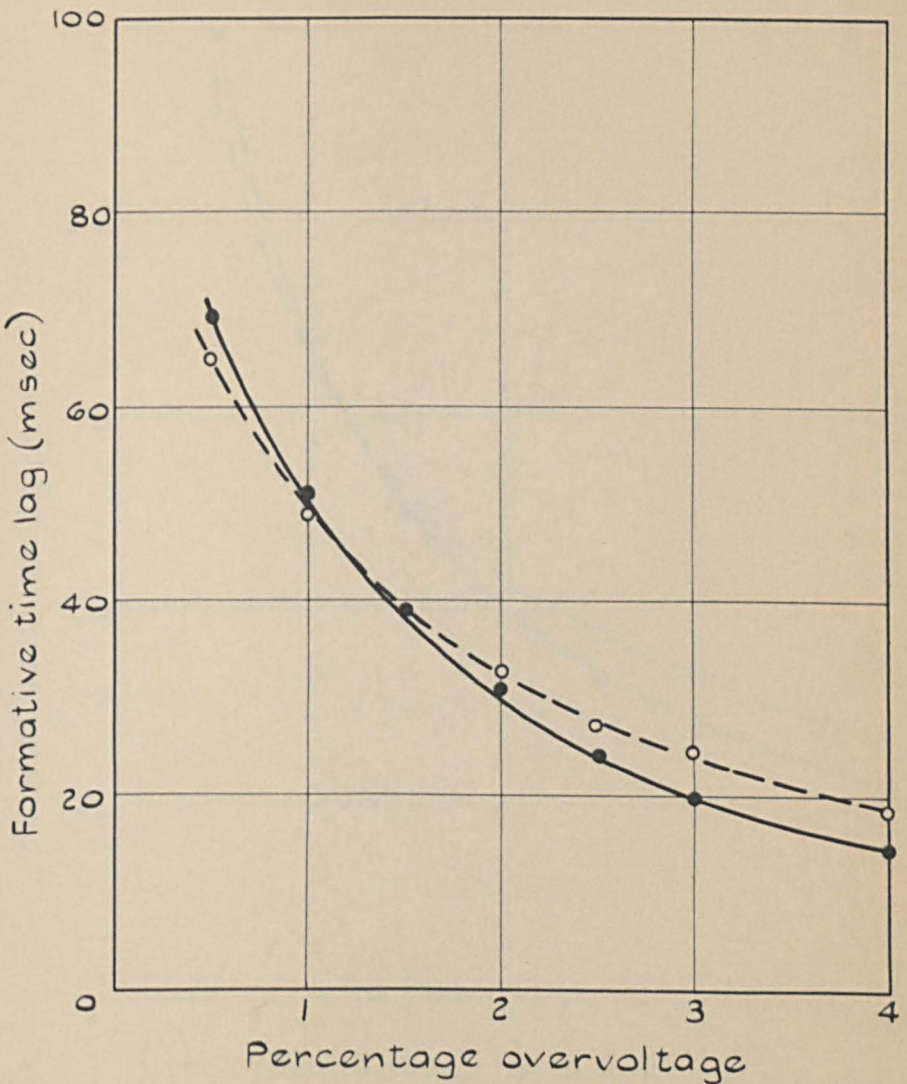

FIG. 63 $p_0 = 44{\cdot}4$ torr, $d = 0{\cdot}54$ cm
$\delta_1/\alpha = 0{\cdot}57\omega/\alpha$, $\delta_2/\alpha = 0{\cdot}43\omega/\alpha$

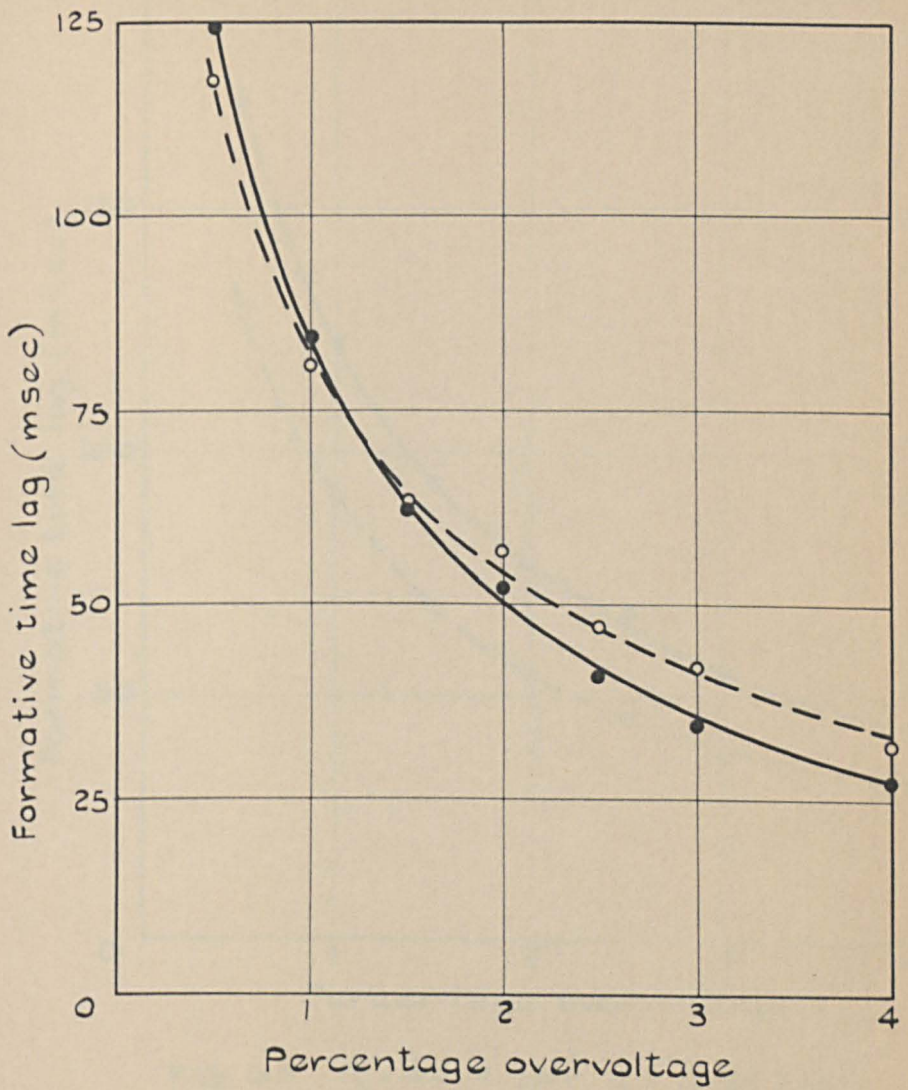

FIG. 64 $p_0 = 44{\cdot}4$ torr, $d = 0{\cdot}69$ cm

$\delta_1/\alpha = 0{\cdot}18\,\omega/\alpha$, $\delta_2/\alpha = 0{\cdot}82\,\omega/\alpha$

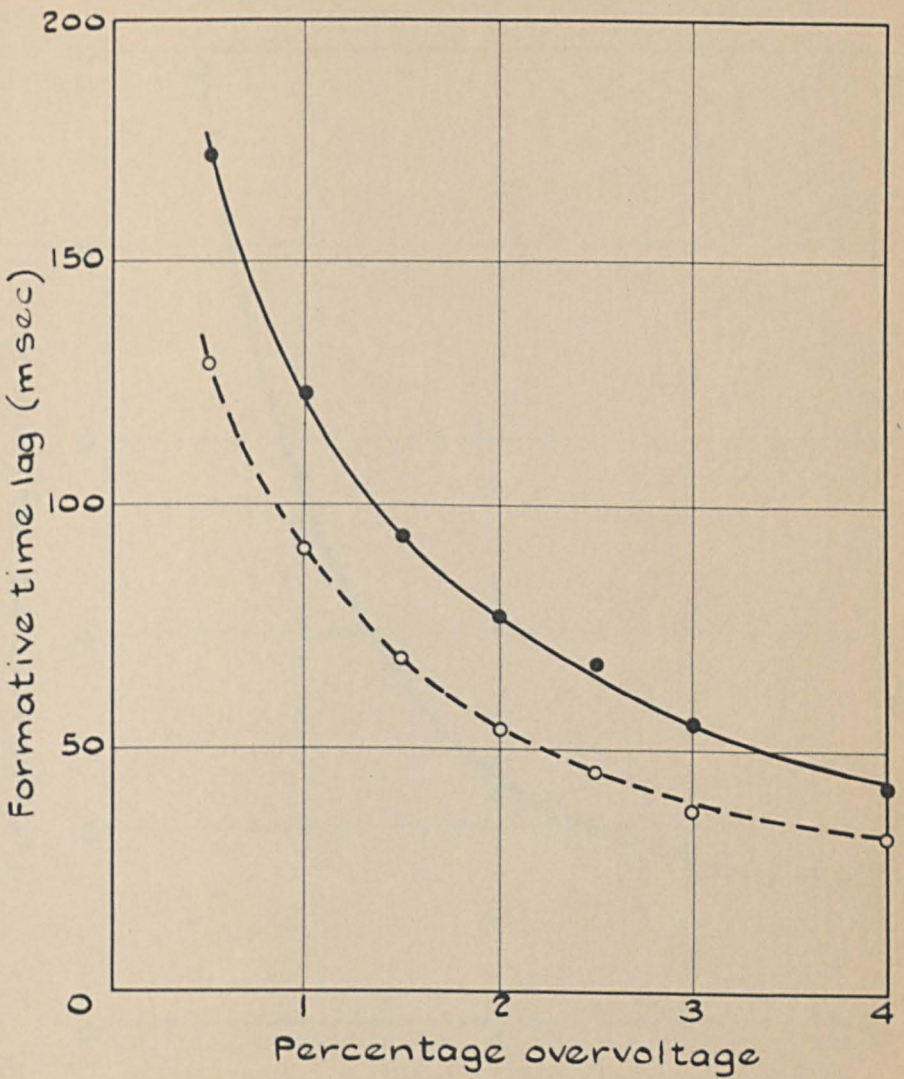

FIG. 65 $P_0 = 44{\cdot}4$ torr, $d = 0{\cdot}82$ cm
$\delta_2/\alpha = \omega/\alpha$.

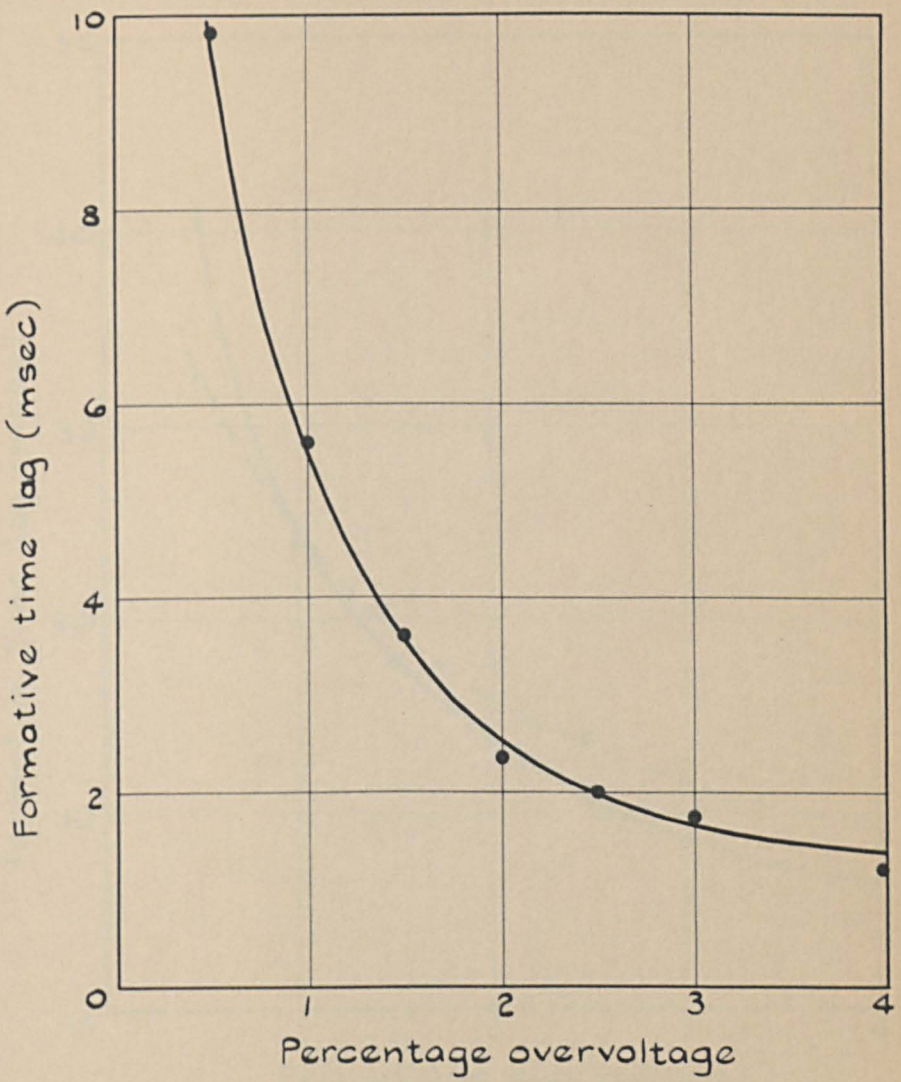

FIG.66 $p_0 = 62{\cdot}2$ torr, $d = 0{\cdot}19$ cm.
EXPERIMENTAL CURVE ONLY.

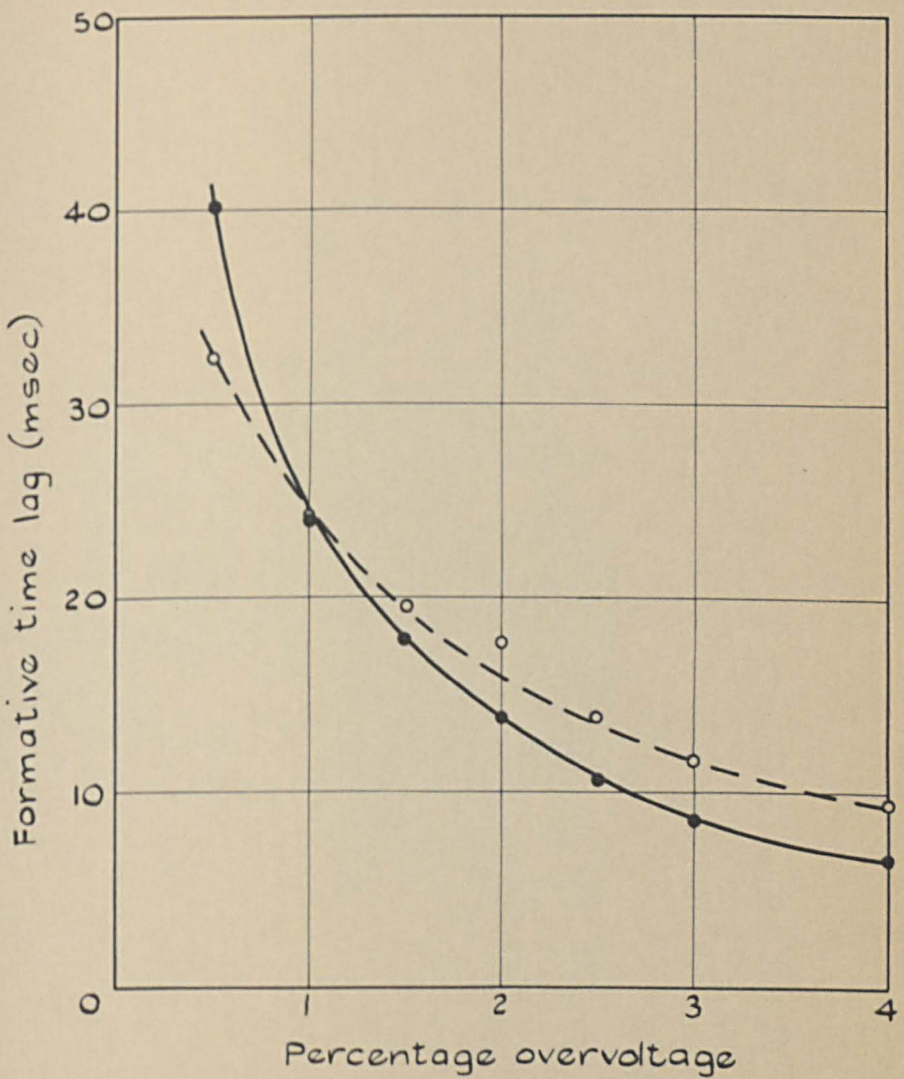

FIG. 67 $p_0 = 62{\cdot}2$ torr, $d = 0{\cdot}34$ cm

$\delta_1/\alpha = 0{\cdot}61\omega/\alpha$, $\delta_2/\alpha = 0{\cdot}39\omega/\alpha$

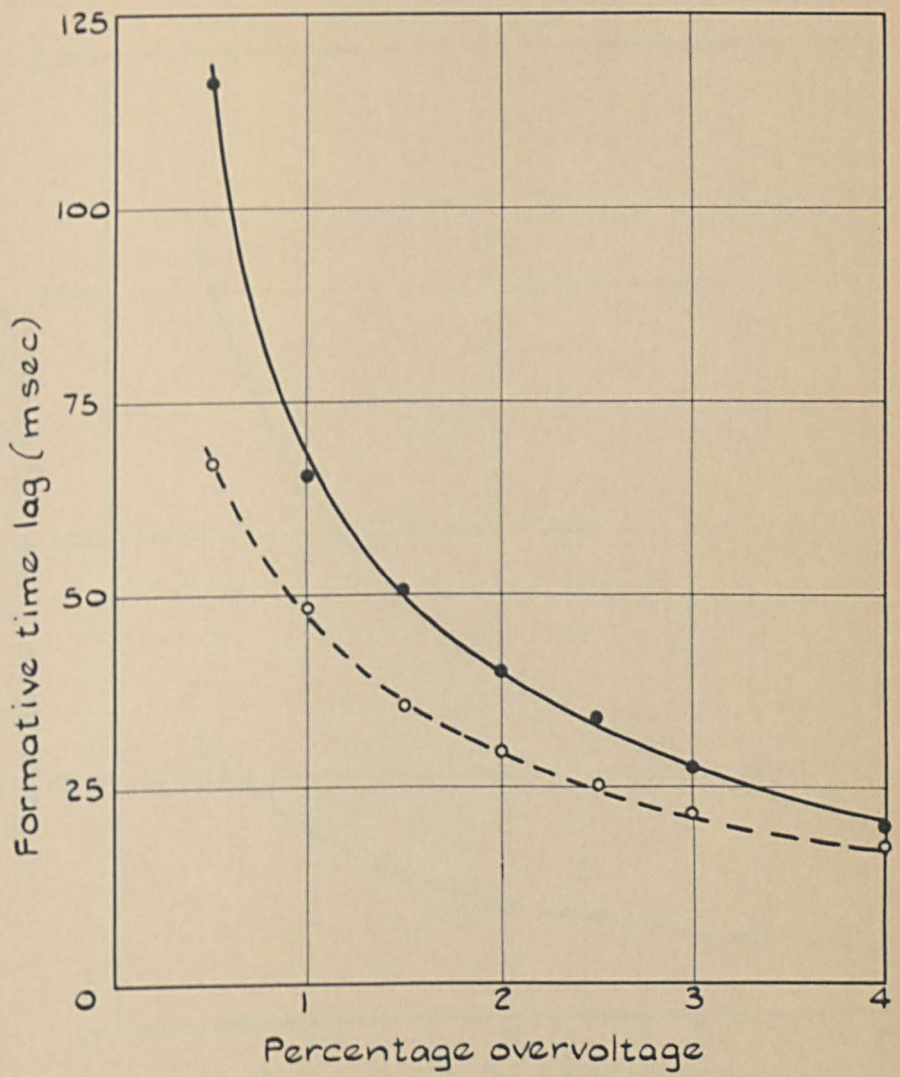

FIG.68 $P_0 = 62{\cdot}2$ torr, $d = 0{\cdot}53$cm
$\delta_2/\alpha = \omega/\alpha$

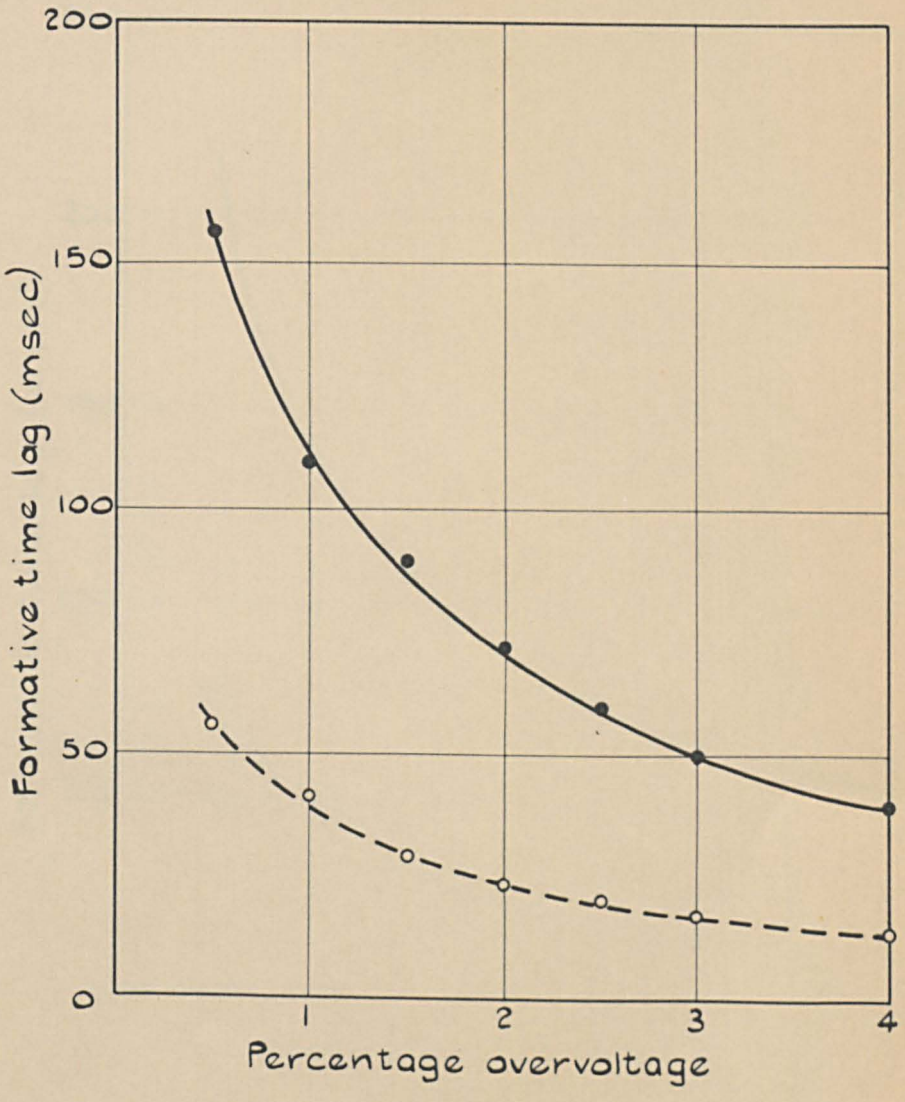

FIG. 69 $p_0 = 62{\cdot}2$ torr, $d = 0{\cdot}72$ cm

$\delta_2/\alpha = \omega/\alpha$

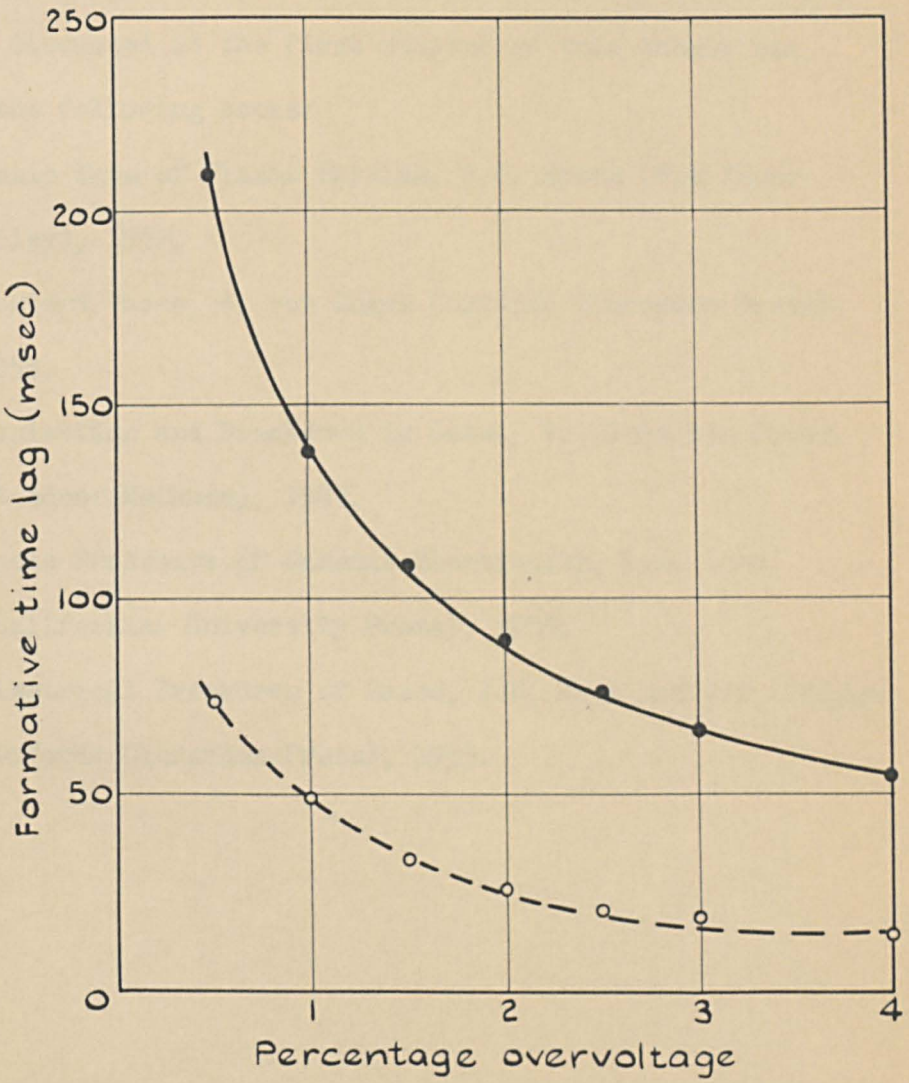

FIG. 70 $p_0 = 62{\cdot}2$ torr, $d = 0{\cdot}82$ cm

$\delta_2/\alpha = \omega/\alpha$.

BIBLIOGRAPHY

A comprehensive survey of some of the topics which are only briefly discussed in the first chapter of this thesis can be found in the following books:

Basic Data of Plasma Physics, S.C. Brown (New York: Wiley), 1959.

Ionized Gases, A. von Engel (Oxford: Clarendon Press), 1955.

Ionization and Breakdown in Gases, F. Llewellyn Jones (London: Methuen), 1957.

Basic Processes of Gaseous Electronics, L.B. Loeb (California: University Press), 1955.

Electrical Breakdown of Gases, J.M. Meek and J.D. Craggs (Oxford: Clarendon Press), 1953.

REFERENCES

1. P.M. Davidson, Proc. Roy. Soc. A, 249, 237 (1959).
2. W.H. Keeson, Helium (Holland: Elsevier), 1942.
3. M. Born, Atomic Physics (London: Blackie), 1957.
4. E.A. Hylleraas, Z. Phys., 65, 209 (1930).
5. W. de Groot and F.M. Penning, Handbuch d. Phys. (Berlin: Springer), 23, 23 (1933).
6. W.P. Allis and P.M. Morse, Z. Phys., 70, 567 (1931).
7. R.B. Brode, Rev. Mod. Phys., 5, 257 (1933).
8. L. Gould and S.C. Brown, Phys. Rev., 95, 897 (1954).
9. A.V. Phelps, O.T. Fundingsland and S.C. Brown, Phys. Rev., 84, 559 (1951).
10. L.J. Varnerin, Phys. Rev., 84, 563 (1951).
11. F.L. Arnot, Collision Processes in Gases (London: Methuen), 1957.
12. P.T. Smith, Phys. Rev., 36, 1293 (1930).
13. F. Horton and D.M. Millest, Proc. Roy. Soc. A, 185, 381 (1946).
14. R.N. Varney, L.B. Loeb and W.R. Haseltine, Phil. Mag., 29, 379 (1940).
15. M.A. Biondi, Phys. Rev., 88, 660 (1952).
16. A.E.D. Heylen and T.J. Lewis, Proc. Roy. Soc. A, 271, 531 (1963).

17. F.H. Reder and S.C. Brown, Phys. Rev., 95, 885 (1954).

18. J.S. Townsend and V.A. Bailey, Phil. Mag., 42, 873 (1921).

19. J.A. Smit, Physica, 3, 543 (1936).

20. A.V. Phelps, J.L. Pack and L.S. Frost, Phys. Rev., 117, 470 (1960).

21. J.A. Hornbeck, Phys. Rev., 84, 615 (1951).

22. A.V. Phelps, Phys. Rev., 99, 1307 (1955).

23. J.S. Townsend, The Theory of Ionization of Gases by Collision (London: Constable), 1910.

24. A. von Engel, Handbuch d. Phys. (Berlin: Springer), 21, 518 (1956).

25. J.S. Townsend and S.P. McCallum, Phil. Mag., 17, 678 (1934).

26. S.H. Dunlop, Nature, 164, 452 (1949).

27. D.K. Davies, F. Llewellyn Jones and C.G. Morgan, Proc. Phys. Soc., 80, 898 (1962).

28. J. Fletcher, Ionization Coefficients in Hydrogen, Helium and Neon (Ph.D. thesis, University of Keele), 1963.

29. L.M. Chanin and G.D. Rork, Phys. Rev., 133, A1005 (1964).

30. A. von Engel, Ionized Gases (Oxford: Clarendon Press), 1955.

31. P.F. Little, Handbuch d. Phys. (Berlin: Springer), 21, 627 (1956); L.B. Loeb, Basic Processes of Gaseous Electronics (California: University Press), 1955; F. Llewellyn Jones, Ionization and Breakdown in Gases (London: Methuen), 1957.

32. H.D. Hagstrum, Phys. Rev., 96, 325 (1954).

33. H.D. Hagstrum, Phys. Rev., 91, 543 (1953).

34. F.M. Propst and E. Lüscher, Phys. Rev., 132, 1037 (1963).

35. R. Dorrestein, Physica, 9, 447 (1942).

36. C. Kenty, Phys. Rev., 44, 891 (1933).

37. S.P. McCallum and L. Klatzow, Phil. Mag., 17, 291 (1934).

38. F. Llewellyn Jones, Phil. Mag., 28, 192 (1939).

39. F. Llewellyn Jones and D.E. Davies, Proc. Phys. Soc. B, 64, 397 (1951).

40. D.E. Davies, R.K. Fitch, B.J. Hopkins and C.F. Gozna, Proc. 4th Int. Conf. on Ionization Phenomena in Gases (Amsterdam: North-Holland), 1, 263 (1960).

41. J.P. Molnar, Phys. Rev., 83, 933, 940 (1951).

42. J.A. Hornbeck, Phys. Rev., 83, 374 (1951).

43. R.N. Varney, Phys. Rev., 93, 1156 (1954).

44. M. Steenbeck, Wiss. Veröff. a.d. Siemens-Werken, 9, 42 (1930).

45. R. Schade, Z. Phys., 104, 487 (1937).

46. M.J. Druyvestyn and F.M. Penning, Rev. Mod. Phys., 12, 87 (1946).

47. W. Bartholomeyczyk, Z. Phys., 116, 235 (1940).

48. P.M. Davidson (Appendix to a paper by J. Dutton, S.C. Haydon and F. Llewellyn Jones), Brit. J. App. Phys., 4, 170 (1953).

49. R.W. Engstrom and W.S. Huxford, Phys. Rev., 58, 67 (1940).

50. G.A. Kachickas and L.H. Fisher, Phys. Rev., 88, 878 (1952).

51. P.M. Davidson, Phys. Rev., 99, 1072 (1955).

52. P.M. Davidson, Phys. Rev., 106, 1 (1957).

53. P.L. Auer, Phys. Rev., 98, 320 (1955); 101, 1243 (1956); 111, 671 (1958).

54. H.W. Bandel, Phys. Rev., 95, 1117 (1954).

55. Y. Miyoshi, Phys. Rev., 103, 1609 (1956).

56. Y. Miyoshi, Phys. Rev., 117, 355 (1960).

57. M. Menes, Phys. Rev., 116, 481 (1959).

58. L. Colli, Phys. Rev., 95, 892 (1954).

59. A.J. Davies, C.J. Evans and F. Llewellyn Jones, Proc. Roy. Soc. A, 281, 164 (1964).

60. P.M. Davidson, Proc. Roy. Soc. A, 249, 237 (1959).

61. P.M. Davidson, Proc. Phys. Soc., 80, 143 (1962).

62. B.T. McClure, Phys. Rev., 125, 11 (1962).

63. H.L. von Gugelberg, Helv. Acta Phys., 20, 307 (1947).

64. D.K. Davies, F. Llewellyn Jones and C.G. Morgan, Proc. Phys. Soc., 81, 677 (1963).

65. D.K. Davies, F. Llewellyn Jones and C.G. Morgan, Proc. Phys. Soc., 83, 137 (1964).

66. A.V. Phelps, Phys. Rev., 117, 619 (1960).

67. T. Holstein, Phys. Rev., 72, 1212 (1947); 83, 1159 (1951).

68. A.C.G. Mitchell and M.W. Zemansky, Resonance Radiation and Excited Atoms (London: Macmillan), 1934.

69. A. Dalgarno and A.L. Stewart, Proc. Phys. Soc., 76, 491 (1960).

70. S.J.B. Corrigan and A. von Engel, Proc. Phys. Soc., 72, 786 (1958).

71. G.B. Evans, The Oxide-coated Cathode and the Hydrogen Discharge (M.Sc. thesis, University of Birmingham), 1962.

72. I.F. Homfrey and A. Titoff, Z. Phys. Chem., 74, 129, 641 (1910).

73. R.E. Wilson, Phys. Rev., 16, 8 (1920).

74. E.C. Baly, Phil. Mag., 35, 200 (1893).

75. F. Skaupy, Z. tech. Phys., 6, 284 (1925).

76. M.J. Druyvestyn, Physica, 2, 255 (1935).

77. R. Riesz and G.H. Dieke, J. App. Phys., 25, 196 (1954).

78. A.L. Schmeltekopf, J. App. Phys., 35, 1712 (1964).

79. L.B. Loeb, J. App. Phys., 29, 1369 (1958).

80. D.A. Wright, Semiconductors (London: Methuen), 1950.

81. J.C. Riviere, Proc. Phys. Soc. B, 70, 676 (1957).

82. R.C. Maddison, Work Function Changes of Clean and Contaminated Metal Films in Vacuum and in Hydrogen (Ph.D. thesis, University of Keele), 1964.

83. D.A. Wright, Semiconductors (London: Methuen), 1966.

84. B.M.W. Trapnell, Proc. Roy. Soc. A, 218, 566 (1953).

85. H.E. Farnsworth, Proc. Phys. Soc., 71, 703 (1958).

86. G.L. Weissler and J.N. Wilson, J. App. Phys., 24, 472 (1953).

87. V.O. Altemose, J. App. Phys., 32, 1309 (1961).

88. H. Bottenbruch, J. Assn. for Computing Machinery, 9, 161 (1962).

89. D. Griffiths, Private Communication.

90. E.H.S. Burhop, Proc. Phys. Soc. A, 67, 276 (1954).

91. M.A. Biondi, Rev. Sci. Instrum., 22, 535 (1951).

GBE/RM